Supplementary Information for

Catalytic Nitrogen-to-Ammonia Conversion by Osmium and Ruthenium Complexes

Javier Fajardo Jr. and Jonas C. Peters*

Division of Chemistry and Chemical Engineering
California Institute of Technology
Pasadena, California 91125, United States

*Email: jpeters@caltech.edu

Table of Contents

Experimental Methods……S2

Synthetic Details & Characterization Data……...S2–S29
$[H_2NPh_2][BAr^F{}_4]$……..S2–S3
$[H_3NPh][BAr^F{}_4]$…… ……..S3
$[P_3{}^{Si}Os{=}NNH_2][OTf]$……...S3–S9
$P_3{}^{Si}Os(N_2)(H)$……...S9–S13
$P_3{}^{Si}OsH_3$……...S13–S21
$P_3{}^{Si}RuH_3$……...S21–S23
Treatment of $[K(THF)_2][P_3{}^{Si}M\text{-}N_2]$ with 10 equiv Acid and 12 equiv Reductant……S23–S29

Ammonia Production & Quantification Studies……S30–S38
Standard NH_3 Generation Reaction Procedure and Results……S30–S35
NH_3 Generation Reaction with Periodic Substrate Reloading – Procedure with $[K(THF)_2][P_3{}^{Si}Os\text{-}N_2]$……..S35
Control Experiments with $[H_2{}^{15}NPh_2][OTf]$ and $[H_3{}^{15}NPh][OTf]$……..S35–S38

Miscellaneous Experiments……...S38–S61
Monitoring the Decomposition of $[P_3{}^{Si}Os{=}NNH_2][OTf]$ in THF Solution at Room Temperature…….....S38–40
Variable Temperature NMR Spectral Analysis of the Reaction of $[K(THF)_2][P_3{}^{Si}Os\text{-}N_2]$ with 1 equiv of $HBAr^F{}_4$ at -78 °C……S40–S46
General Procedure for the Variable Temperature NMR Spectral Analysis of the Reaction of $P_3{}^{Si}M\text{-}N_2$ (M = Os, Ru, Fe) with 5 equiv of $Cp^*{}_2Co$...S47–S60
UV-vis Spectral Analysis of the Reaction of $P_3{}^{Si}Os\text{-}N_2$ with 5 equiv of $Cp^*{}_2Co$……..S60–S61

X-Ray Data……S62–S63

References…….....S63–S64

Experimental Methods

General Considerations: Unless otherwise noted, all manipulations were carried out using standard Schlenk or glovebox techniques under an N_2 atmosphere. Solvents were deoxygenated and dried by thoroughly sparging with N_2 gas followed by passage through an activated alumina column in the solvent purification system by SG Water, USA LLC. Non-halogenated solvents were tested with sodium benzophenone ketyl in tetrahydrofuran (THF) in order to confirm effective oxygen and moisture removal. Deuterated solvents were purchased from Cambridge Isotope Laboratories, Inc., degassed, and dried over activated 3-Å molecular sieves prior to use.

$[H_2NPh_2][BAr^F{}_4]$ and $[H_3NPh][BAr^F{}_4]$ were synthesized from a modified literature procedure.[1] $P_3{}^{Si}Os\text{-}Cl$,[2] $P_3{}^{Si}Os\text{-}N_2$,[2] $[K(THF)_2][P_3{}^{Si}Os\text{-}N_2]$,[2] $P_3{}^{Si}Ru\text{-}Cl$,[2] $P_3{}^{Si}Ru\text{-}N_2$,[2] $[K(THF)_2][P_3{}^{Si}Ru\text{-}N_2]$,[2] $P_3{}^{Si}Fe\text{-}N_2$,[3] $[Na(12\text{-crown-}4)_2][P_3{}^{Si}Fe\text{-}N_2]$,[3] $[Na(12\text{-crown-}4)_2][P_3{}^{B}Fe\text{-}N_2]$,[4] $[H(OEt_2)_2][BAr^F{}_4]$ ($HBAr^F{}_4$, $BAr^F{}_4$ = tetrakis(3,5-bis(trifluoromethyl)phenyl)borate),[5] KC_8,[6] $[H_2NPh_2][OTf]$,[7,8] $[H_2{}^{15}NPh_2][OTf]$,[7,9] $[H_3NPh][OTf]$,[8] $[H_2N(Me)(Ph)][OTf]$,[8] and $Cp^*{}_2Co$[10] were prepared according to literature methods. $H_2{}^{15}NPh$ was obtained from Sigma-Aldrich, Inc., degassed, and dried over activated 3-Å molecular sieves prior to use**.** All other reagents were purchased from commercial vendors and used without further purification unless otherwise stated. Diethyl ether (Et_2O) and THF used for NH_3 generation experiments were stirred over Na/K (≥ 1 hour) and filtered before use. *Note:* $P_3{}^{Si}M$ is equivalent to the abbreviated **[M]** notation in the maintext.

NMR: NMR measurements were obtained on Varian 300, 400, or 500 MHz spectrometers. ^1H NMR chemical shifts are reported in ppm and referenced to residual protio solvent. ^{31}P NMR chemical shifts were externally referenced to 85% H_3PO_4 in H_2O.

IR: IR measurements were obtained as solids or thin films formed by evaporation of solutions using a Bruker Alpha Platinum ATR spectrometer with OPUS software.

UV-Vis: Optical spectroscopy measurements were collected with a Cary 50 UV-vis spectrophotometer using a 1 cm path length quartz cuvette. Variable temperature measurements were collected with a Unisoku CoolSpek cryostat mounted within the Cary spectrophotometer. All samples had a blank sample background subtraction applied. Density corrections were applied using literature temperature versus density data available for THF.[11]

X-ray Crystallography: XRD studies were carried out at the Caltech Division of Chemistry and Chemical Engineering X-ray Crystallography Facility on a Bruker three-circle SMART diffractometer with a SMART 1K CCD detector or Bruker Kappa Apex II diffractometer. Data was collected at 100 K using Mo Kα radiation (λ = 0.71073 Å). Using OLEX2,[12] structures were solved with the XT[13] structure solution program using Direct Methods and refined with the XL[14] refinement package using Least Squares minimization. All non-hydrogen atoms were refined anisotropically. All hydrogen atoms were placed at geometrically calculated positions and refined using a riding model. The isotropic displacement parameters of all hydrogen atoms were fixed at 1.2 (1.5 for methyl groups) times the U_{eq} of the atoms to which they are bonded.

Synthetic Details & Characterization Data

$[H_2NPh_2][BAr^F{}_4]$. This compound was synthesized from a modified literature procedure as

follows.[1] Inside the glovebox, $HNPh_2$ (0.0855 g, 0.504 mmol) was weighed out into a 20 mL scintillation vial, equipped with a stir bar, and dissolved in 5 mL of Et_2O. While stirring at room temperature, an $HBAr^F{}_4$ (1.00 equiv, 0.504 mmol, 0.5107 g) solution in Et_2O (5 mL) was added dropwise. The reaction was allowed to stir at room temperature for 1 hour before concentrating the volume of the solution to 2 mL, layering with pentane, and cooling to -30 °C. The white crystals obtained from the crystallization were dried under vacuum to yield $[H_2NPh_2][BAr^F{}_4]$ in quantitative yield.

$[H_3NPh][BAr^F{}_4]$. $[H_3NPh][BAr^F{}_4]$ was prepared from H_2NPh via a procedure analogous to that for $[H_2NPh_2][BAr^F{}_4]$.

$[P_3{}^{Si}Os{=}NNH_2][OTf]$. This compound was synthesized from a modified literature procedure as follows.[15] Inside the glovebox, $[K(THF)_2][P_3{}^{Si}Os\text{-}N_2]$ (0.0574 g, 0.0569 mmol) was dissolved in 2 mL of 2-MeTHF, filtered through glass filter paper into a 20 mL scintillation vial, and frozen inside the coldwell chilled with an external liquid nitrogen bath. A second vial containing a solution of HOTf acid (3.02 equiv, 0.172 mmol, 15.2 μL) in 1 mL of 2-MeTHF was similarly frozen. In addition, a pair of large forceps, a spatula, two pipets, and a vial containing 15 mL of pentane were cooled inside the coldwell.

After freezing and allowing the temperature to equilibrate, the acid solution was briefly thawed by elevating it off of the floor of the coldwell with the forceps. Using the pre-chilled pipet, the acid solution was layered dropwise on top of the frozen solution of $[K(THF)_2][P_3{}^{Si}Os\text{-}N_2]$. Following the refreezing of the solutions, the two layers were combined by first elevating the vial off the coldwell floor with the forceps until the solutions thawed to a viscous mixture, and then stirring mechanically with the pre-chilled spatula. (*Note:* It is critical to combine the layers as soon as the solvent glass melts and while the solution remains rather viscous.) The two layers were mixed in this fashion for ca. 10 minutes, at which point the reaction mixture had changed color from dark red to orange.

Upon completion of mixing, the reaction mixture was allowed to glass. While still at 77 K, it was layered with 15 mL of pre-chilled pentane using a pre-chilled pipet. (*Note:* The pentane was added in small fractions and allowed to freeze in between so as not to allow the reaction layer to thaw). The contents of the vial were then allowed to freeze and equilibrate at 77 K for 10 minutes. During this time, a vial containing 20 mL of pentane, two pipets, a 50 mL filter flask, and a M-porosity frit were similarly cooled to 77 K inside the glovebox coldwell.

The coldwell bath was then switched from a liquid nitrogen bath to a dry ice/acetone bath (-78 °C), and the pentane-layered reaction was allowed to thaw for 1 hour. The layers were further mixed with a pre-chilled pipet to give a cloudy orange mixture that was vacuum filtered through the M-frit inside the glovebox coldwell. While still at -78 °C, the collected pale orange solid was rinsed with pre-chilled pentane. Transferring the solid to a tared vial and drying under vacuum thus afforded 0.0518 g (< 93 % yield) of $[P_3{}^{Si}Os{=}NNH_2][OTf]$ as a pale orange solid. Crystals suitable for XRD were obtained by vapor diffusion of pentane into a concentrated THF solution of $[P_3{}^{Si}Os{=}NNH_2][OTf]$ at room temperature.

*********Note:* $[P_3{}^{Si}Os{=}NNH_2][OTf]$ prepared in this manner contains variable amounts of KOTf.

^{1}H NMR (500 MHz, THF-d_8, 25 ^{o}C): δ(ppm) 9.87 (s, 2H, NNH_2), 8.17 (d, J = 7.2 Hz, 3H, Ar–H), 7.60 (d, J = 7.6 Hz, 3H, Ar–H), 7.40 (t, J = 7.4 Hz, 3H, Ar–H), 7.27 (t, J = 7.4 Hz, 3H, Ar–H), 2.70 (br s, 6H, CH(CH$_3$)$_2$), 1.10–1.04 (br m, 18H, CH(CH_3)$_2$), 0.69 (br s, 18H, CH(CH_3)$_2$).

^{31}P{^{1}H} NMR (202 MHz, THF-d_8, 25 ^{o}C): δ(ppm) 56.5 (s).

^{19}F NMR (376 MHz, THF-d_8, 25 ^{o}C): δ(ppm) -82.2 (s).

IR (solid-state): ν(N–H) = 3232 cm^{-1}.

E.A.: No combustion analysis data was obtained due to the presence of KOTf salts that could not be separated from the [P$_3^{Si}$Os=NNH$_2$][OTf] product.

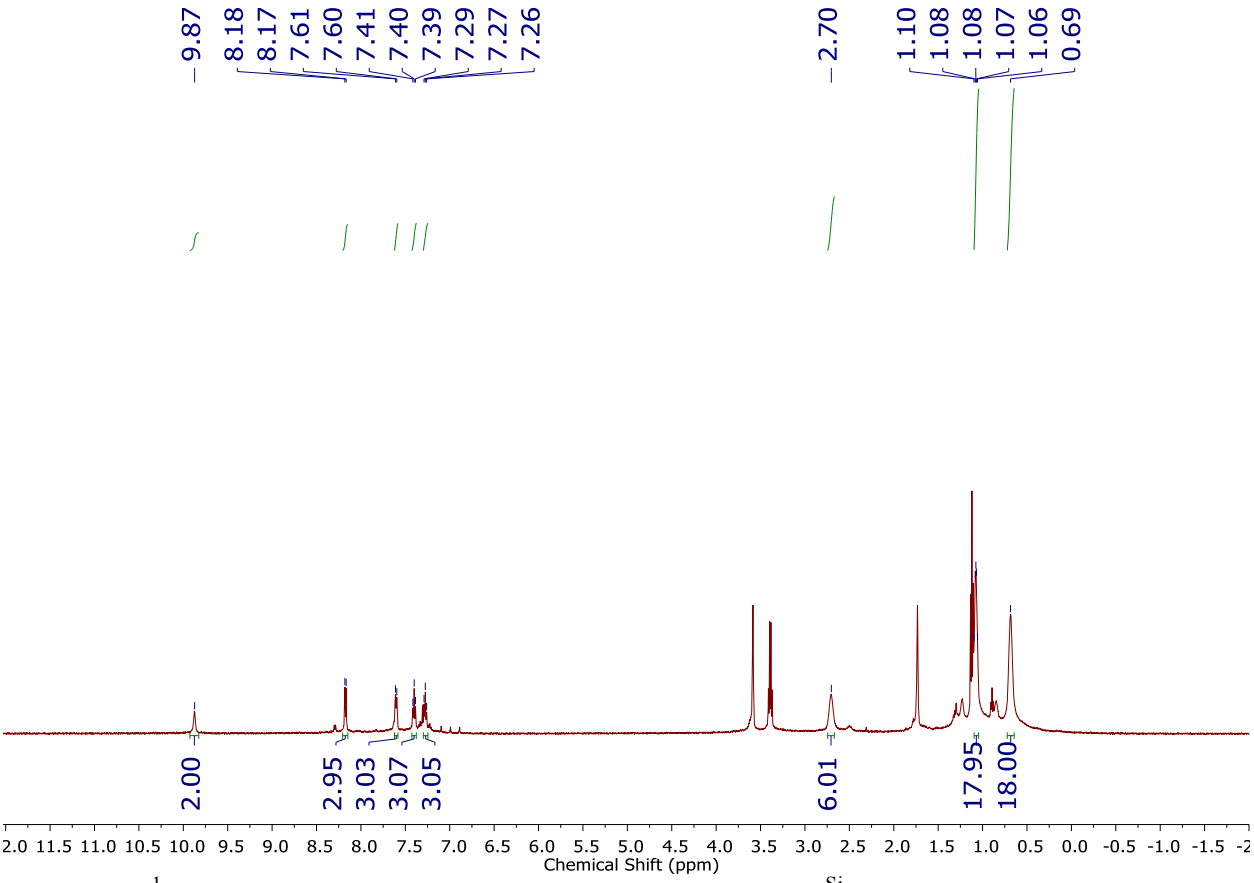

Figure S1. ^{1}H NMR spectrum (500 MHz, THF-d_8, 25 °C) of [P$_3^{Si}$Os=NNH$_2$][OTf].

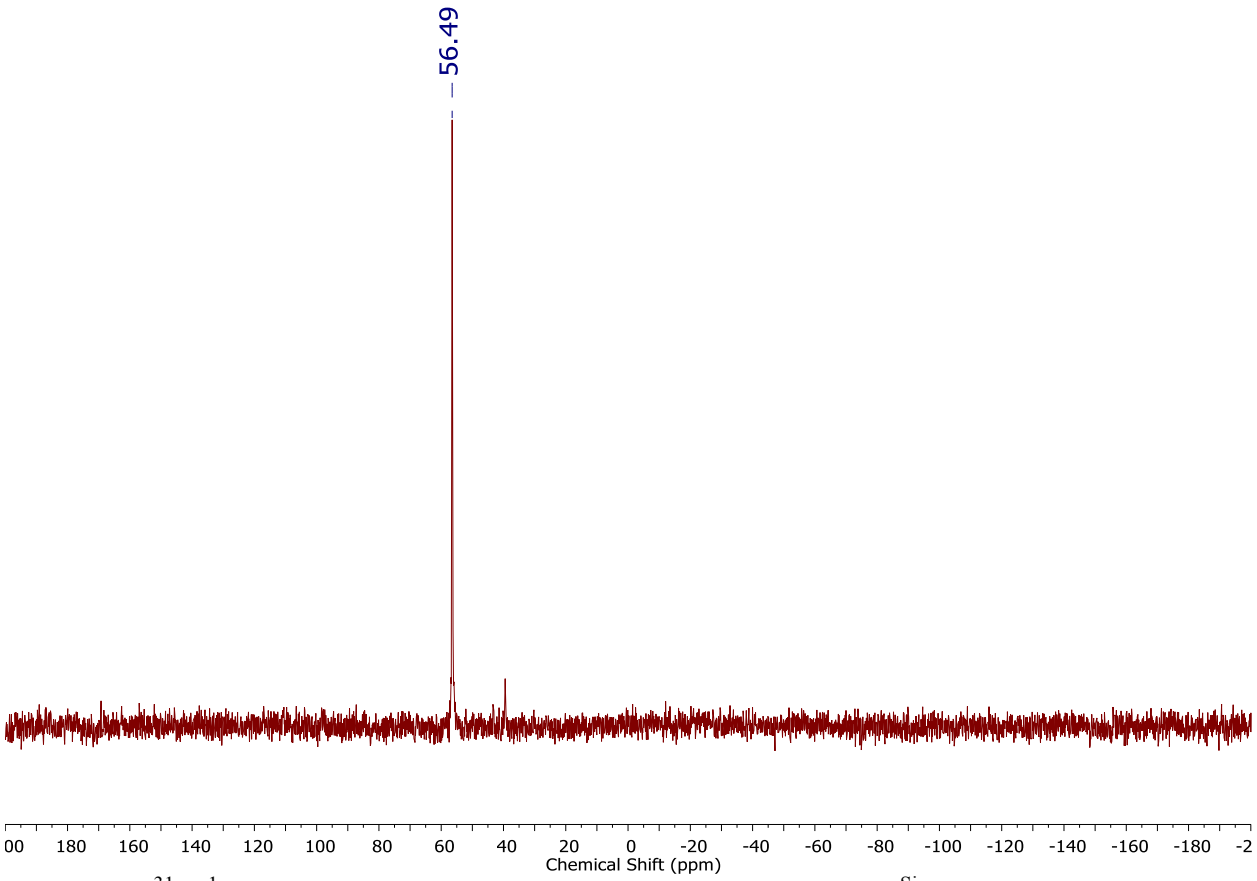

Figure S2. $^{31}P\{^{1}H\}$ NMR spectrum (202 MHz, THF-d_8, 25 °C) of $[P_3{}^{Si}Os{=}NNH_2][OTf]$.

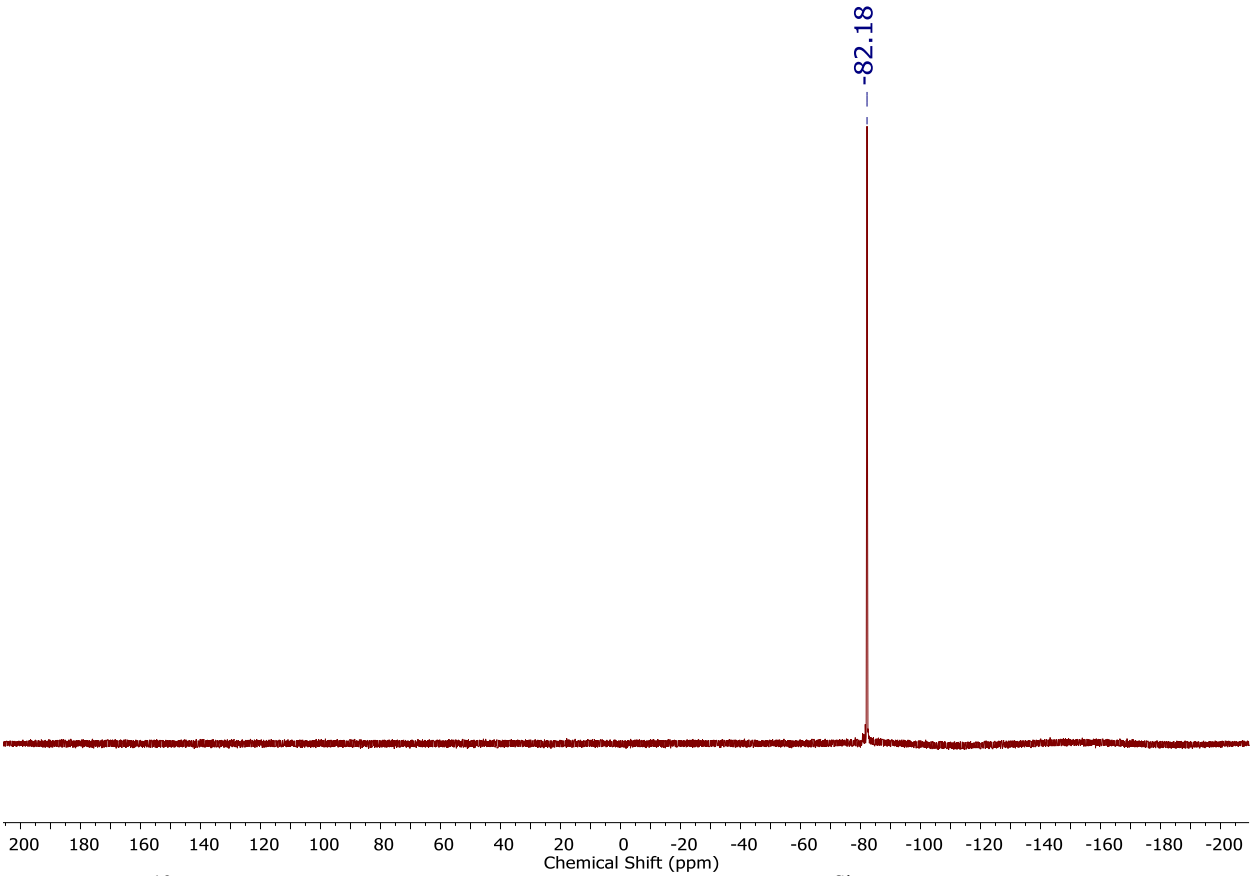

Figure S3. ^{19}F NMR spectrum (376 MHz, THF-d_8, 25 °C) of $[P_3^{Si}Os{=}NNH_2][OTf]$.

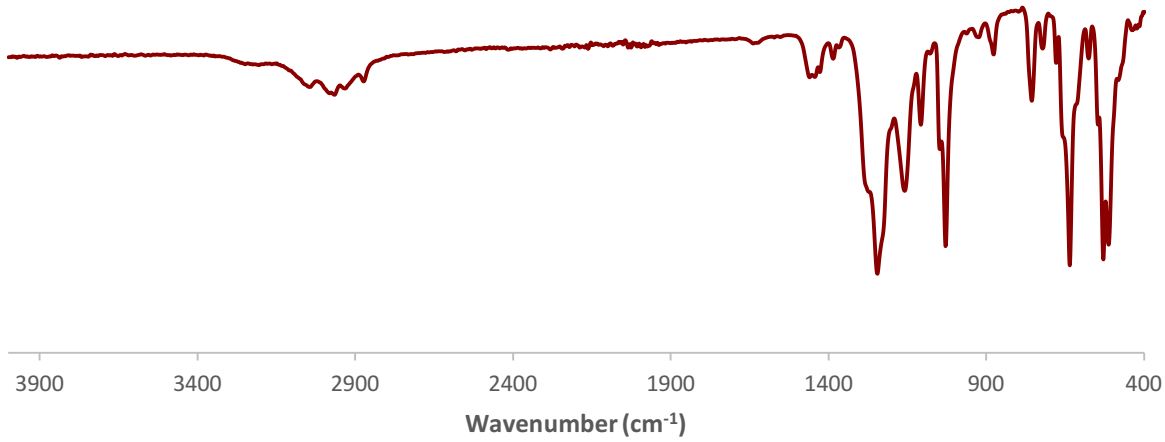

Figure S4. Solid-state IR spectrum of $[P_3^{Si}Os{=}NNH_2][OTf]$.

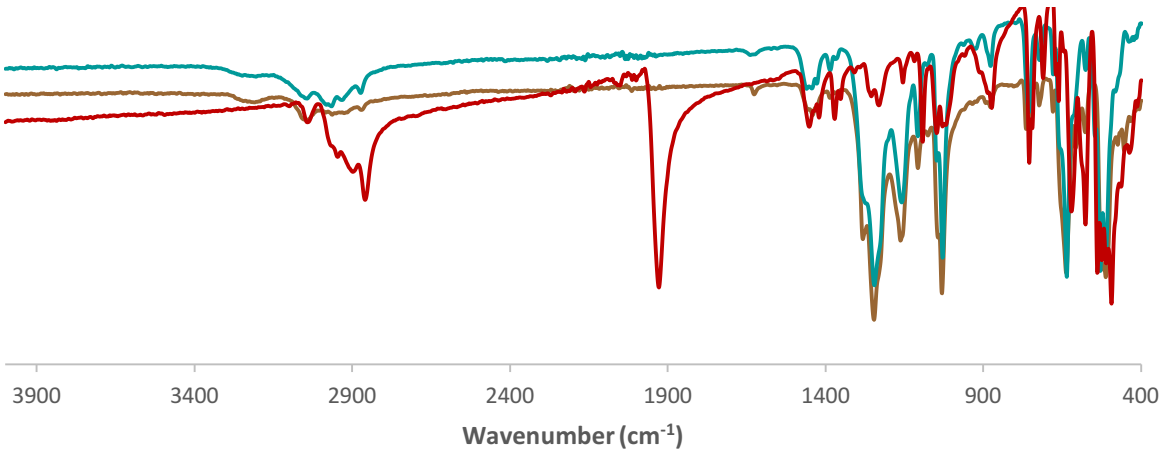

Figure S5. Overlaid solid-state IR spectra of $[K(THF)_2][P_3^{Si}Os\text{-}N_2]$ (red), $[P_3^{Si}Os{=}NNH_2][OTf]$ (teal), and $[P_3^{Si}Fe{=}NNH_2][OTf]$ (brown).

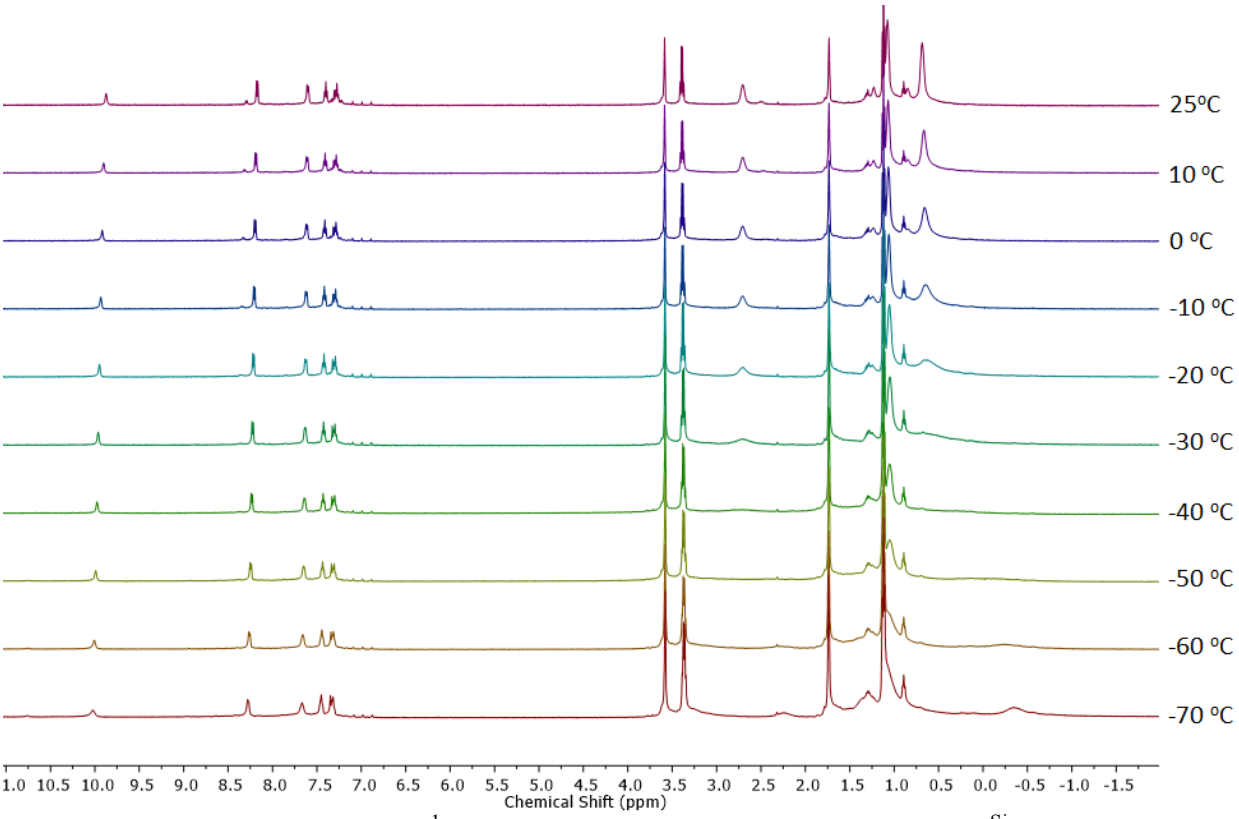

Figure S6. Variable temperature ^{1}H NMR spectra (500 MHz, THF-d_8) of $[P_3^{Si}Os{=}NNH_2][OTf]$.

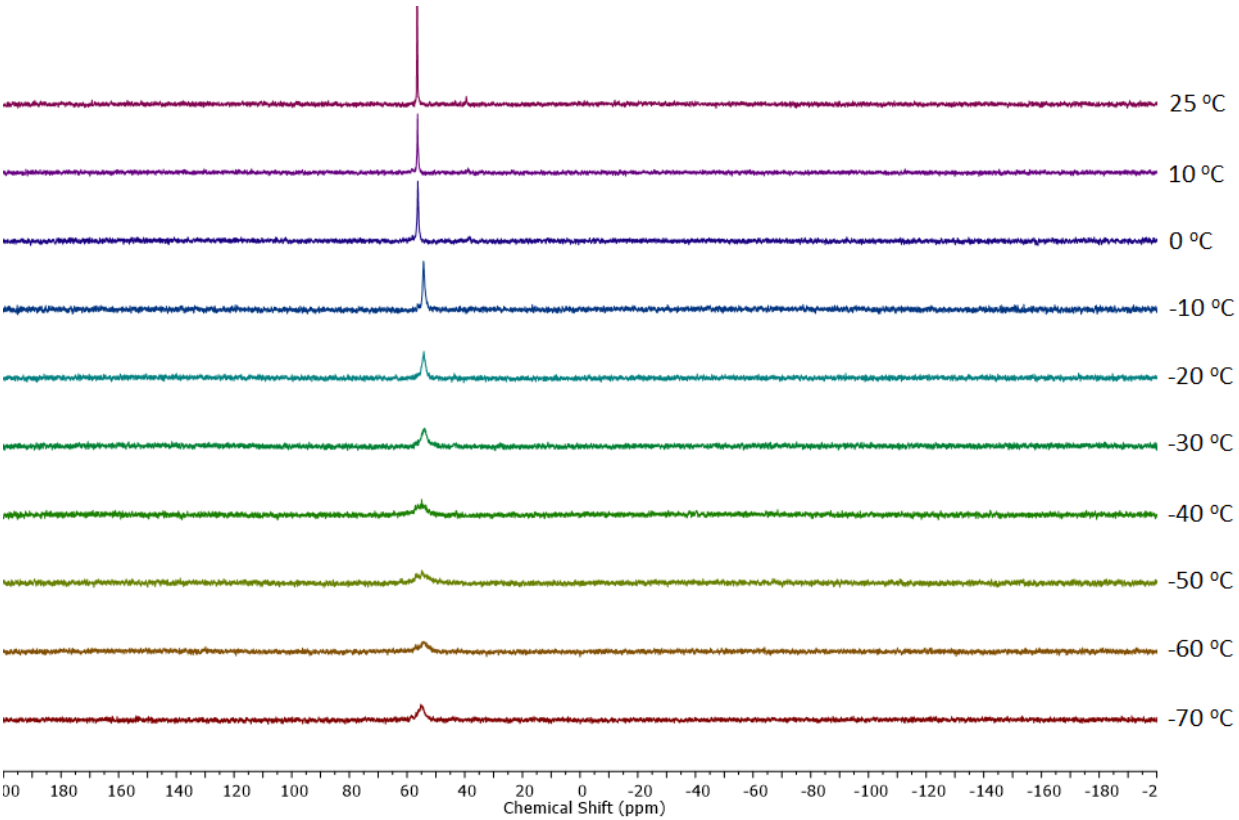

Figure S7. Variable temperature $^{31}P\{^{1}H\}$ NMR spectra (202 MHz, THF-d_8) of $[P_3^{Si}Os{=}NNH_2][OTf]$.

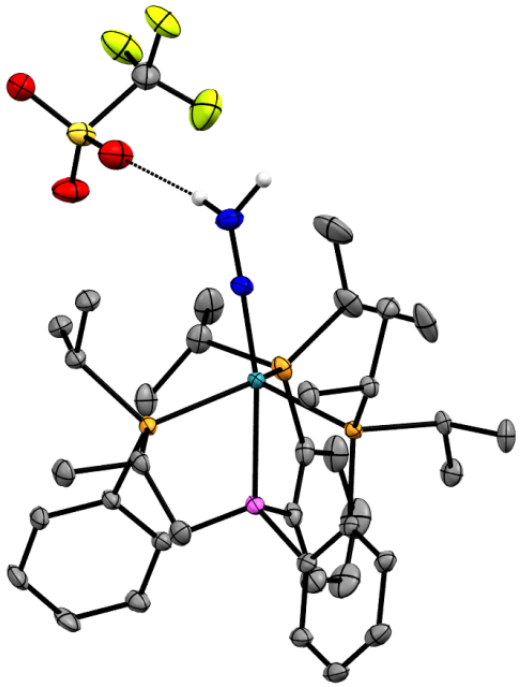

Figure S8. XRD structure of $[P_3^{Si}Os{=}NNH_2][OTf]$ with thermal ellipsoids set at 50% probability. Hydrogen atoms (except N–H's) are omitted for clarity. Color code: Os = aqua, S = yellow, P = orange, Si = pink, F = green-yellow, O = red, N = blue, C = gray, H = white.

Table S1. Comparison of the structural data of $[P_3^{Si}Os{=}NNH_2][OTf]$ with that of $[K(THF)_2][P_3^{Si}Os\text{-}N_2]$, $[P_3^{Si}Fe{=}NNH_2][OTf]$, and $P_3^{Si}Os{=}N\text{-}Ar$ (Ar = *p*-trifluoromethylphenyl).

Metric	[Os]-N_2^-	[Os]=NNH_2^+	[Fe]=NNH_2^+	[Os]=N-Ar
M–N1	1.965	1.815	1.668	1.859
N1–N2	1.136	1.271	1.273	-----
M–Si	2.339	2.440	2.344	2.408
∠Si–M–N1	179	168	171	162
∠M–N1–N2	178	176	175	-----
Σ∠P–M–P	352	346	350	346
Σ∠C–Si–C	321	324	325	323
Σ∢Nβ	-----	358	359	-----

$P_3^{Si}Os(N_2)(H)$. $P_3^{Si}Os\text{-}N_2$ (0.0145 g, 0.0176 mmol) was dissolved in 4 mL of Et_2O to give a green solution. While stirring vigorously, 166 µL of an N_2H_4 stock solution in Et_2O (10.0 µL of anhydrous N_2H_4 in 3 mL of Et_2O; 0.106 M, 1.15 equiv, 0.0202 mmol) was delivered via micropipette. After a few moments, the color of the reaction gradually changed from green to orange. The reaction was then stirred vigorously at room temperature for 1 hour before removing the Et_2O under vacuum. The remaining residue was extracted into C_6H_6, filtered through celite, and lyophilized to yield $P_3^{Si}Os(N_2)(H)$ as an aqua solid (0.0135 g, ~90% $P_3^{Si}Os(N_2)(H)$ as determined by ^1H and ^{31}P NMR spectroscopies).

******Note:*** $P_3^{Si}Os(N_2)(H)$ prepared in this fashion contains a small amount of $P_3^{Si}OsH_3$ as an impurity. Attempts to purify $P_3^{Si}Os(N_2)(H)$ were unsuccessful due to the similar solubility properties of the compounds. Other reaction conditions canvassed afforded a similar distribution of products.

^1H NMR (400 MHz, C_6D_6, 25 °C): δ(ppm) 8.25 (d, *J* = 7.4 Hz, 2H, Ar–*H*), 8.06 (d, *J* = 7.2 Hz, 1H, Ar–*H*), 7.40 (d, *J* = 6.5 Hz, 2H, Ar–*H*), 7.23–7.17 (m, 3H, Ar–*H*), 7.11 (t, *J* = 7.4 Hz, 1H, Ar–*H*), 7.04 (t, *J* = 7.5 Hz, 2H, Ar–*H*), 7.00–6.96 (t, *J* = 7.4 Hz, 1H, Ar–*H*), 2.82 (br m, 2H, C*H*$(CH_3)_2$), 2.50 (m, 2H, C*H*$(CH_3)_2$), 2.34 (m, 2H, C*H*$(CH_3)_2$), 1.33 (m, 6H, CH(C*H*$_3)_2$), 1.25 (m, 6H, CH(C*H*$_3)_2$), 1.11 (m, 6H, CH(C*H*$_3)_2$), 0.78–0.68 (m, 12H, CH(C*H*$_3)_2$), 0.59 (br s, 6H, CH(C*H*$_3)_2$), -11.18 (dt, *J* = 50 Hz, 1H, Os–*H*).

$^{31}P\{^1H\}$ NMR (162 MHz, C_6D_6, 25 °C): δ(ppm) 38.3 (br, 2P), 36.1 (m, 1P).

$^{31}P\{^1H\}$ NMR (202 MHz, toluene-d_8, -78 °C): δ(ppm) 56.5 (d, 1P), 39.6 (s, 1P), 28.8 (d, 1P).

IR (thin film from C_6D_6): ν(NN) = 2098 cm^{-1}.

E.A.: No combustion analysis data was obtained due to the lability of the dinitrogen ligand under vacuum.

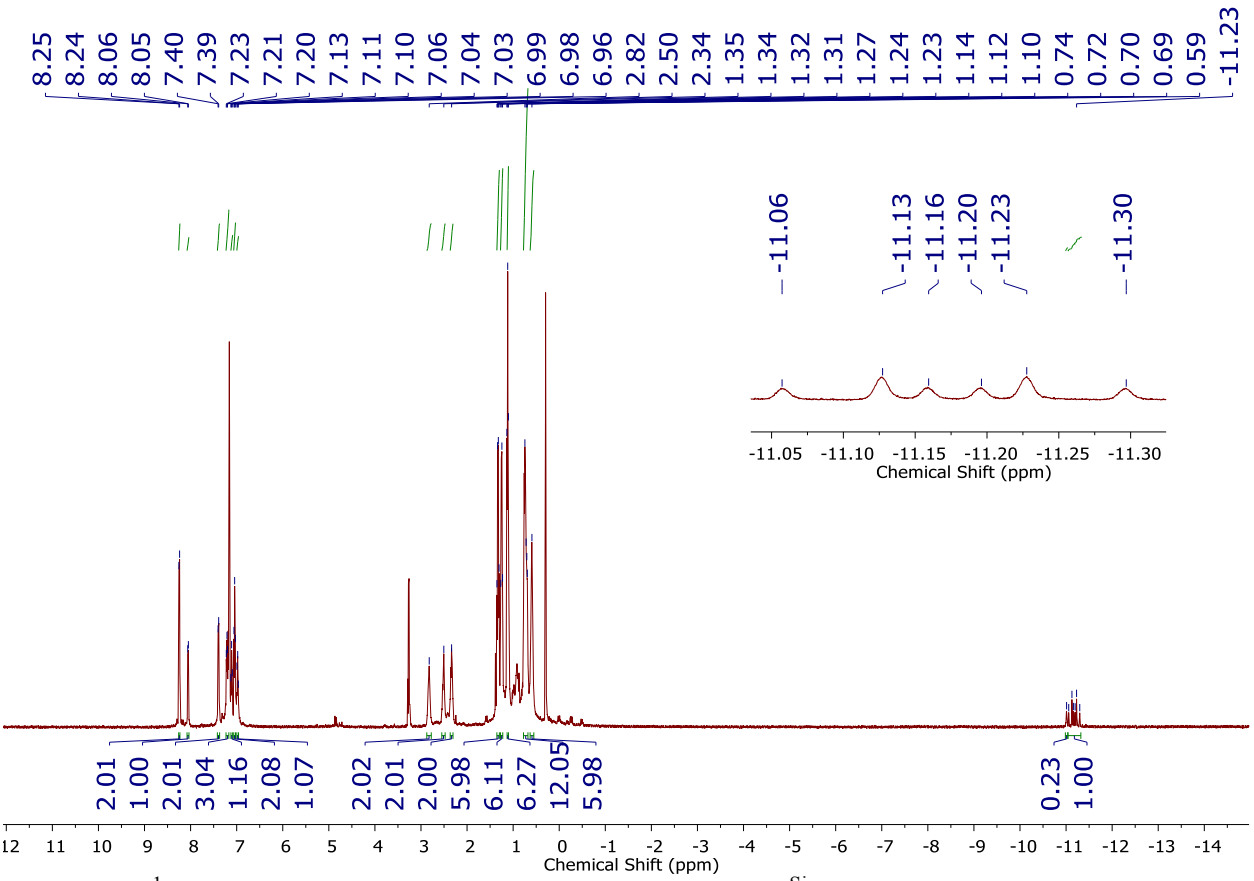

Figure S9. ^{1}H NMR spectrum (400 MHz, C_6D_6, 25 °C) of $P_3^{Si}Os(N_2)(H)$. The hydride resonance at -11.01 ppm corresponds to a small amount of $P_3^{Si}OsH_3$ present as an impurity.

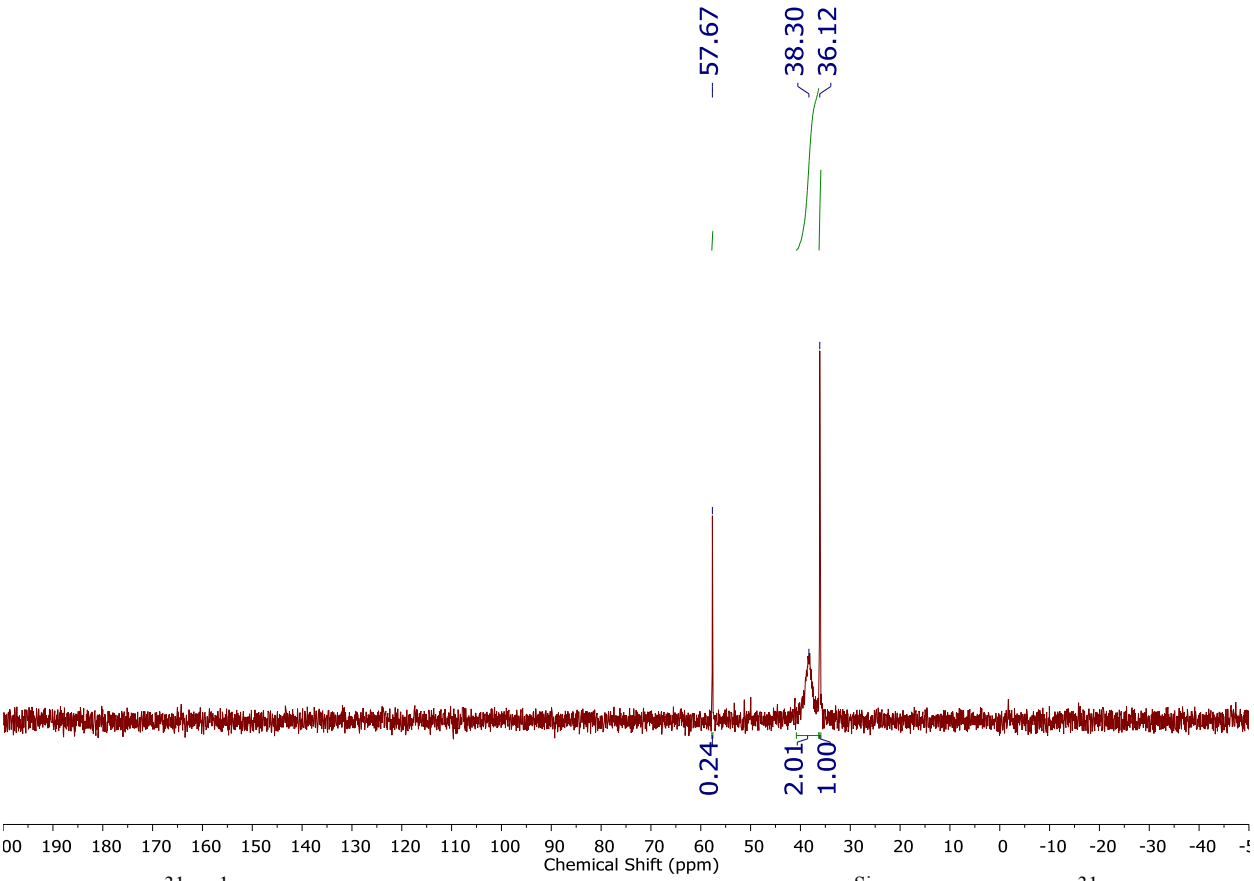

Figure S10. $^{31}P\{^{1}H\}$ NMR spectrum (162 MHz, C_6D_6, 25 °C) of $P_3{}^{Si}Os(N_2)(H)$. The ^{31}P resonance at 57.7 ppm corresponds to a small amount of $P_3{}^{Si}OsH_3$ present as an impurity.

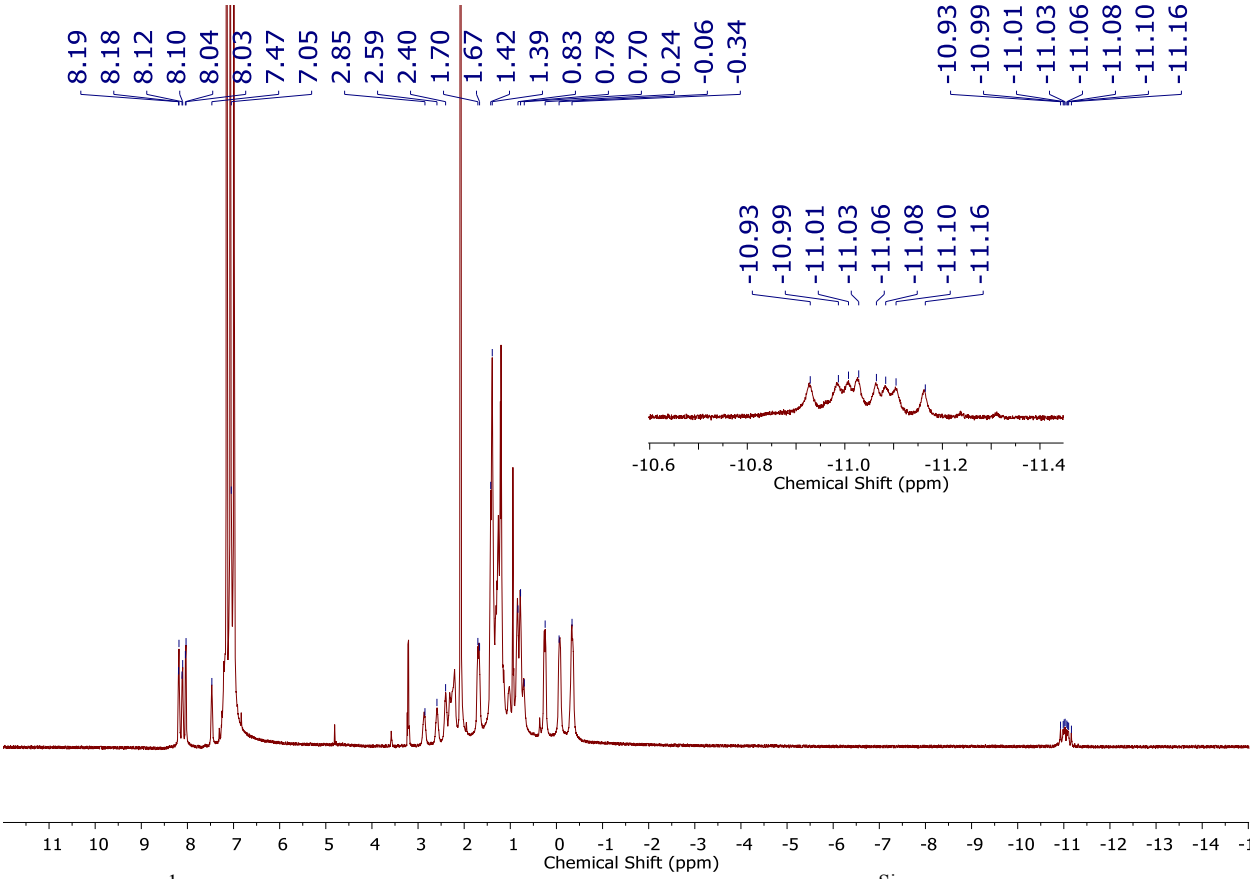

Figure S11. ^{1}H NMR spectrum (500 MHz, toluene-d_8, -78 °C) of $P_3^{Si}Os(N_2)(H)$. There is a small amount of $P_3^{Si}OsH_3$ present as an impurity.

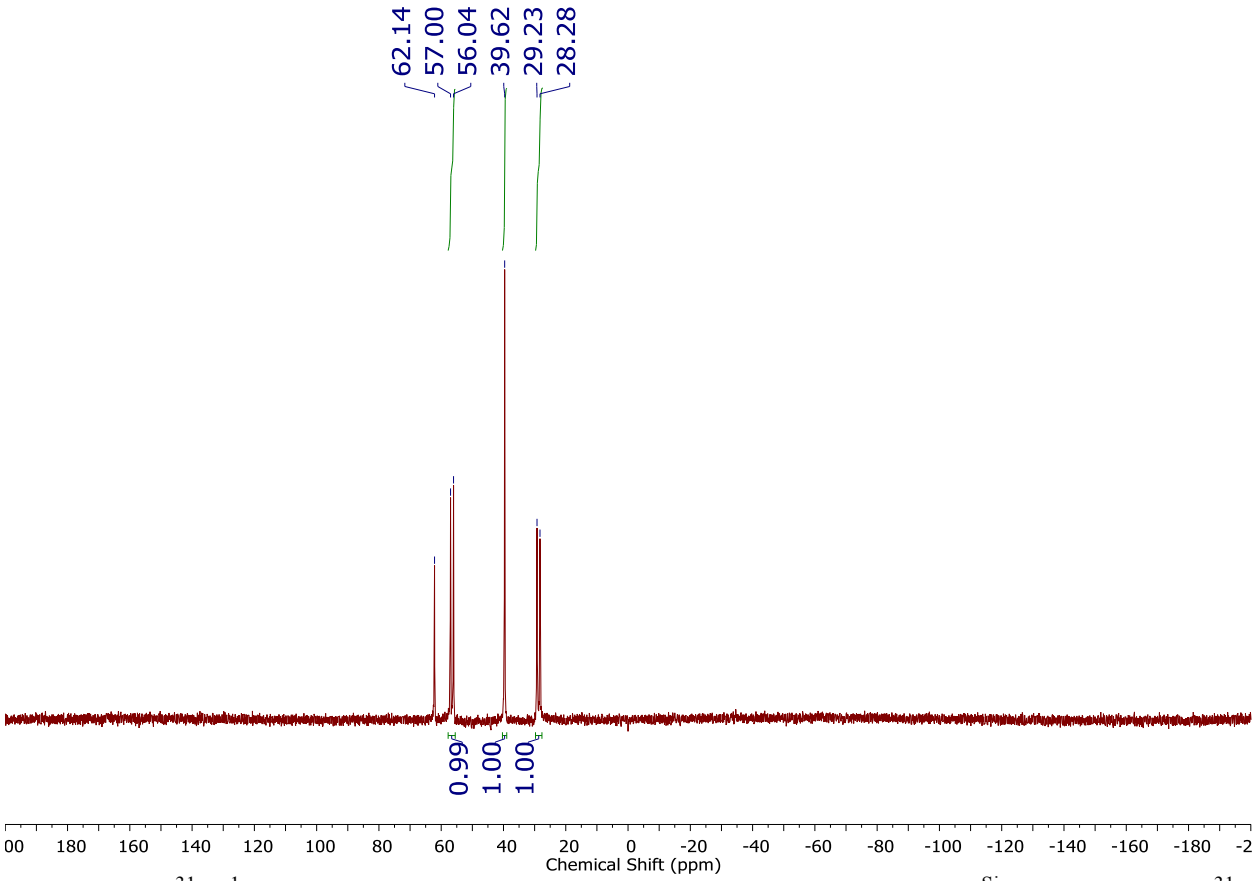

Figure S12. $^{31}P\{^{1}H\}$ NMR spectrum (202 MHz, toluene-d_8, -78 °C) of $P_3^{Si}Os(N_2)(H)$. The ^{31}P resonance at 62.1 ppm corresponds to a small amount of $P_3^{Si}OsH_3$ present as an impurity.

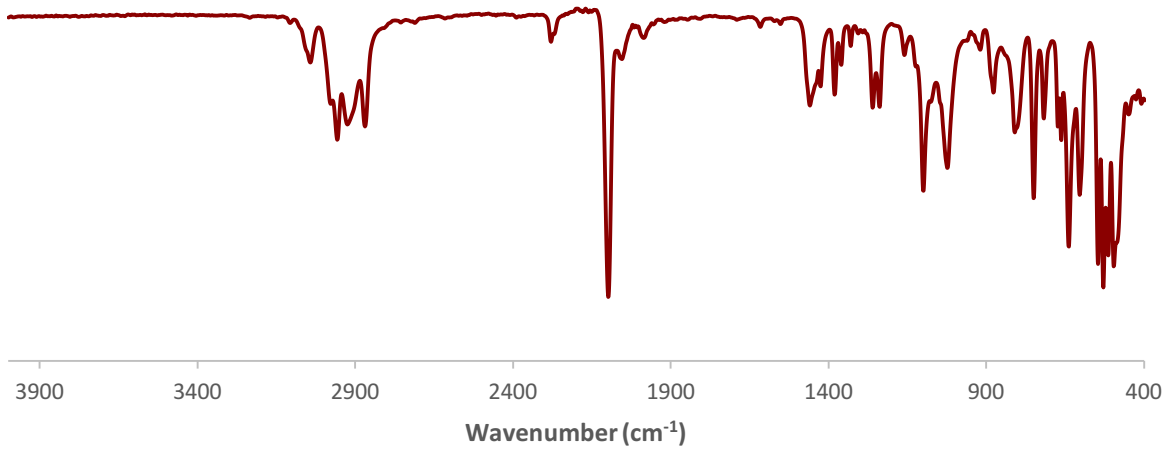

Figure S13. IR spectrum of $P_3^{Si}Os(N_2)(H)$ deposited as a thin film from C_6D_6.

$P_3^{Si}OsH_3$. P_3^{Si}Os-Cl (0.0375 g, 0.0440 mmol) was dissolved in 3 mL of THF to give a brown solution. $LiEt_3BH$ (1.0 M in THF, 3.00 equiv, 0.135 mmol, 135 µL) was then added at room temperature via micropipette. The reaction was stirred vigorously for two days at room temperature, after which the color of the reaction had changed from brown to yellow. The THF

was removed under vacuum, and the product was extracted into pentane (3 x 3 mL), filtered through celite, and dried under vacuum to yield $P_3^{Si}OsH_3$ as an off-white solid (0.0348 g, 0.0434 mmol) in 96% yield. Crystals suitable for XRD were obtained by slow concentration of a C_6H_6 solution of $P_3^{Si}OsH_3$ in a closed vessel containing HMDSO.

Alternatively, $P_3^{Si}OsH_3$ can be synthesized by addition of an atmosphere of H_2(g) to a degassed solution of $P_3^{Si}Os\text{-}N_2$ or $P_3^{Si}Os(N_2)(H)$ and stirring vigorously at room temperature. The reaction is shown to go to completion after 4 days or 12 hours, respectively, as determined by NMR and IR spectroscopies.

^{1}H NMR (400 MHz, C_6D_6, 25 ^{o}C): δ(ppm) 8.24 (d, J = 7.2 Hz, 3H, Ar–*H*), 7.25–7.18 (m, 6H, Ar–*H*), 7.01 (t, J = 7.4 Hz, 3H, Ar–*H*), 2.41 (br s, 6H, C*H*(CH_3)$_2$), 1.05–0.80 (m, 24H, CH(C*H*$_3$)$_2$), 0.28 (br s, 12H, CH(C*H*$_3$)$_2$), -11.01 (t, J = 3.5 Hz, 3H, Os–*H*).

^{31}P{^{1}H} NMR (162 MHz, C_6D_6, 25 ^{o}C): δ(ppm) 57.6 (s).

^{1}H NMR (500 MHz, toluene-d_8, -78 ^{o}C): δ(ppm) δ 8.18 (d, J = 7.2 Hz, 3H, Ar–*H*), 7.25 (t, J = 7.0 Hz, 3H, Ar–*H*), 7.15–6.99 (remaining Ar–*H* signals overlap with toluene peaks), 2.40 (br s, 3H, C*H*(CH_3)$_2$), 2.21 (br s, 3H, C*H*(CH_3)$_2$), 1.37 (br s, 9H, CH(C*H*$_3$)$_2$), 1.02 (br s, 9H, CH(C*H*$_3$)$_2$), 0.71 (br s, 9H, CH(C*H*$_3$)$_2$), -0.32 (br s, 9H, CH(C*H*$_3$)$_2$), -10.79 – -11.18 (m, 3H, Os–*H*).

^{1}H{^{31}P} NMR (500 MHz, toluene-d_8, -78 ^{o}C): δ(ppm) δ 8.18 (d, J = 7.4 Hz, 3H, Ar–*H*), 7.25 (t, J = 6.7 Hz, 3H, Ar–*H*), 7.15–6.99 (remaining Ar–*H* signals overlap with toluene peaks), 2.40 (br m, 3H, C*H*(CH_3)$_2$), 2.21 (br m, 3H, C*H*(CH_3)$_2$), 1.38 (br s, 9H, CH(C*H*$_3$)$_2$), 1.02 (br s, 9H, CH(C*H*$_3$)$_2$), 0.71 (br s, 9H, CH(C*H*$_3$)$_2$), -0.32 (br s, 9H, CH(C*H*$_3$)$_2$), -10.37 (s, 3H, Os–*H*).

^{31}P{^{1}H} NMR (202 MHz, toluene-d_8, -78 ^{o}C): δ(ppm) 62.1 (s).

^{31}P NMR (202 MHz, toluene-d_8, -78 ^{o}C): δ(ppm) 62.2 (br s).

IR (thin film from C_6D_6): ν(Os–H) = 1985 cm^{-1}.

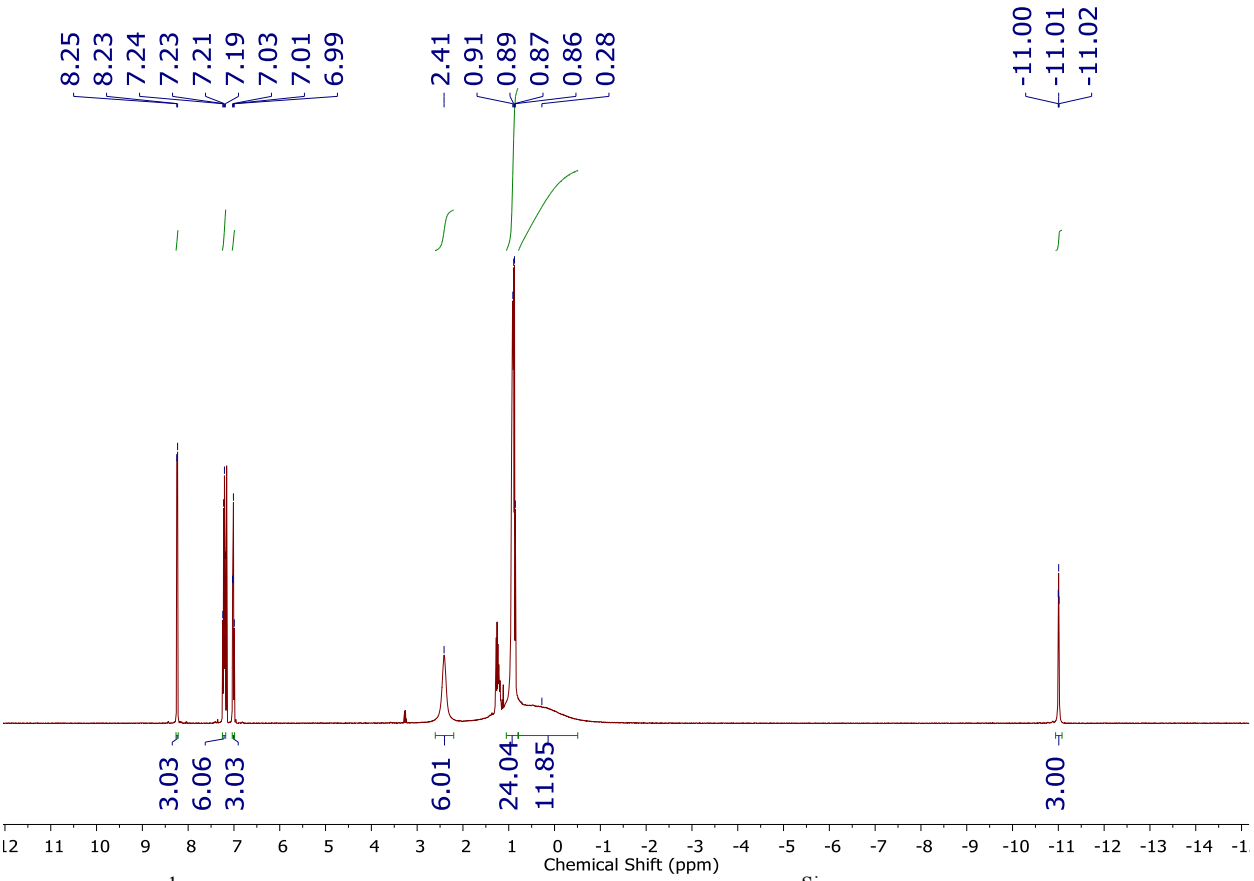

Figure S14. ^{1}H NMR spectrum (400 MHz, C_6D_6, 25 °C) of $P_3{}^{Si}OsH_3$.

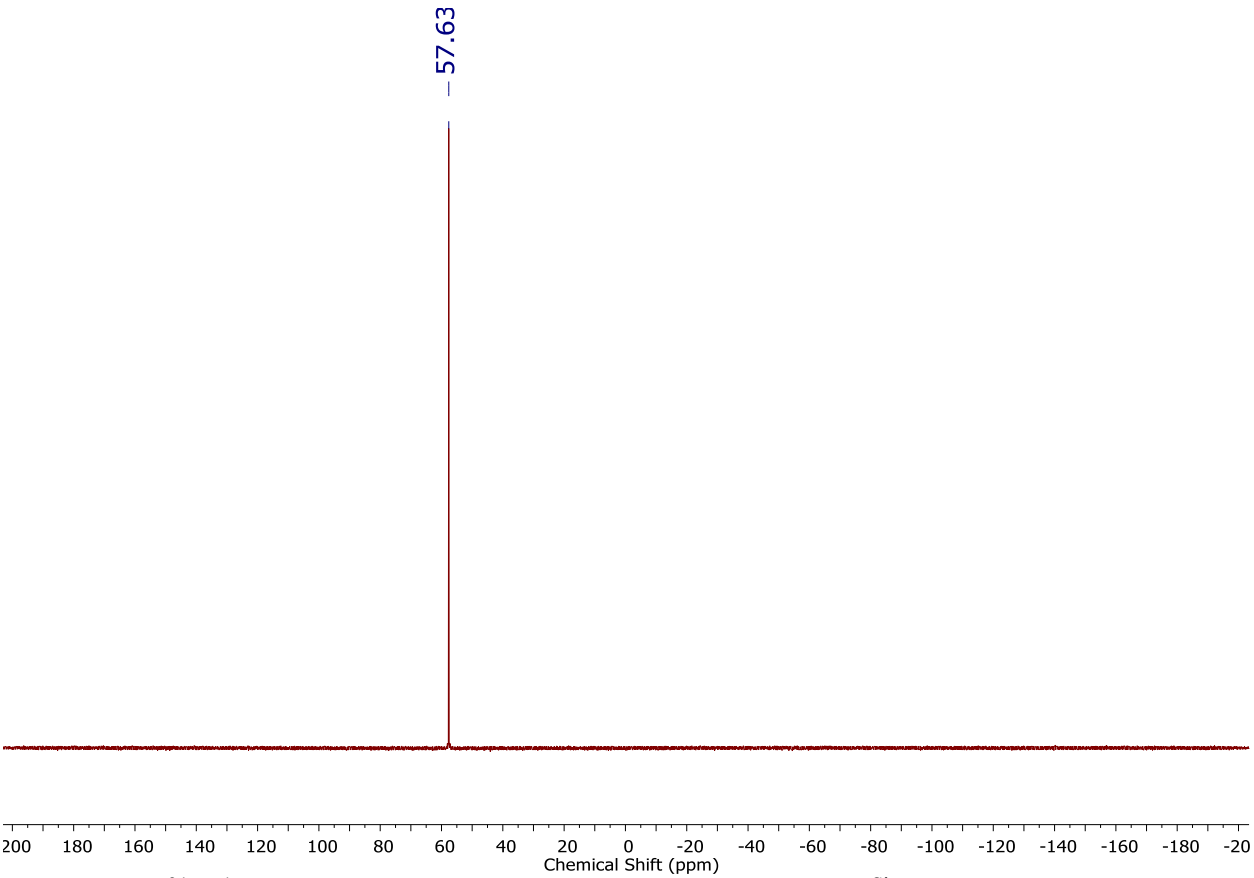

Figure S15. $^{31}P\{^{1}H\}$ NMR spectrum (162 MHz, C_6D_6, 25 °C) of $P_3{}^{Si}OsH_3$.

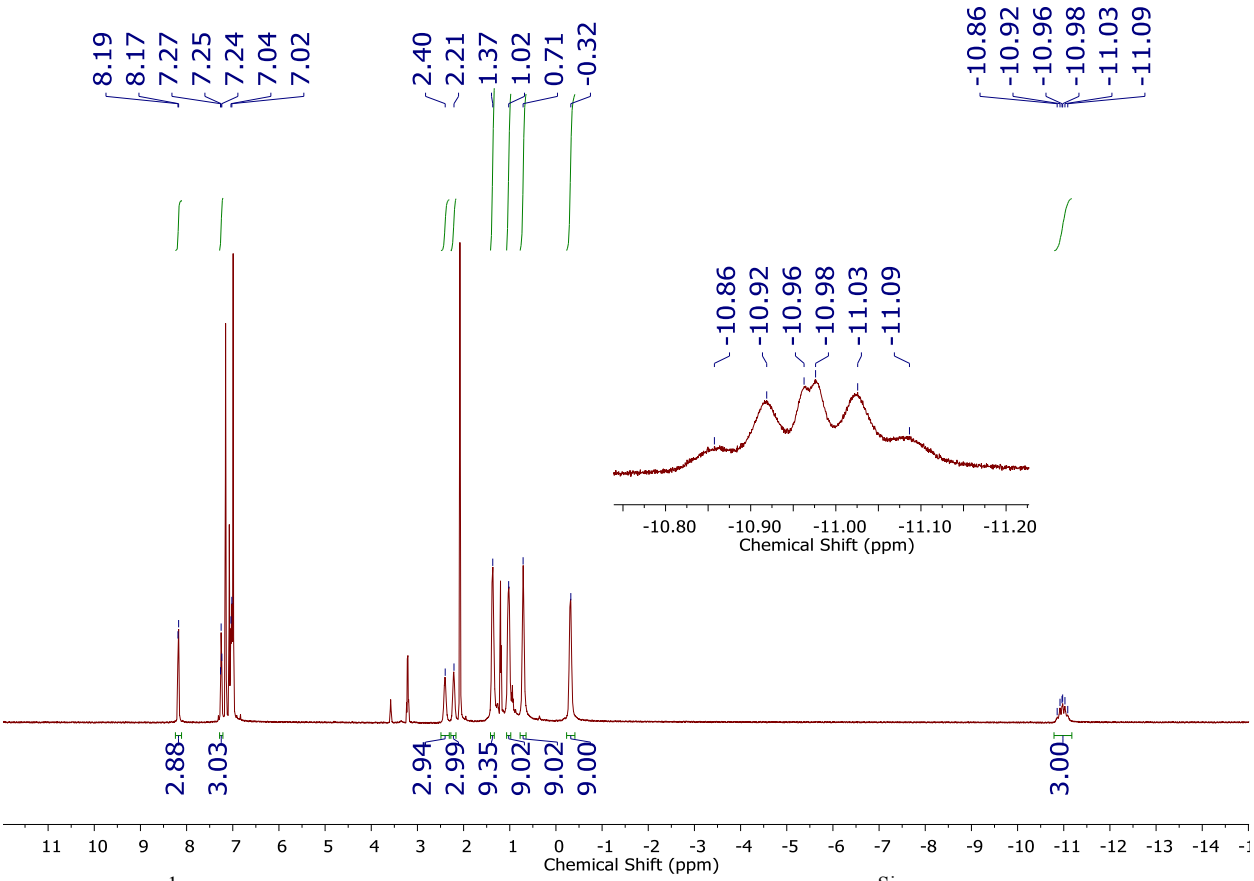

Figure S16. ^{1}H NMR spectrum (500 MHz, toluene-d_8, -78 °C) of $P_3{}^{Si}OsH_3$.

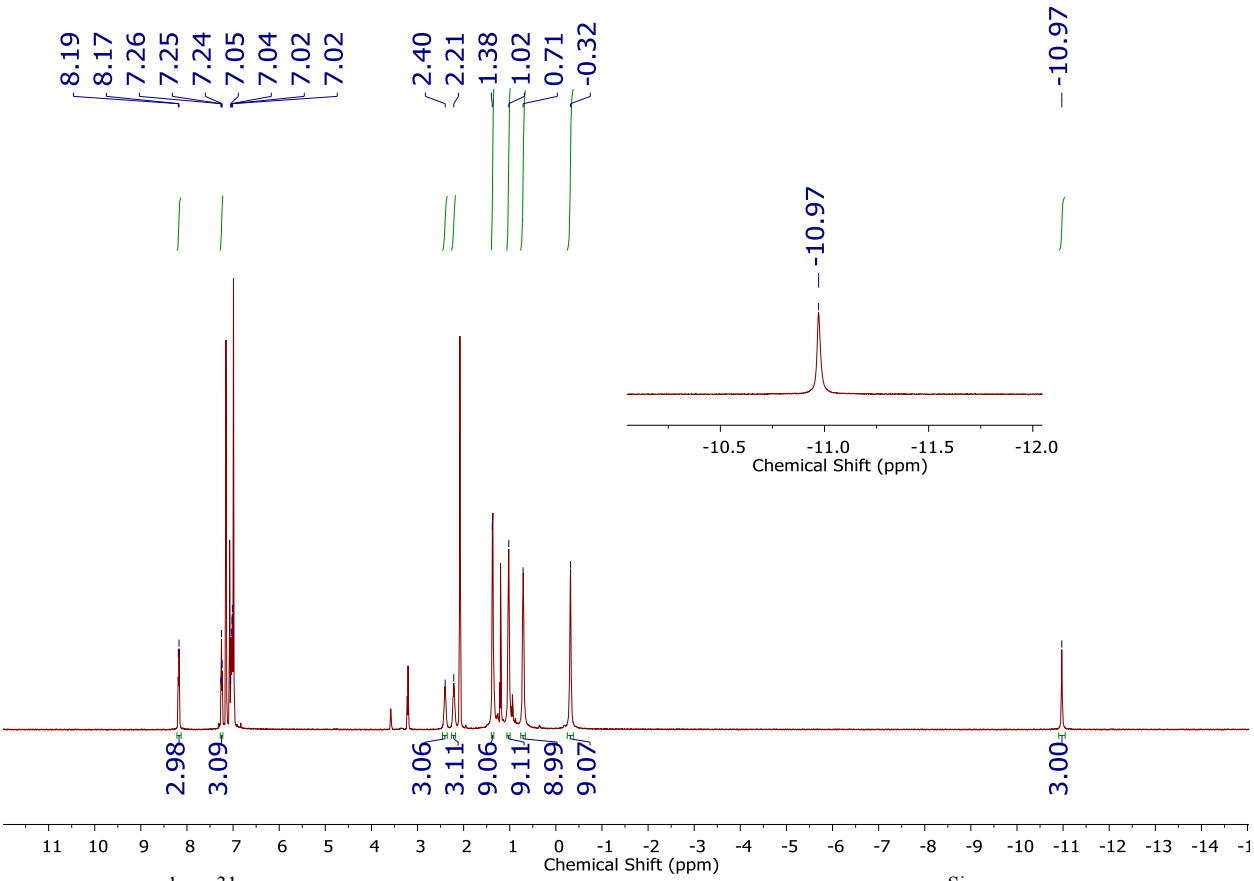

Figure S17. $^{1}H\{^{31}P\}$ NMR spectrum (500 MHz, toluene-d_8, -78 °C) of $P_3{}^{Si}OsH_3$.

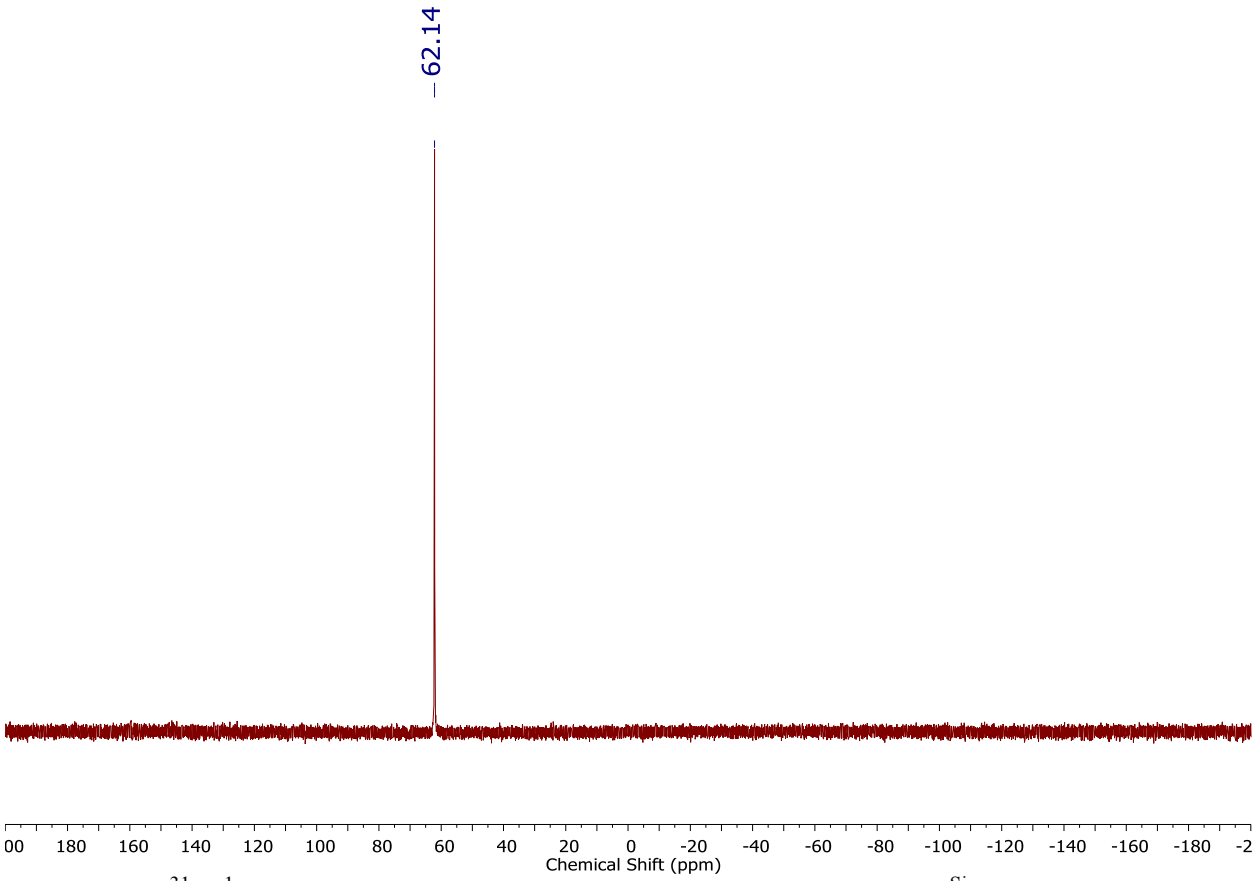

Figure S18. $^{31}P\{^{1}H\}$ NMR spectrum (202 MHz, toluene-d_8, -78 °C) of $P_3{}^{Si}OsH_3$.

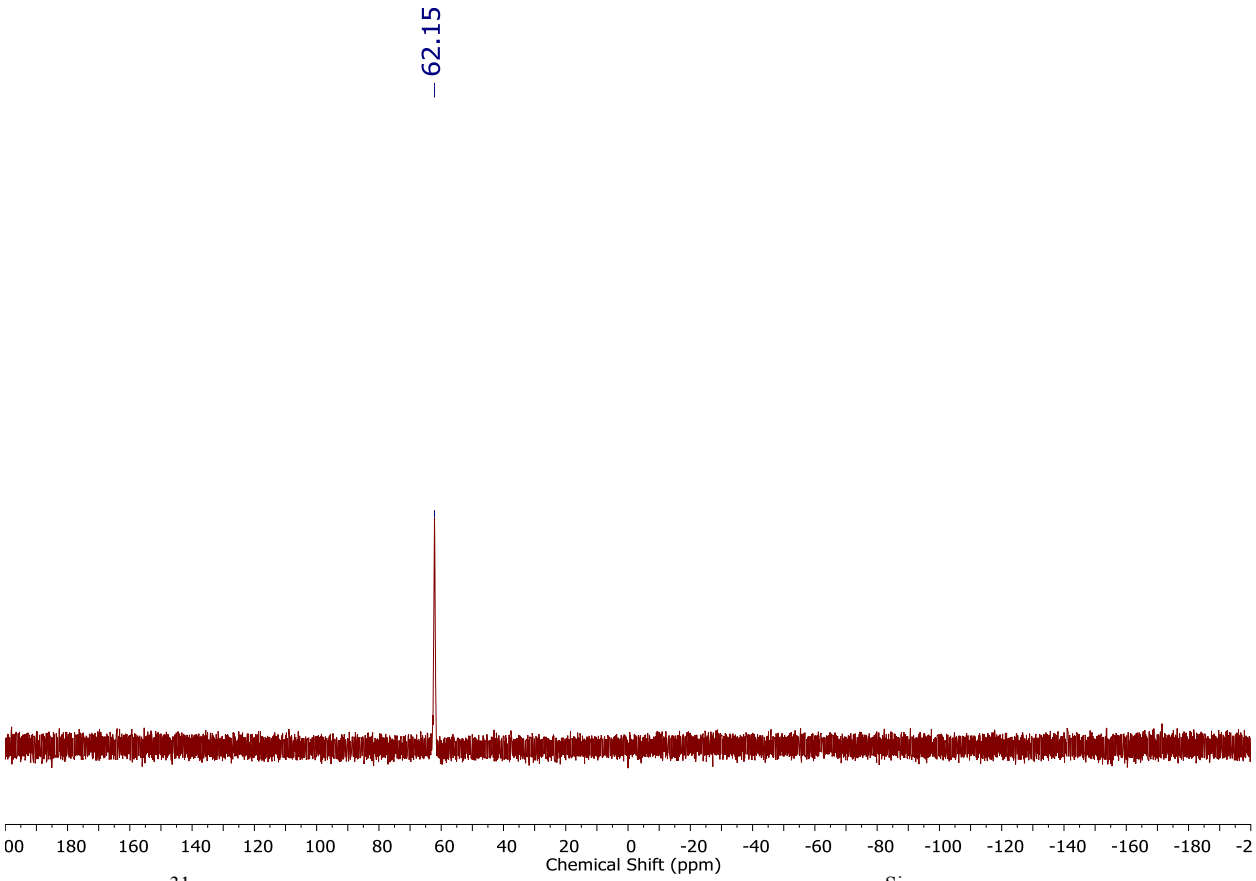

Figure S19. ^{31}P NMR spectrum (202 MHz, toluene-d_8, -78 °C) of $P_3{}^{Si}OsH_3$.

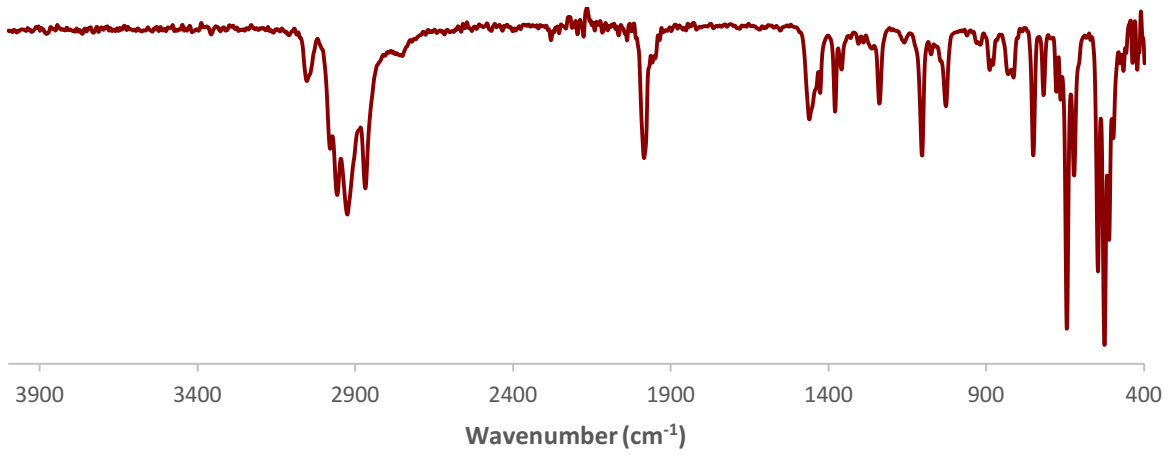

Figure S20. IR spectrum of $P_3{}^{Si}OsH_3$ deposited as a thin film from C_6D_6.

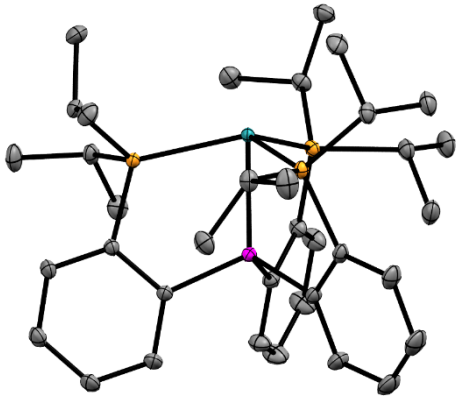

Figure S21. XRD structure of $P_3^{Si}OsH_3$ with thermal ellipsoids set at 50% probability. Hydrogen atoms are omitted for clarity. The terminal hydride ligand could not be located in the Fourier difference map. Color code: Os = aqua, P = orange, Si = pink, C = gray.

$P_3^{Si}RuH_3$. P_3^{Si}Ru-Cl (0.0200 g, 0.0269 mmol) was dissolved in 2 mL of THF to give a red-brown solution. $LiEt_3BH$ (1.0 M in THF, 3.00 equiv, 0.806 mmol, 80.6 µL) was then added at room temperature via micropipette. The reaction was stirred vigorously for two days at room temperature, after which the color of the reaction had changed from red-brown to yellow. The THF was removed under vacuum, and the product was extracted into pentane (3 x 3 mL), filtered through celite, and dried under vacuum to yield $P_3^{Si}RuH_3$ (0.0159 g, 0.0223 mmol) in 83% yield. While no combustion analysis data or XRD structure was obtained, $P_3^{Si}RuH_3$ features a nearly identical ^{1}H NMR spectrum to that of $P_3^{Si}OsH_3$.

^{1}H NMR (400 MHz, C_6D_6, 25 ^{o}C): δ(ppm) 8.16 (d, *J* = 7.3 Hz, 3H, Ar–*H*), 7.20–7.18 (m, 6H, Ar–*H*), 7.01 (t, *J* = 7.3 Hz, 3H, Ar–*H*), 2.31 (br s, 6H, C*H*$(CH_3)_2$), 0.91 (br s, 18H, CH(C*H*$_3)_2$), 0.57 (br s, 18H, CH(C*H*$_3)_2$), -8.44 (s, 3H, Ru–*H*).

^{31}P{^{1}H} NMR (162 MHz, C_6D_6, 25 ^{o}C): δ(ppm) 92.9 (s).

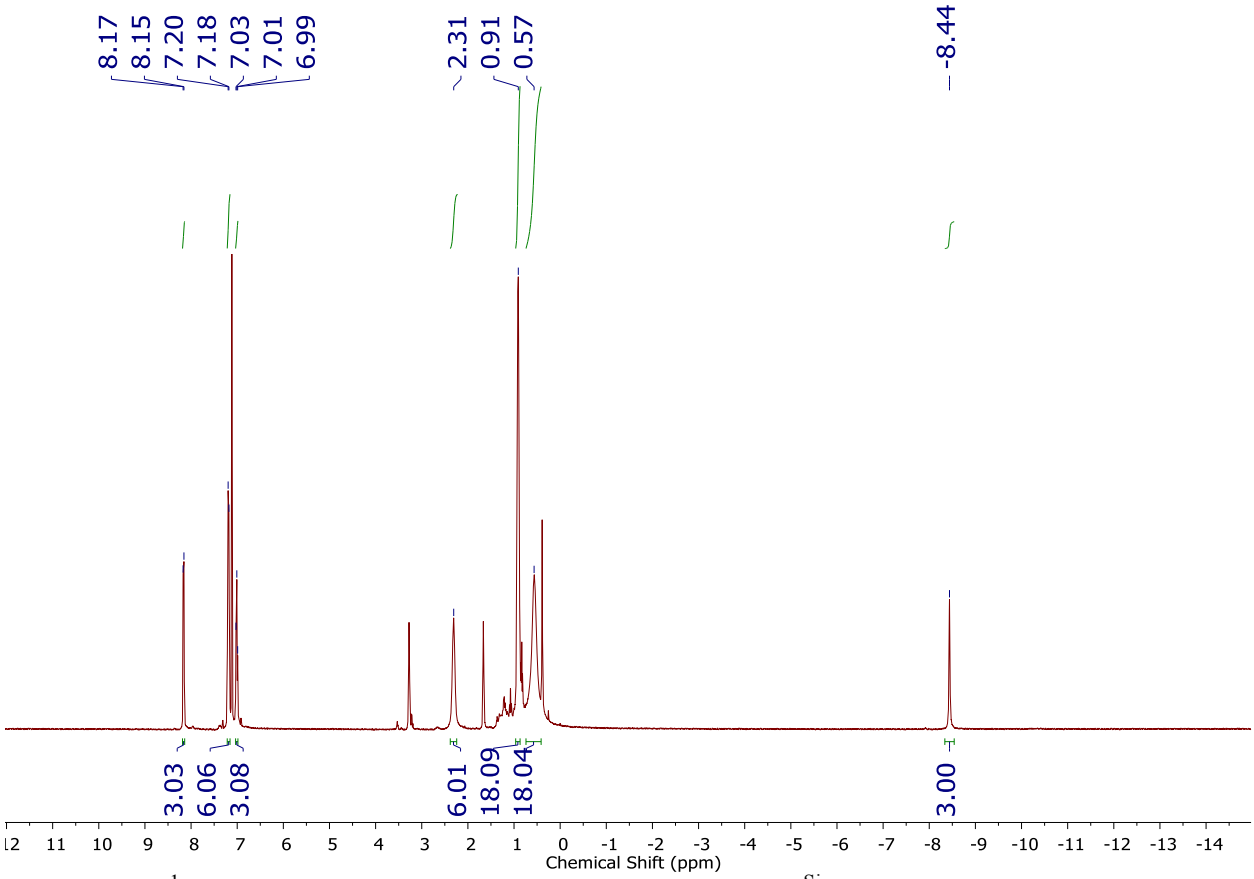

Figure S22. ^{1}H NMR spectrum (400 MHz, C_6D_6, 25 °C) of $P_3{}^{Si}RuH_3$.

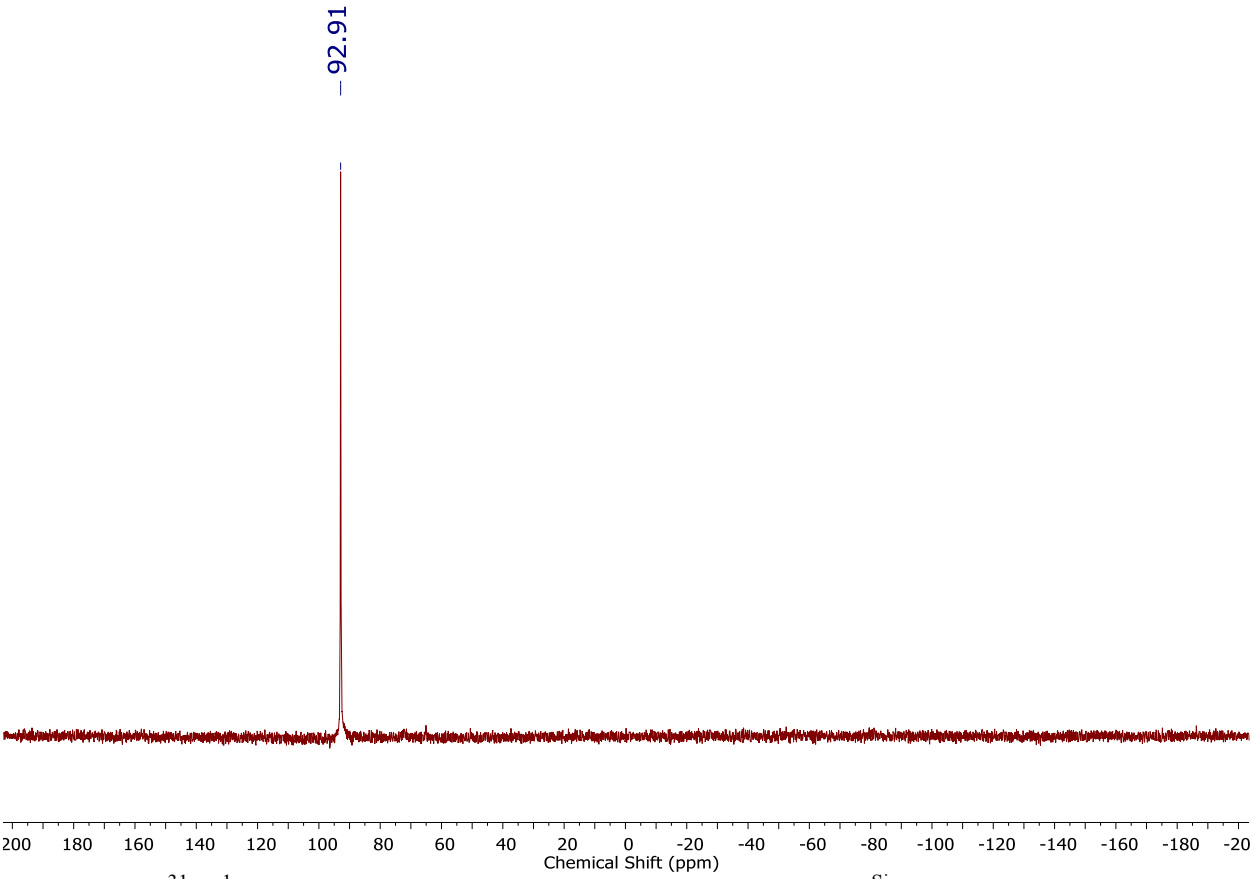

Figure S23. $^{31}P\{^{1}H\}$ NMR spectrum (162 MHz, C_6D_6, 25 °C) of $P_3{}^{Si}RuH_3$.

Treatment of $[K(THF)_2][P_3{}^{Si}Os\text{-}N_2]$ with 10 equiv $HBAr^F{}_4$ and 12 equiv KC_8: In the glovebox, $[K(THF)_2][P_3{}^{Si}Os\text{-}N_2]$ (0.0088 g, $8.7x10^{-3}$ mmol) was weighed out into a 20 mL scintillation vial, equipped with a stir bar, and cooled to 77 K inside the coldwell chilled with an external liquid nitrogen bath. 1 mL of Et_2O was added dropwise to the vial and allowed to freeze. A solution of $HBAr^F{}_4$ (10 equiv, 0.087 mmol, 0.088 g) in Et_2O (1 mL) was then layered dropwise. Residual acid was dissolved in Et_2O (0.5 mL) and added subsequently. This was allowed to chill in the coldwell until the contents of the vial were frozen. Finally, KC_8 (12 equiv. 0.10 mmol, 0.014 g) was transferred as a suspension in Et_2O (1 mL) to the reaction vial. The vial was then sealed and its contents were cooled until the mixture was again frozen.

After thawing the mixture by replacing the liquid nitrogen bath with a dry ice/acetone bath (-78 °C), the reaction was stirred for 1 hour at -78 °C followed by 45 minutes at room temperature. The reaction mixture was then filtered through glass filter paper into a 20 mL vial containing triphenylphosphine (3.0 equiv, 0.026 mmol, 0.0068 g) as a ^{31}P NMR internal standard, concentrated to ½ the original volume, and transferred to an NMR tube. The integration of the ^{31}P resonances suggested the formation of $P_3{}^{Si}Os(N_2)(H)$ and $P_3{}^{Si}OsH_3$ in approximately 32% yield and 48% yield, respectively. The NMR solution was then transferred to a 20 mL vial in the glovebox, concentrated, redissolved in C_6D_6, and analyzed by ^{1}H and ^{31}P NMR spectroscopies. The data obtained matched the data reported above.

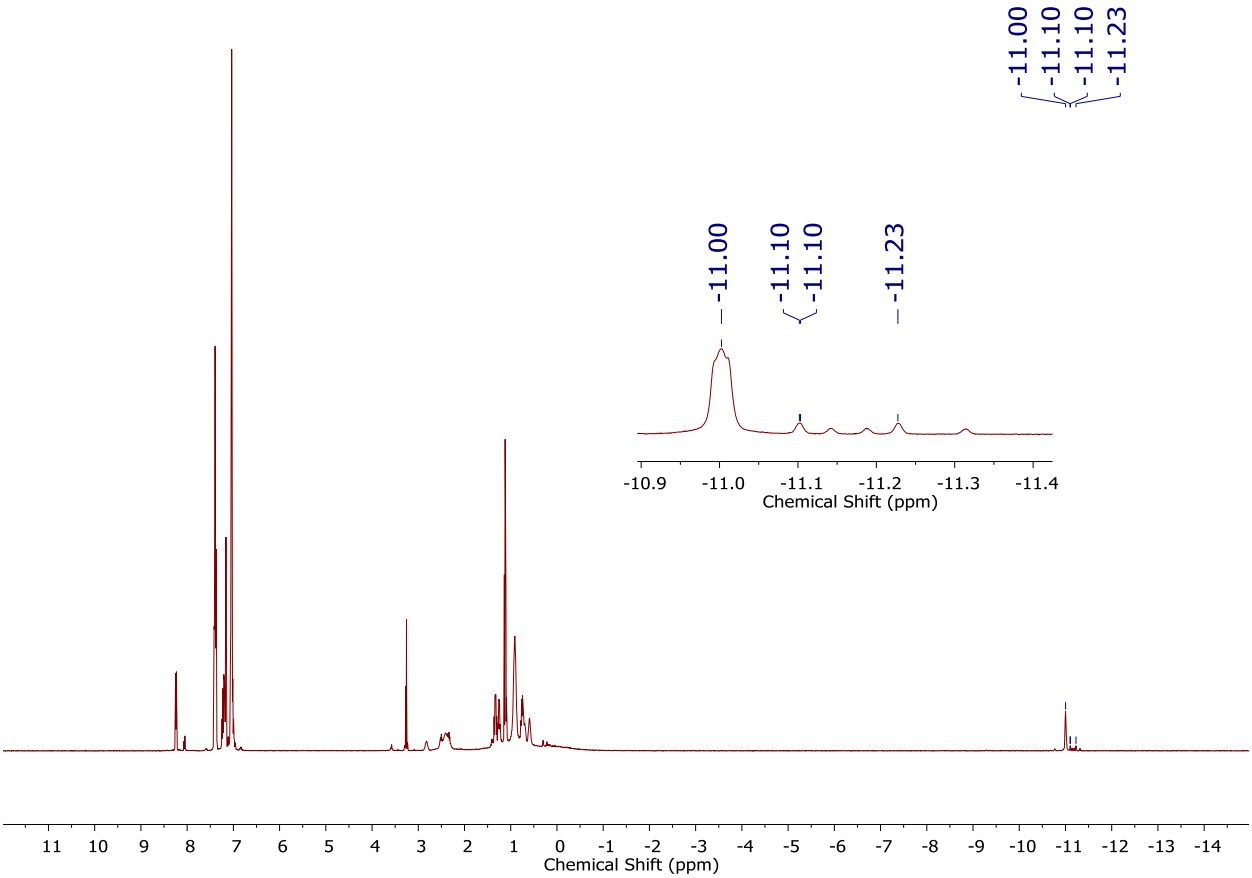

Figure S24. ^{1}H NMR spectrum (400 MHz, C_6D_6, 25 °C) for the addition of 10 equiv $HBAr^{F}_{4}$ and 12 equiv KC_8 to $[K(THF)_2][P_3{}^{Si}Os\text{-}N_2]$.

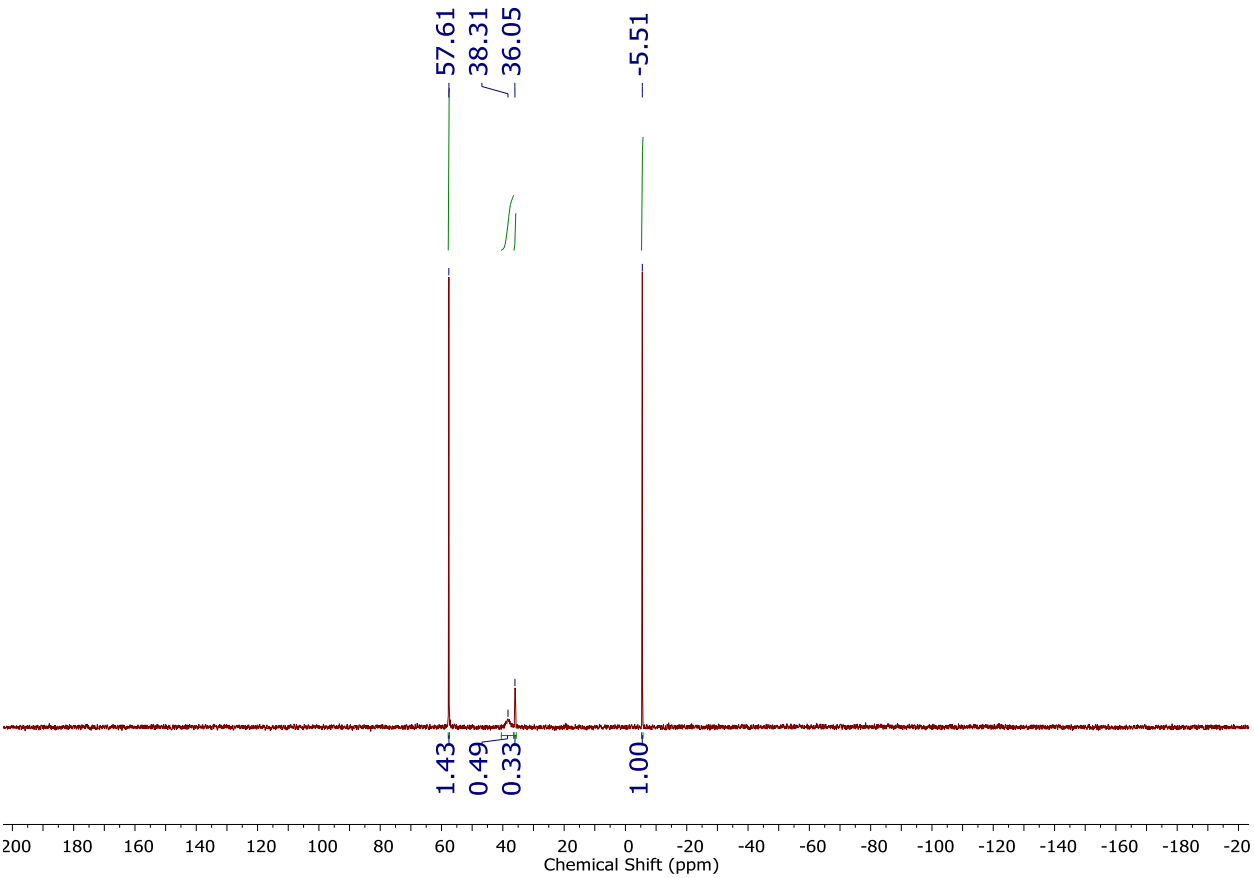

Figure S25. $^{31}P\{^{1}H\}$ NMR spectrum (162 MHz, C_6D_6, 25 °C) for the addition of 10 equiv $HBAr^{F}_{4}$ and 12 equiv KC_8 to $[K(THF)_2][P_3{}^{Si}Os\text{-}N_2]$.

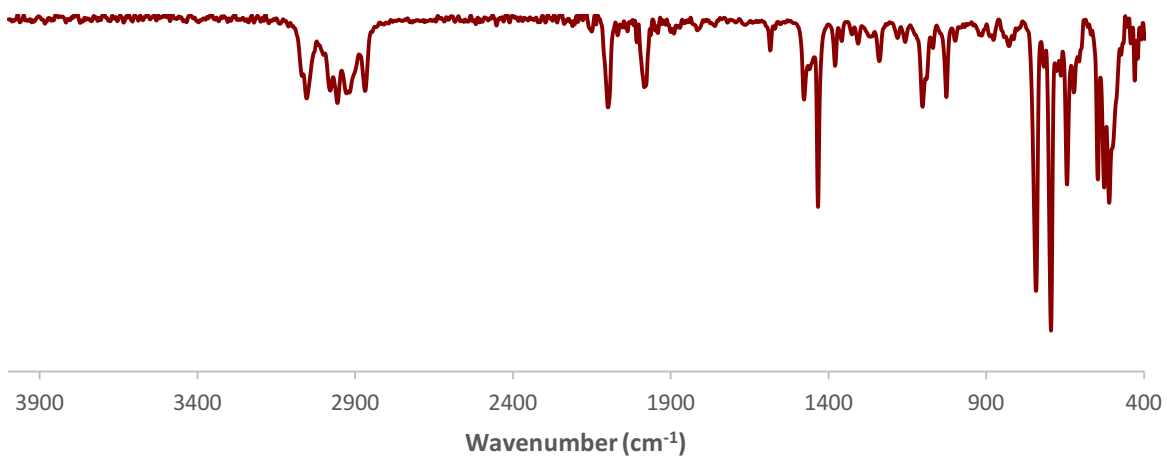

Figure S26. IR spectrum for the addition of 10 equiv $HBAr^{F}_{4}$ and 12 equiv KC_8 to $[K(THF)_2][P_3{}^{Si}Os\text{-}N_2]$; deposited as a thin film from C_6D_6.

Treatment of $[K(THF)_2][P_3{}^{Si}Ru\text{-}N_2]$ with 10 equiv $HBAr^{F}_{4}$ and 12 equiv KC_8: In the glovebox, $[K(THF)_2][P_3{}^{Si}Ru\text{-}N_2]$ (0.0088 g, $9.6\text{x}10^{-3}$ mmol) was weighed out into a 20 mL scintillation vial, equipped with a stir bar, and cooled to 77 K inside the coldwell chilled with an external liquid

nitrogen bath. 1 mL of Et_2O was added dropwise to the vial and allowed to freeze. A solution of $HBAr^F_4$ (10 equiv, 0.096 mmol, 0.097 g) in Et_2O (1 mL) was then layered dropwise. Residual acid was dissolved in Et_2O (0.5 mL) and added subsequently. This was allowed to chill in the coldwell until the contents of the vial were frozen. Finally, KC_8 (12 equiv. 0.11 mmol, 0.016 g) was transferred as a suspension in Et_2O (1 mL) to the reaction vial. The vial was then sealed and its contents were cooled until the mixture was again frozen.

After thawing the mixture by replacing the liquid nitrogen bath with a dry ice/acetone bath (-78 °C), the reaction was stirred for 1 hour at -78 °C followed by 45 minutes at room temperature. The reaction mixture was then filtered through glass filter paper into a 20 mL vial containing triphenylphosphine (3.0 equiv, 0.029 mmol, 0.0075 g) as a ^{31}P NMR internal standard, concentrated to ½ the original volume, and transferred to an NMR tube. The integration of the ^{31}P resonances suggested the formation of $P_3^{Si}Ru(N_2)(H)$ and $P_3^{Si}RuH_3$ in approximately 39% yield and 21% yield, respectively. The NMR solution was then transferred to a 20 mL vial in the glovebox, concentrated, redissolved in C_6D_6, and analyzed by ^1H and ^{31}P NMR spectroscopies. The data obtained matched the data reported above.

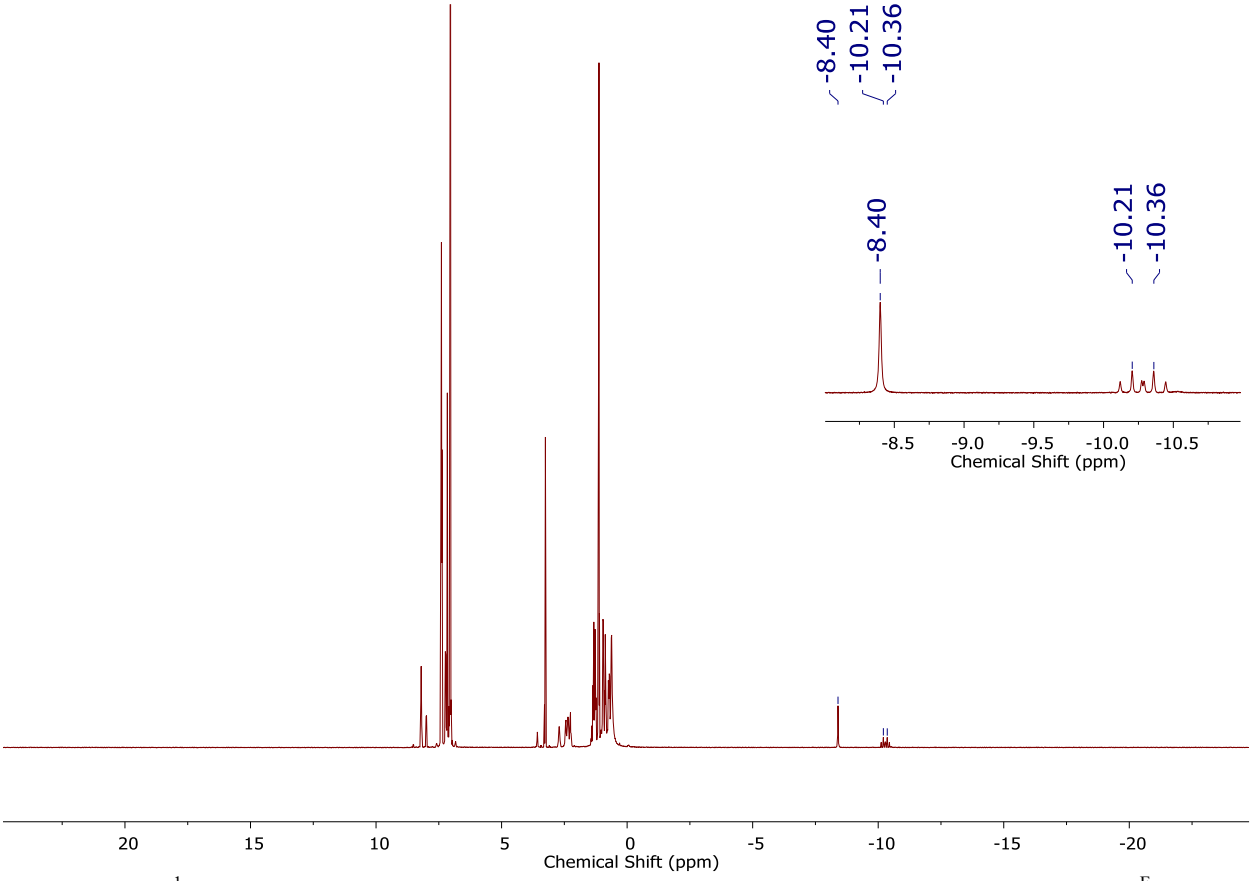

Figure S27. ^1H NMR spectrum (400 MHz, C_6D_6, 25 °C) for the addition of 10 equiv $HBAr^F_4$ and 12 equiv KC_8 to $[K(THF)_2][P_3^{Si}Ru\text{-}N_2]$.

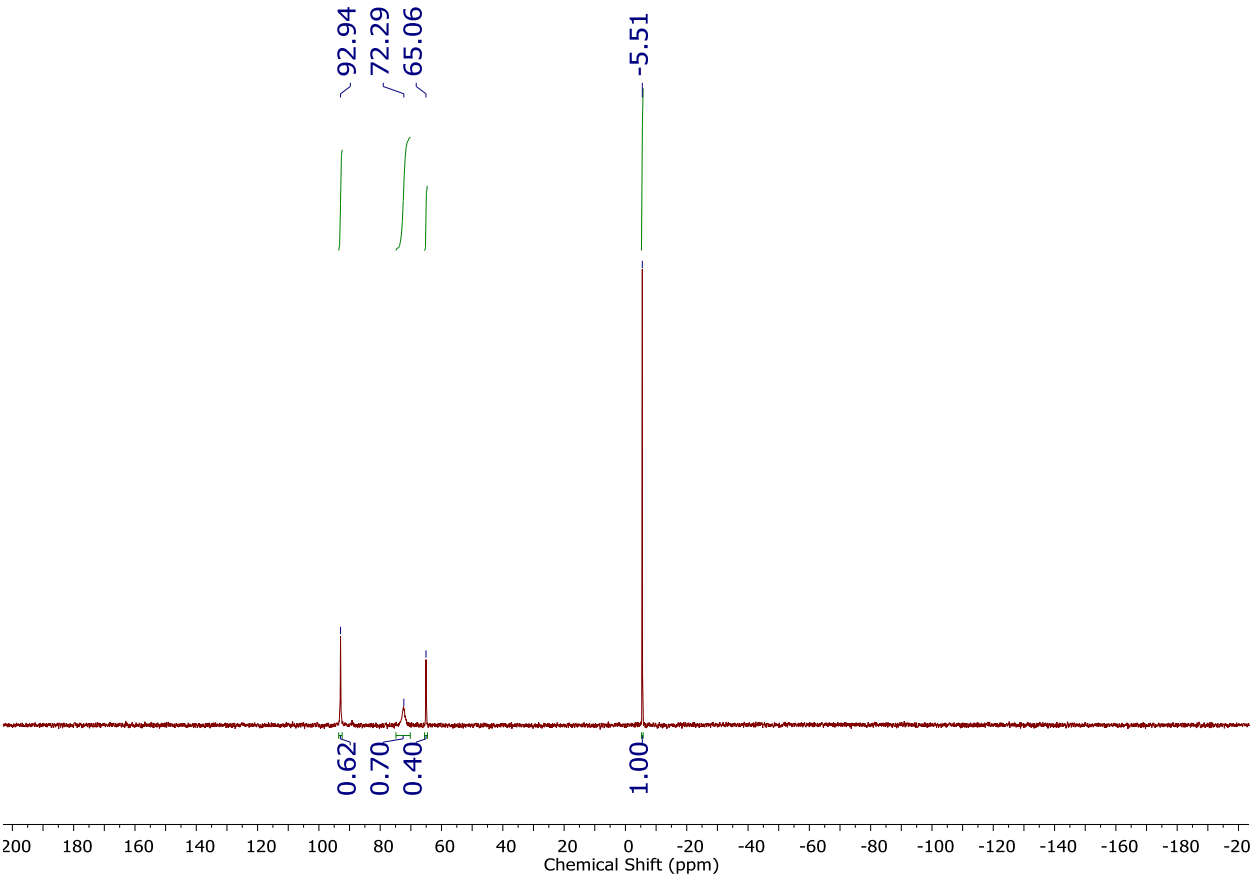

Figure S28. $^{31}P\{^{1}H\}$ NMR spectrum (162 MHz, C_6D_6, 25 °C) for the addition of 10 equiv $HBAr^{F}_{4}$ and 12 equiv KC_8 to $[K(THF)_2][P_3{}^{Si}Ru\text{-}N_2]$.

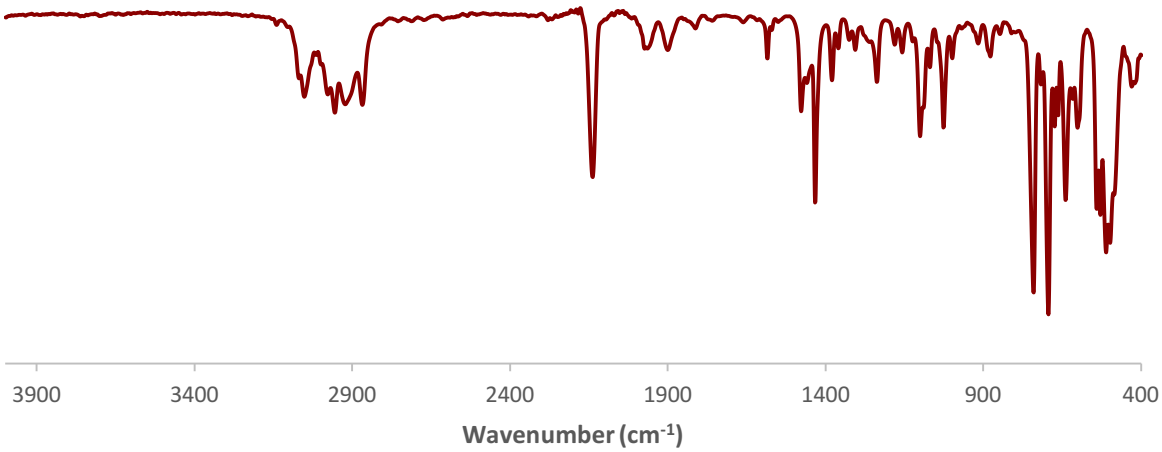

Figure S29. IR spectrum for the addition of 10 equiv $HBAr^{F}_{4}$ and 12 equiv KC_8 to $[K(THF)_2][P_3{}^{Si}Ru\text{-}N_2]$; deposited as a thin film from C_6D_6.

Treatment of $[K(THF)_2][P_3{}^{Si}Os\text{-}N_2]$ with 10 equiv $[H_2NPh_2][OTf]$ and 12 equiv Cp^*_2Co: In the glovebox, $[K(THF)_2][P_3{}^{Si}Os\text{-}N_2]$ (0.0091 g, $9.0\text{x}10^{-3}$ mmol) was weighed out into a 20 mL scintillation vial, equipped with a stir bar, and cooled to 77 K inside the coldwell chilled with an

external liquid nitrogen bath. 1 mL of Et_2O was added dropwise to the vial and allowed to freeze. A suspension of Cp^*_2Co (12 equiv, 0.11 mmol, 0.036 g) in Et_2O (1 mL) was then layered dropwise. This was allowed to chill in the coldwell until the contents of the vial were frozen. Finally, $[H_2NPh_2][OTf]$ (10 equiv. 0.090 mmol, 0.029 g) was transferred as a suspension in Et_2O (1 mL) to the reaction vial. The vial was then sealed and its contents were cooled until the mixture was again frozen.

After thawing the mixture by replacing the liquid nitrogen bath with a dry ice/acetone bath (-78 °C), the reaction was stirred for 3 hours at -78 °C followed by 1 hour at room temperature. The reaction mixture was then filtered through glass filter paper into a 20 mL vial containing triphenylphosphine (3.0 equiv, 0.027 mmol, 0.0071 g) as a ^{31}P NMR internal standard, concentrated to ½ the original volume, and transferred to an NMR tube. The integration of the ^{31}P resonances suggested the formation of $P_3{}^{Si}OsH_3$ in approximately 64% yield. The NMR solution was then transferred to a 20 mL vial in the glovebox, concentrated, redissolved in C_6D_6, and analyzed by ^1H and ^{31}P NMR spectroscopies. The data obtained matched the data reported above.

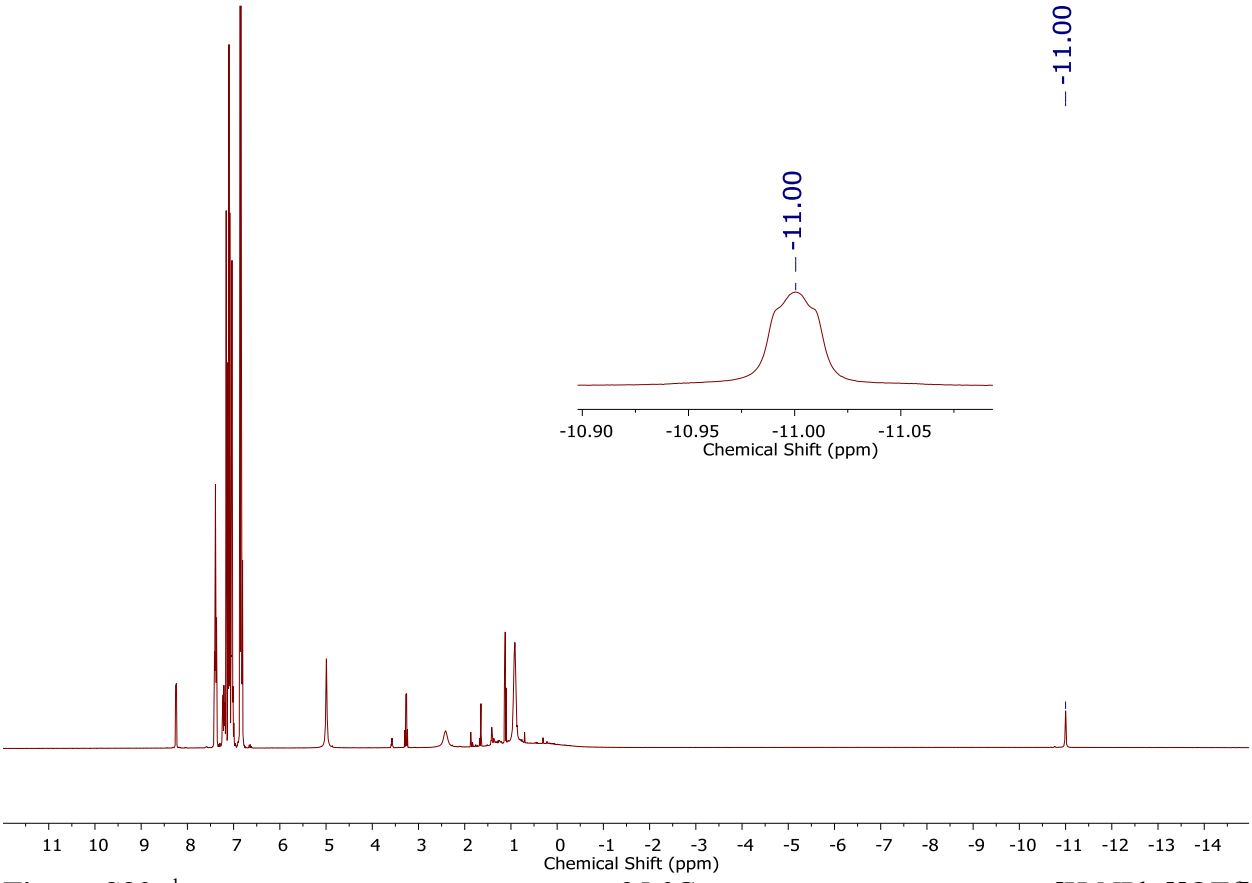

Figure S30. ^1H NMR spectrum (400 MHz, C_6D_6, 25 °C) for the addition of 10 equiv $[H_2NPh_2][OTf]$ and 12 equiv Cp^*_2Co to $[K(THF)_2][P_3{}^{Si}Os\text{-}N_2]$.

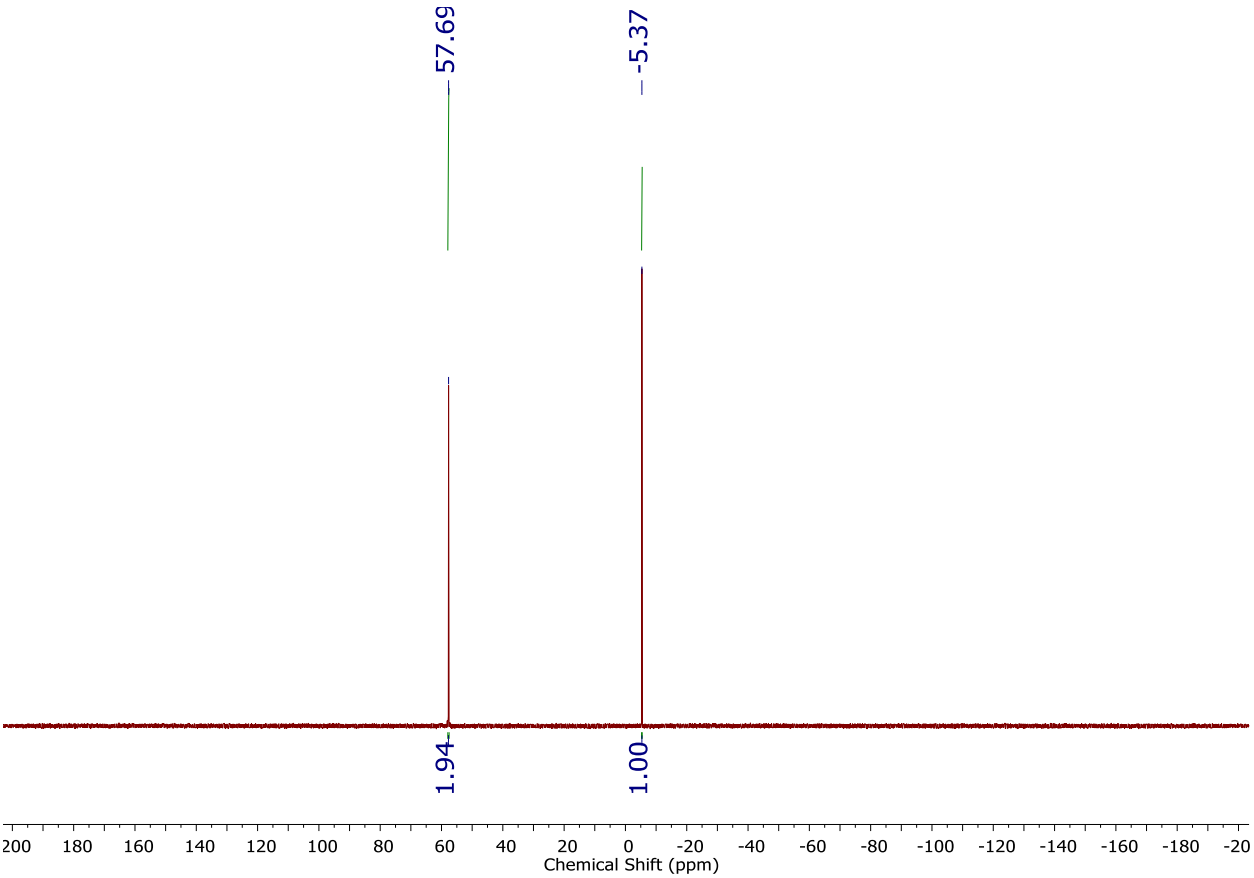

Figure S31. $^{31}P\{^{1}H\}$ NMR spectrum (162 MHz, C_6D_6, 25 °C) for the addition of 10 equiv $[H_2NPh_2][OTf]$ and 12 equiv Cp^*_2Co to $[K(THF)_2][P_3^{Si}Os\text{-}N_2]$.

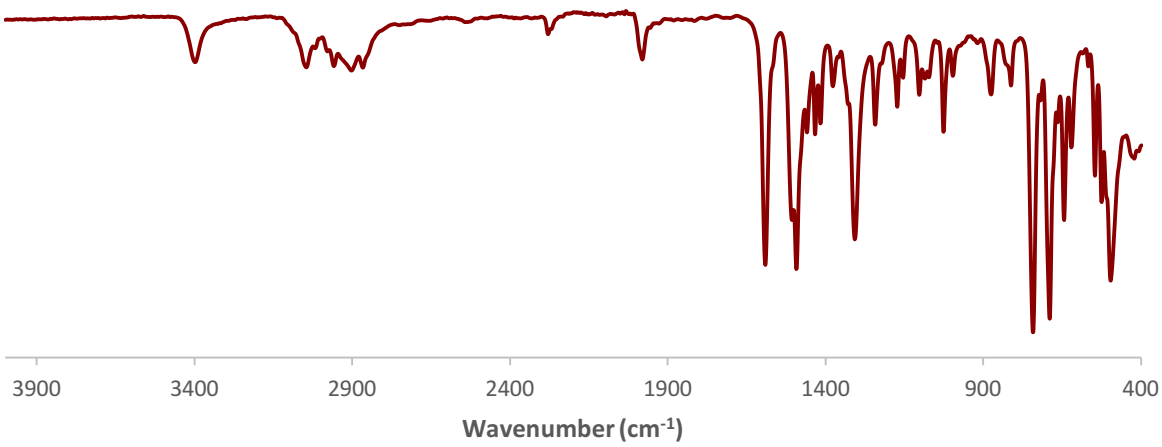

Figure S32. IR spectrum for the addition of 10 equiv $[H_2NPh_2][OTf]$ and 12 equiv Cp^*_2Co to $[K(THF)_2][P_3^{Si}Os\text{-}N_2]$; deposited as a thin film from C_6D_6.

Ammonia Production & Quantification Studies

***Standard NH_3 Generation Reaction Procedure*:** All solvents were stirred with Na/K for ≥ 1 hour and filtered prior to use. In a nitrogen-filled glovebox, the precatalyst (2.0 μmol) was weighed into a vial.* The precatalyst was then transferred quantitatively into a Schlenk tube as a suspension in Et_2O. The Et_2O was then evaporated to provide a solid layer (or thin film) of precatalyst at the bottom of the Schlenk tube. The acid and reductant were then added as solids and the tube was equipped with a stir bar. The tube was then cooled to 77 K in the coldwell. To the cold tube was added Et_2O to produce the desired concentration of precatalyst. The temperature of the system was allowed to equilibrate for 5 minutes and then the tube was sealed with a Teflon screw-valve. This tube was passed out of the box into a liquid nitrogen bath and transported to a fume hood. The tube was then transferred to a dry ice/acetone bath (-78 °C) where it thawed and was allowed to stir at -78 °C. For runs utilizing $HBAr^F_4$, reactions were stirred at -78 °C for 1 hour, followed by stirring at room temperature for 45 minutes. For all other runs, reactions were allowed to stir and gradually warm to room temperature overnight. To ensure reproducibility, all experiments were conducted in 200 mL Schlenk tubes (51 mm OD) using 25 mm stir bars, and stirring was conducted at ~900 rpm.

* In cases where less than 2.0 μmol of precatalyst was used, stock solutions (in THF) were used to avoid having to weigh very small amounts.

***Ammonia and Hydrazine Quantification*:** The catalytic reaction mixture was cooled to 77 K and allowed to freeze. The reaction vessel was then opened to atmosphere and to the frozen solution was added an excess (with respect to acid) solution of a NaO*t*Bu solution in MeOH (0.25 mM) dropwise over 1-2 minutes. This solution was allowed to freeze, then the headspace of the tube was evacuated and the tube was sealed. The tube was then allowed to warm to room temperature and stirred at room temperature for at least 10 minutes. An additional Schlenk tube was charged with HCl (3 mL of a 2.0 M solution in Et_2O, 6 mmol) to serve as a collection flask. The volatiles of the reaction mixture were vacuum transferred at room temperature into this collection flask. After completion of the vacuum transfer, the collection flask was sealed and warmed to room temperature. Solvent was removed *in vacuo*, and the remaining residue dissolved in 1 mL of DI H_2O. A 20 μL aliquot of this solution was then analyzed for the presence of NH_3 (present as $[NH_4][Cl]$) by the indophenol method.[16] Quantification was performed with UV-vis spectroscopy by analyzing the absorbance at 635 nm. A further aliquot of this solution was analyzed for the presence of N_2H_4 (present as $[N_2H_5][Cl]$) by a standard colorimetric method.[17] Quantification was performed with UV-vis spectroscopy by analyzing the absorbance at 458 nm.

In the case of runs with $[H_3NPh][OTf]$, $[H_3N\text{-}2,5\text{-}Cl_2C_6H_3][OTf]$, [*N*-Me-$H_2NPh$][OTf], and $[H_3NPh][BAr^F_4]$, it was found that the corresponding aniline derivative in the form of anilinium chloride was present in the receiving vessel. The anilinium chloride interfered with the indophenol and hydrazine detection methods. Therefore, quantification for NH_3 was performed by extracting the solid residue into 1 mL of DMSO-d_6 that had 1,4-dioxane as an internal standard. Integration of the ^{1}H NMR peak observed for $[NH_4][Cl]$ was then integrated against the peak of 1,4-dioxane to quantify the ammonium present. This ^{1}H NMR detection method was also used to differentiate $[^{14}NH_4][Cl]$ and $[^{15}NH_4][Cl]$ produced in the control reactions conducted with $[H_2{}^{15}NPh_2][OTf]$ and $[H_3{}^{15}NPh][OTf]$.

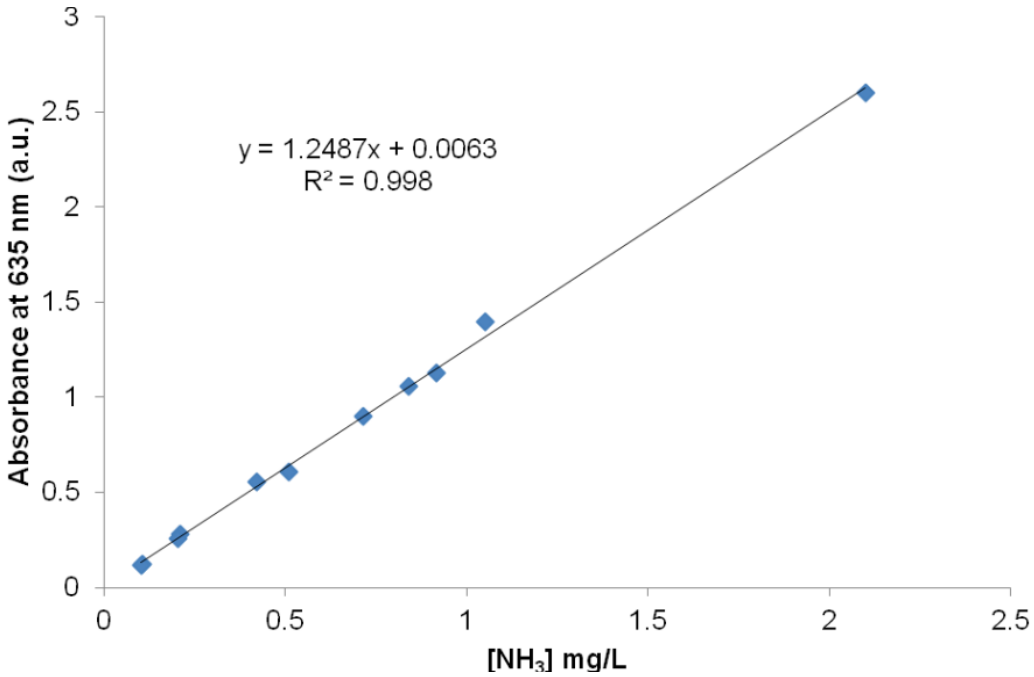

Figure S33. Calibration curve used for NH_3 quantification.

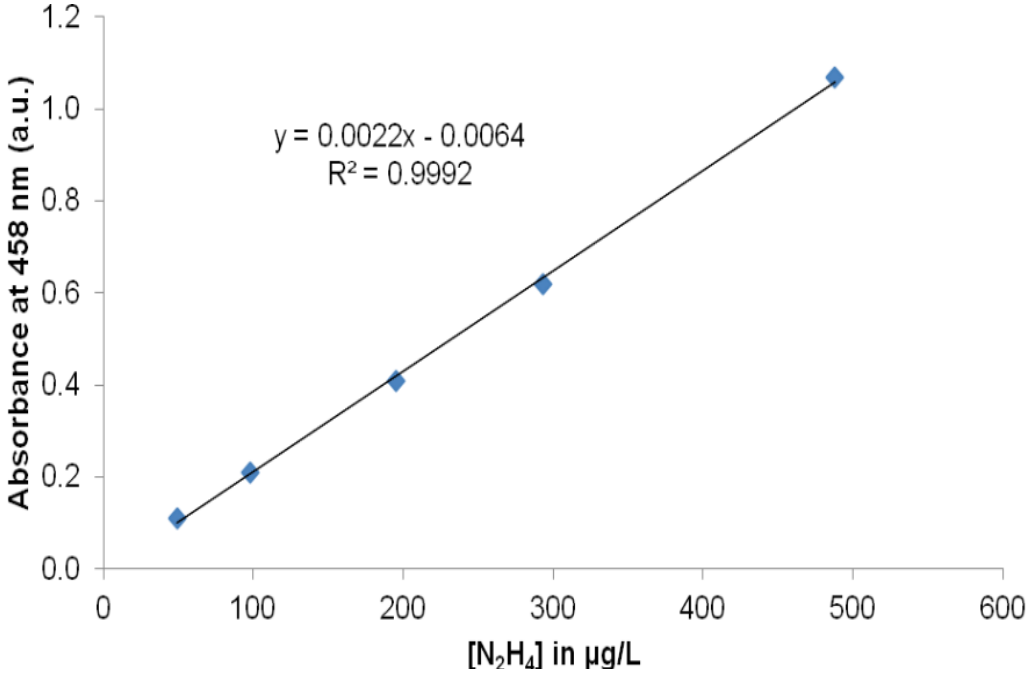

Figure S34. Calibration curve used for N_2H_4 quantification.

Table S2. UV-vis quantification results for standard NH_3 generation experiments with $[K(THF)_2][P_3^{Si}Os\text{-}N_2]$.

Entry	Total volume of Et_2O (mL)	[Os]-N_2^- (μmol)	Acid (equiv)	Reductant (equiv)	NH_4Cl (μmol)	NH_3/Os (equiv)	Yield NH_3/H^+ (%)
A	2.0	2.0	46[a]	50[b]	2.5	1.2	8.0
B	2.0	2.0	46[a]	50[b]	3.4	1.7	11.1
C	2.0	2.0	46[a]	50[b]	3.7	1.9	12.1
Avg.						1.6 ± 0.3	10 ± 2
D	2.0	2.0	46[c]	50[d]	12.7	6.4	41.9
E	2.0	2.0	46[c]	50[d]	13.5	6.8	44.0
F	2.0	2.0	46[c]	50[d]	14.7	7.4	48.5
G	2.0	2.0	46[c]	50[d]	15.4	7.8	50.8
Avg.						7.1 ± 0.6	46 ± 4
H	1.1	0.48	150[c]	180[d]	8.3	17.2	34.5
I	1.1	0.48	150[c]	180[d]	8.5	17.8	35.6
J	1.1	0.48	150[c]	180[d]	8.5	17.9	35.7
Avg.						18 ± 1	35 ± 1
K	1.5	0.19	500[c]	800[d]	9.1	47.9	28.7
L	1.5	0.19	500[c]	800[d]	9.9	52.5	31.5
Avg.						50 ± 3	30 ± 2
M	2.0	0.16	800[c]	960[d]	12.9	82.1	30.8
N	2.0	0.16	800[c]	960[d]	13.2	83.9	31.5
O	2.0	0.16	800[c]	960[d]	14.4	91.8	34.4
Avg.						86 ± 5	32 ± 2
P	2.8	0.12	1500[c]	1800[d]	13.1	110.4	22.1
Q	2.8	0.12	1500[c]	1800[d]	13.5	112.9	22.6
R	2.8	0.12	1500[c]	1800[d]	13.8	115.1	23.0
S	2.8	0.12	1500[c]	1800[d]	15.2	126.4	25.3
T	2.8	0.12	1500[c]	1800[d]	16.4	136.3	27.3
Avg.						120 ± 11	24 ± 2
U	2.0	2.0	46[e]	50[a]	15.3	7.7	50.3
V	2.0	2.0	46[e]	50[d]	16.0	8.1	52.7
Avg.						7.9 ± 0.3	52 ± 2
W	2.0	2.0	46[f]	50[a]	15.7	7.9	52
X	2.0	2.0	46[g]	50[a]	11.7	5.9	38.7
Y	2.0	2.0	46[g]	50[d]	13.2	6.6	43.2
Avg.						6.3 ± 0.5	41 ± 3
Z	2.0	2.0	46[h]	50[a]	0.2	0.1	0.7
AA	2.0	2.0	46[h]	50[d]	0.3	0.15	1.0
Avg.						0.1 ± 0.1	0.8 ± 0.2
BB	2.0	2.0	46[i]	50[a]	2.1	1.1	7.0
CC	2.0	2.0	46[i]	50[d]	2.5	1.3	8.2
Avg.						1.2 ± 0.1	7.6 ± 0.8
DD	2.0	2.0	46[f]	50[a]	1.2	0.6	4.1

EE	2.0	2.0	46[j]	50[d]	1.5	0.8	5.1
Avg.						0.7 ± 0.1	4.6 ± 0.7
FF**	2.0	2.0	46[c]	50[d]	12.3	6.2	40.4
GG	2.0	2.0	46[c]	50[k]	0	0	0
HH	2.0	2.0	46[c]	50[l]	0	0	0

[a]$HBAr^F_4$. [b]KC_8. [c]$[H_2NPh_2][OTf]$. [d]Cp^*_2Co. [e]$[H_3NPh][OTf]$. [f]$[H_3N\text{-}2,5\text{-}Cl_2C_6H_3][OTf]$. [g][*N*-Me-$H_2NPh$][OTf]. [h]$[H_2NPh_2][BAr^F_4]$. [i]$[H_3NPh][BAr^F_4]$. [j]HOTf. [k]$Cp_2Co$. [l]$Cp^*_2Cr$.
*N_2H_4 was not detected in the catalytic runs.
**Run at -40 °C instead of -78 °C.

Table S3. UV-vis quantification results for standard NH_3 generation experiments with $[K(THF)_2][P_3{}^{Si}Ru\text{-}N_2]$.

Entry	Total volume of Et_2O (mL)	[Ru]-N_2^- (μmol)	Acid (equiv)	Reductant (equiv)	NH_4Cl (μmol)	NH_3/Ru (equiv)	Yield NH_3/H^+ (%)
A	2.0	2.0	46[a]	50[b]	7.8	4.0	25.8
B	2.0	2.0	46[a]	50[b]	8.8	4.3	27.7
C	2.0	2.0	46[a]	50[b]	8.9	4.6	29.7
Avg.						4.3 ± 0.3	28 ± 2
D	2.0	2.0	46[c]	50[d]	0.7	0.4	2.4
E	2.0	2.0	46[c]	50[d]	2.2	1.1	7.4
Avg.						0.8 ± 0.5	4.9 ± 3.5

[a]$HBAr^F_4$. [b]KC_8. [c]$[H_2NPh_2][OTf]$. [d]Cp^*_2Co.
*N_2H_4 was not detected in the catalytic runs.

Table S4. UV-vis quantification results for standard NH_3 generation experiments with $[Na(12\text{-crown-}4)_2][P_3{}^{Si}Fe\text{-}N_2]$.

Entry	Total volume of Et_2O (mL)	[Fe]-N_2^- (μmol)	Acid (equiv)	Reductant (equiv)	NH_4Cl (μmol)	NH_3/Fe (equiv)	Yield NH_3/H^+ (%)
A	2.0	2.0	46[a]	50[b]	2.2	1.1	7.3
B	2.0	2.0	46[a]	50[b]	2.9	1.5	9.8
C	2.0	2.0	46[a]	50[b]	3.4	1.7	10.8
Avg.						1.4 ± 0.3	9.3 ± 1.8

[a]$[H_2NPh_2][OTf]$. [b]Cp^*_2Co.
*N_2H_4 was not detected in the catalytic runs.

Table S5. UV-vis quantification results for standard NH_3 generation experiments with $[Na(12\text{-crown-}4)_2][P_3{}^{B}Fe\text{-}N_2]$.

Entry	Total volume of Et_2O (mL)	$P_3{}^BFe\text{-}N_2^-$ (μmol)	Acid (equiv)	Reductant (equiv)	NH_4Cl (μmol)	NH_3/Fe (equiv)	Yield NH_3/H^+ (%)
A	2.8	0.12	1500[a]	1800[b]	2.2	18.3	3.7
B	2.8	0.12	1500[a]	1800[b]	3.1	25.5	5.1

Avg.	22 ± 5	4.4 ± 1.0

[a][H_2NPh_2][OTf]. [b]Cp^*_2Co.
*N_2H_4 was not detected in the catalytic runs.

Table S6. UV-vis quantification results for standard NH_3 generation experiments with $P_3^{Si}Os(N_2)(H)$.

Entry	Total volume of Et_2O (mL)	[Os](N$_2$)(H) (μmol)	Acid (equiv)	Reductant (equiv)	NH_4Cl (μmol)	NH_3/Os (equiv)	Yield NH_3/H^+ (%)
A	2.0	2.0	46[a]	50[b]	0	0	0
B	2.0	2.0	46[c]	50[a]	0	0	0

[a]$HBAr^F_4$. [b]KC_8. [c][H_2NPh_2][OTf]. [d]Cp^*_2Co.
*N_2H_4 was not detected in the catalytic runs.

Table S7. UV-vis quantification results for standard NH_3 generation experiments with $P_3^{Si}OsH_3$.

Entry	Total volume of Et_2O (mL)	[Os]H$_3$ (μmol)	Acid (equiv)	Reductant (equiv)	NH_4Cl (μmol)	NH_3/Os (equiv)	Yield NH_3/H^+ (%)
A	2.0	2.0	46[a]	50[b]	0	0	0
B	2.0	2.0	46[c]	50[a]	0	0	0

[a]$HBAr^F_4$. [b]KC_8. [c][H_2NPh_2][OTf]. [d]Cp^*_2Co.
*N_2H_4 was not detected in the catalytic runs.

Table S8. UV-vis quantification results for standard NH_3 generation experiments with $[P_3^{Si}Os{=}NNH_2][OTf]$.

Entry	Total volume of Et_2O (mL)	[Os]=NNH_2^+ (μmol)	Acid (equiv)	Reductant (equiv)	NH_4Cl (μmol)	NH_3/Os (equiv)	Yield NH_3/H^+ (%)
A	2.0	2.0	46[a]	50[b]	5.3	2.6	17

[a][H_2NPh_2][OTf]. [b]Cp^*_2Co.
*N_2H_4 was not detected in the catalytic runs.

Table S9. UV-vis quantification results for standard NH_3 generation experiments with $P_3^{Si}Os$-Cl.

Entry	Total volume of Et_2O (mL)	[Os]-Cl (μmol)	Acid (equiv)	Reductant (equiv)	NH_4Cl (μmol)	NH_3/Os (equiv)	Yield NH_3/H^+ (%)
A	2.0	2.0	46[a]	50[b]	5.0	2.5	16

[a][H_2NPh_2][OTf]. [b]Cp^*_2Co.
*N_2H_4 was not detected in the catalytic runs.

Table S10. UV-vis quantification results for standard NH_3 generation experiments with $[(\eta^6\text{-}C_6H_6)Os(Cl)(\mu\text{-}Cl)]_2$.

Entry	Total volume of Et_2O (mL)	Os-dimer (µmol)	Acid (equiv)	Reductant (equiv)	NH_4Cl (µmol)	NH_3/Os (equiv)	Yield NH_3/H^+ (%)
A	2.0	2.0	46[a]	50[b]	0	0	0

[a] $[H_2NPh_2][OTf]$. [b] Cp^*_2Co.
*N_2H_4 was not detected in the catalytic runs.

NH_3 Generation Reaction with Periodic Substrate Reloading – Procedure with $[K(THF)_2][P_3^{Si}Os\text{-}N_2]$: All solvents were stirred with Na/K for ≥ 1 hour and filtered prior to use. In a nitrogen-filled glovebox, a stock solution of the precatalyst in THF was used to deliver the precatalyst to the Schlenk tube. The THF was then evaporated to provide a thin film of the precatalyst at the bottom of the Schlenk tube. The acid and reductant were then added as solids and the tube was equipped with a stir bar. The tube was then cooled to 77 K in the coldwell. To the cold tube was added Et_2O. The temperature of the system was allowed to equilibrate for 5 minutes and then the tube was sealed with a Teflon screw-valve. The coldwell cooling bath was switched from a liquid nitrogen bath to a dry ice/acetone bath (-78 °C). In the coldwell, the mixture in the sealed tube was stirred at -78 °C for 3 hours. Then, without allowing the tube to warm above -78 °C, the coldwell bath was switched from dry ice/acetone to a liquid nitrogen bath. After fifteen minutes the reaction mixture was observed to have frozen, and at this time the tube was opened. To the cold tube was added acid and reductant as solids. To the tube then an additional fraction of Et_2O was added. The coldwell cooling bath was switched from a liquid nitrogen bath to a dry ice/acetone bath. In the coldwell, the mixture in the sealed tube was stirred at -78 °C for 3 hours. These reloading steps were repeated the desired number of times. Then the tube was allowed to stir and gradually warm to room temperature overnight.

Table S11. UV-vis quantification results for NH_3 generation experiments with $[K(THF)_2][P_3^{Si}Os\text{-}N_2]$, with reloading.

Entry	Number of Loadings	Total volume of Et_2O (mL)	[Os]-N_2^- (µmol)	Acid (equiv)	Reductant (equiv)	NH_4Cl (µmol)	NH_3/Os (equiv)	Yield NH_3/H^+ (%)
A	2	2.0 x 2	0.16	800[a] x 2	960[b] x 2	19.3	122	23.0

[a] $[H_2NPh_2][OTf]$. [b] Cp^*_2Co.
*N_2H_4 was not detected in the catalytic runs.

Control Experiments with $[H_2^{15}NPh_2][OTf]$ and $[H_3^{15}NPh][OTf]$: The procedure was the same as the standard NH_3 generation reaction procedure with 2.0 µmol of $[K(THF)_2][P_3^{Si}Os\text{-}N_2]$ catalyst, 46 equiv of $[H_2{}^{15}NPh_2][OTf]$ or $[H_3{}^{15}NPh][OTf]$, and 50 equiv of Cp^*_2Co. The product was analyzed by ^1H NMR and only the diagnostic triplet of $[^{14}NH_4][Cl]$ was observed.

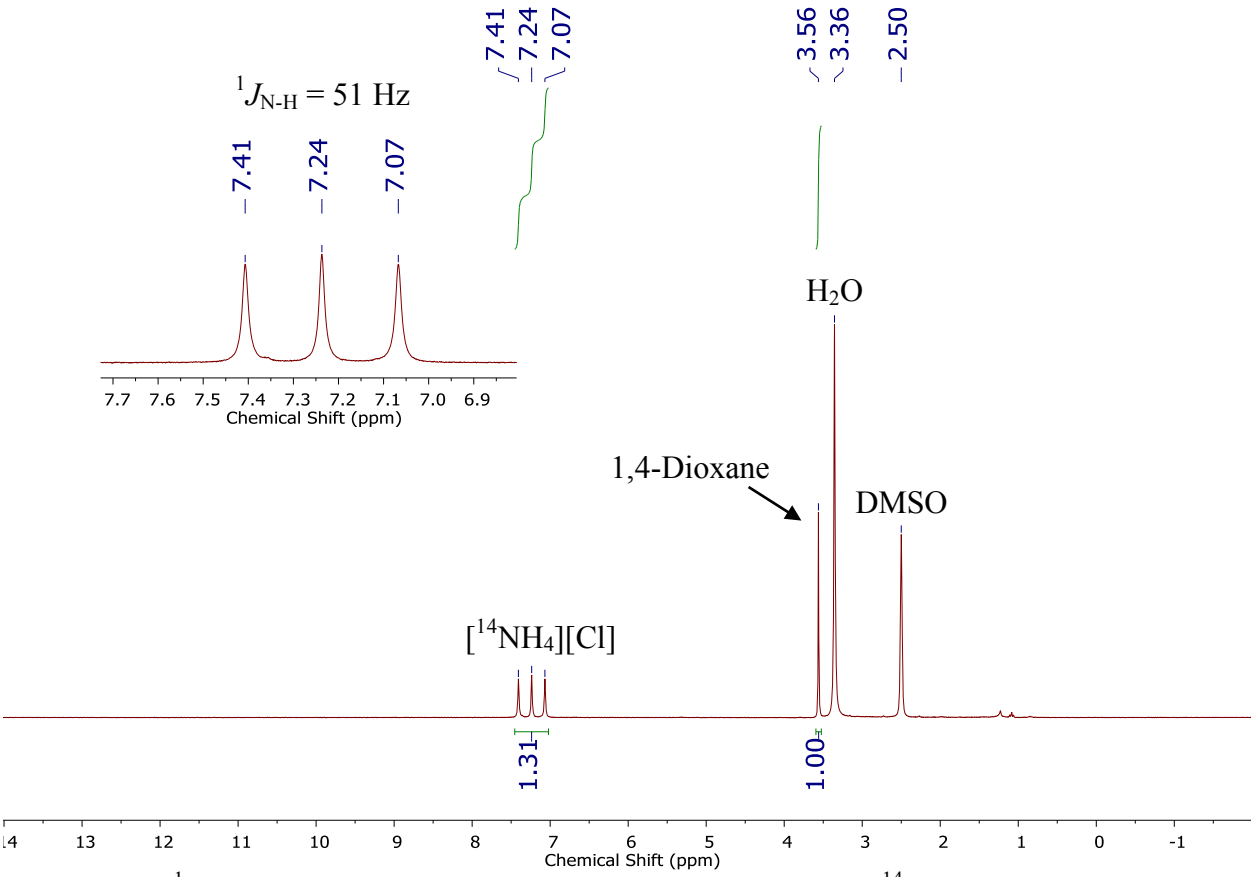

Figure S35. ^{1}H NMR spectrum (300 MHz, DMSO-d_6, 25 °C) of [^{14}NH$_4$][Cl] produced from a catalytic reaction with [K(THF)$_2$][P$_3^{Si}$Os-N$_2$] catalyst, 46 equiv of [H$_2$^{15}NPh$_2$][OTf], and 50 equiv of Cp*$_2$Co under an atmosphere of ^{14}N$_2$.

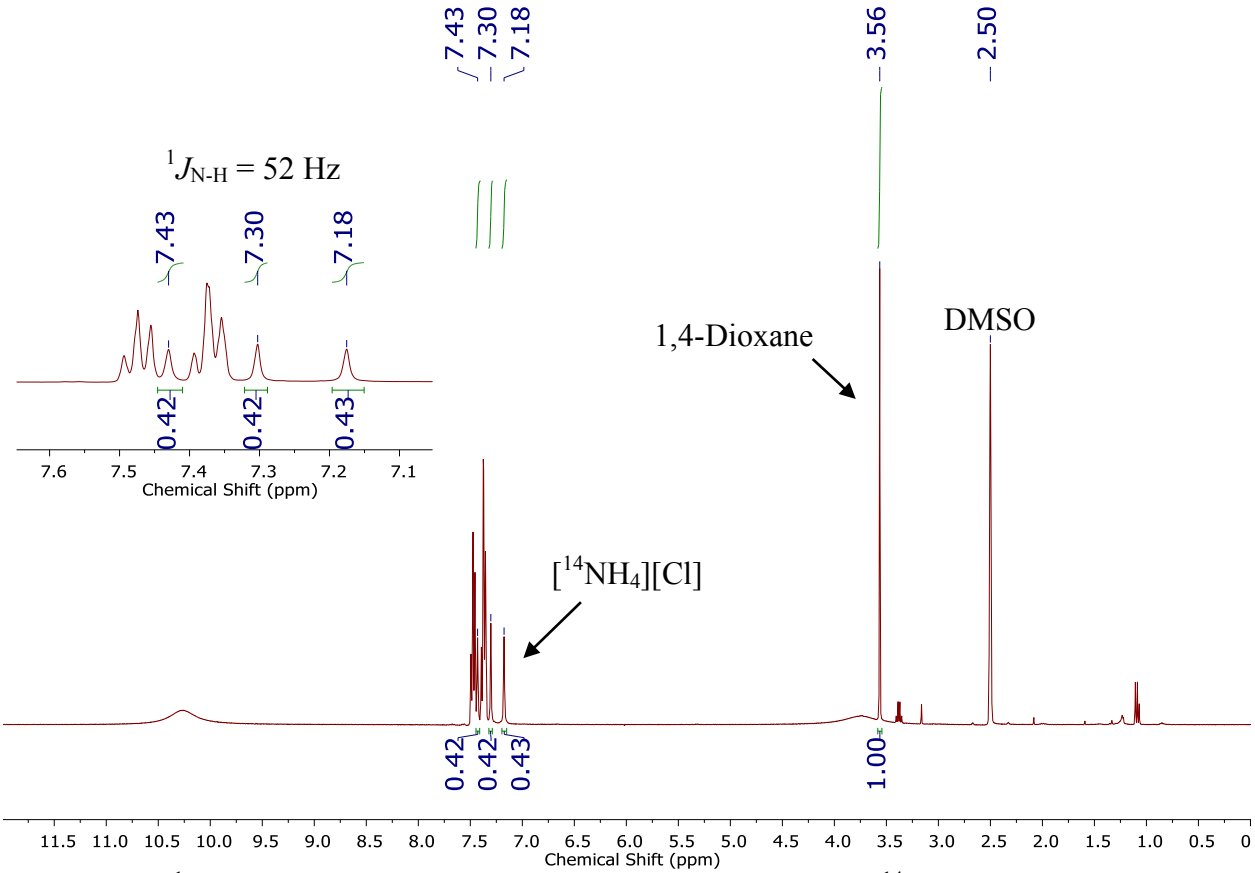

Figure S36. ^{1}H NMR spectrum (400 MHz, DMSO-d_6, 25 °C) of [$^{14}NH_4$][Cl] produced from a catalytic reaction with [K(THF)$_2$][P$_3^{Si}$Os-N$_2$] catalyst, 46 equiv of [H$_3$^{15}NPh][OTf], and 50 equiv of Cp*$_2$Co under an atmosphere of $^{14}N_2$.

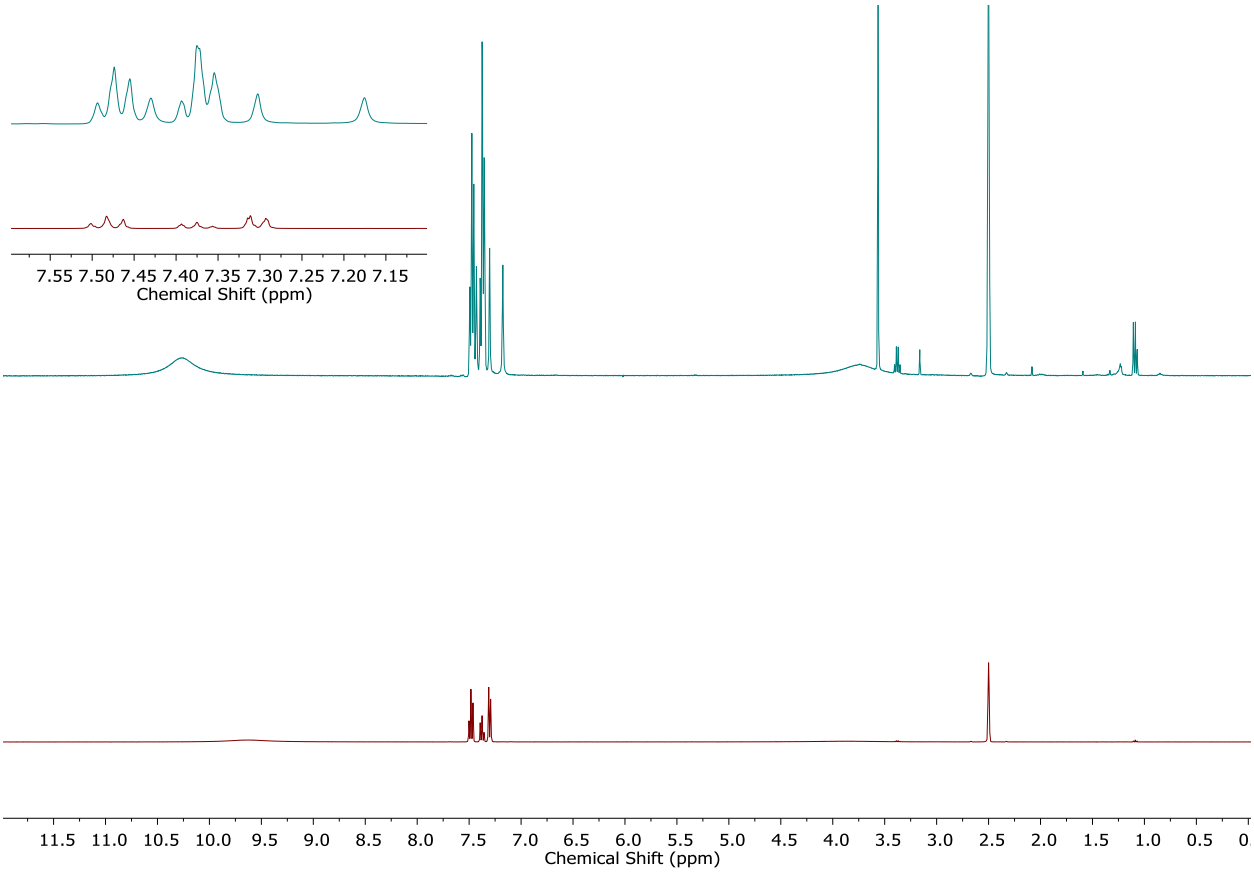

Figure S37. Stacked ^{1}H NMR spectra (400 MHz, DMSO-d_6, 25 °C) of the volatiles from the catalytic reaction described in Figure S36 (top) and an authentic sample of $[H_3NPh][OTf]$ (bottom).

Miscellaneous Experiments

Monitoring the Decomposition of $[P_3^{Si}Os{=}NNH_2][OTf]$ in THF Solution at Room Temperature:
A sample of $[P_3^{Si}Os{=}NNH_2][OTf]$ was dissolved in THF-d_8 and filtered through glass filter paper into a J-Young NMR tube. The sample was allowed to sit at room temperature, and spectra were acquired at various time points.

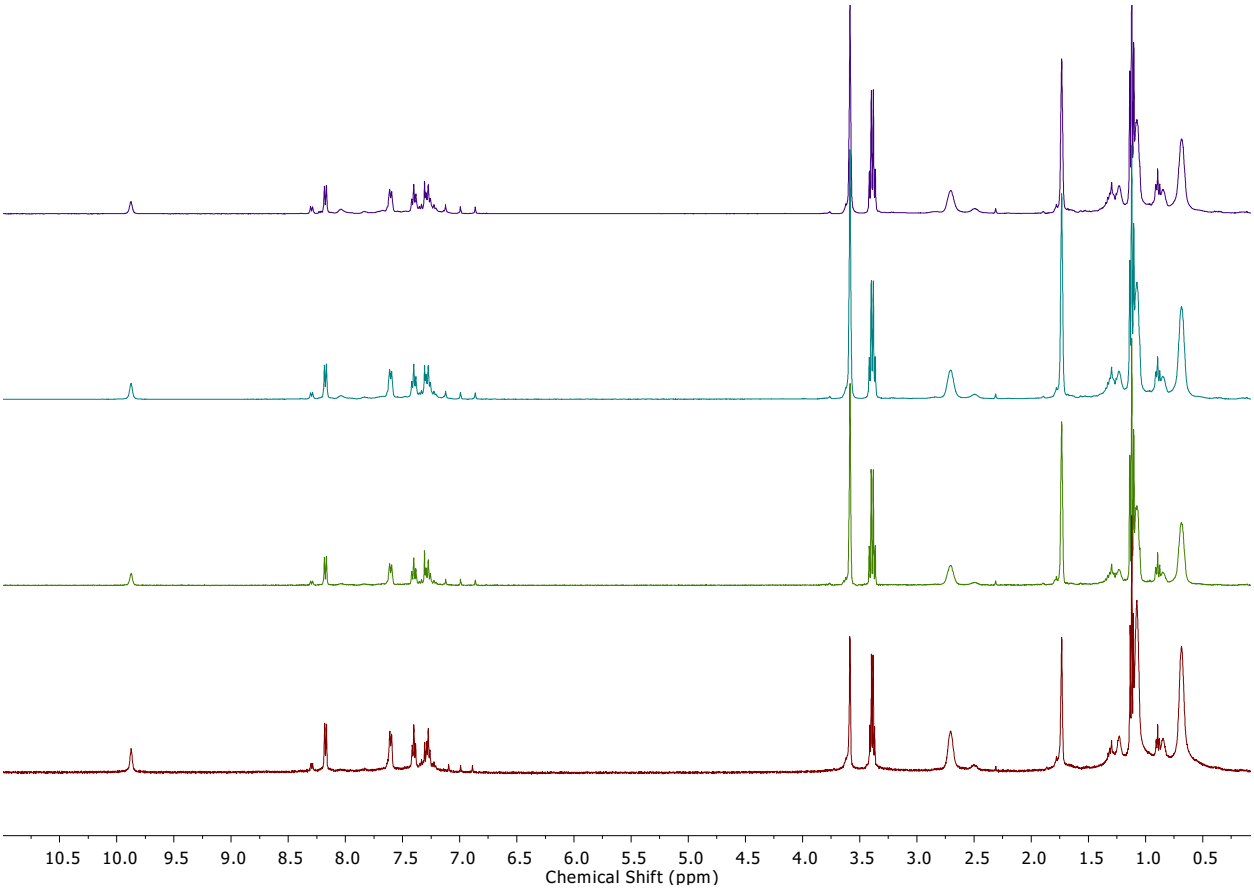

Figure S38. Stacked ^{1}H NMR spectra (400 MHz, THF-d_8, 25 °C) of [$P_3{}^{Si}$Os=NNH2][OTf] after preparing the sample (red), 2 days (light green), 5 days (aqua), and 7 days (purple).

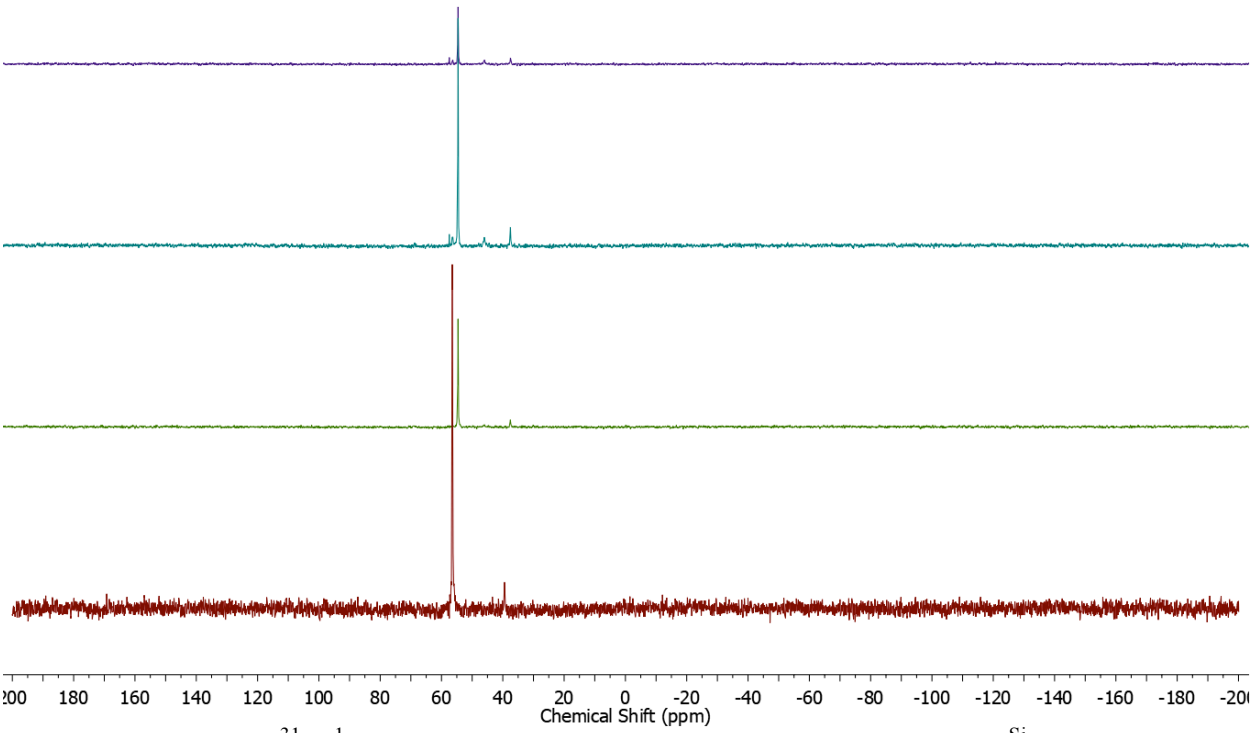

Figure S39. Stacked $^{31}P\{^{1}H\}$ NMR spectra (162 MHz, THF-d_8, 25 °C) of $[P_3^{Si}Os{=}NNH2][OTf]$ after preparing the sample (red), 2 days (light green), 5 days (aqua), and 7 days (purple).

Variable Temperature NMR Spectral Analysis of the Reaction of $[K(THF)_2][P_3^{Si}Os\text{-}N_2]$ with 1 equiv of $HBAr^F{}_4$ at -78 °C: In the glovebox, 0.0056 g ($5.5x10^{-3}$ mmol) of $[K(THF)_2][P_3^{Si}Os\text{-}N_2]$ was dissolved in 400 µL of THF-d_8 to give a dark red solution that was cooled to -78 °C in the coldwell. In a separate vial, $HBAr^F{}_4$ (1.0 equiv, $5.5x10^{-3}$ mmol, 0.0056 g) was dissolved in 200 µL of THF-d_8 and similarly cooled. After allowing the temperature to equilibrate for 15 minutes, the $HBAr^F{}_4$ solution was added dropwise to the stirring solution of $[K(THF)_2][P_3^{Si}Os\text{-}N_2]$ inside the coldwell. The reaction was stirred for 15 minutes at -78 °C before being transferred to a pre-chilled J-Young NMR tube using a pre-chilled pipet. The sample was removed quickly from the glovebox and transferred to a waiting dry/ice acetone bath (-78 °C). The sample was analyzed by variable temperature NMR spectroscopy (beginning at -78 °C) on a Varian 500 MHz instrument, allowing the probe temperature to equilibrate for 5 minutes before acquiring the spectra.

After warming to room temperature, ^{1}H and ^{31}P NMR spectra, as well as an IR spectrum of a thin film from the THF-d_8 solution, were acquired. These analyses revealed the products to be $P_3^{Si}Os(N_2)(H)$ (major), $P_3^{Si}Os\text{-}N_2$ (minor), and $P_3^{Si}OsH_3$ (minor).

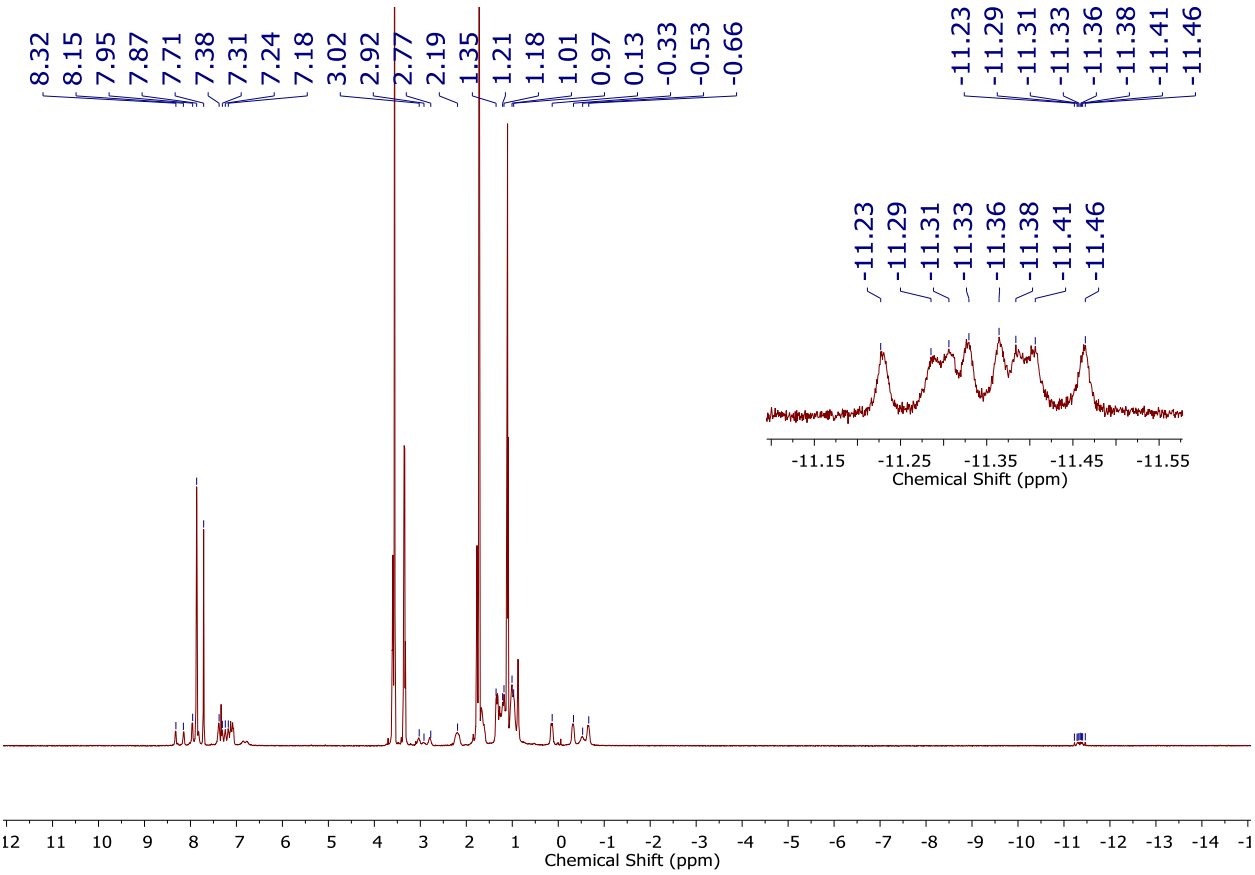

Figure S40. ^{1}H NMR spectrum (500 MHz, THF-d_8, -78 °C) for the reaction of $[K(THF)_2][P_3^{Si}Os\text{-}N_2]$ with 1 equiv of $HBAr^F_4$.

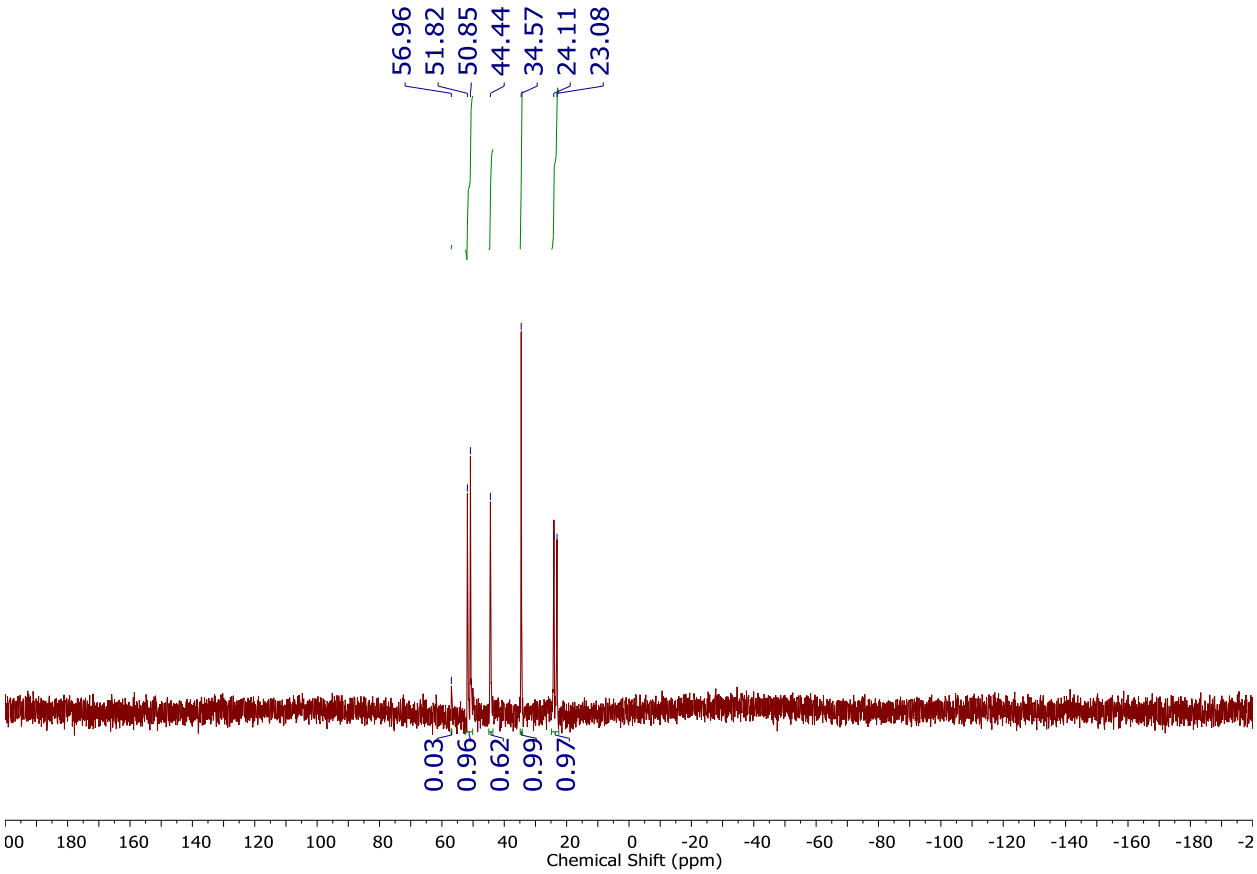

Figure S41. $^{31}P\{^{1}H\}$ NMR spectrum (202 MHz, THF-d_8, -78 °C) for the reaction of $[K(THF)_2][P_3{}^{Si}Os\text{-}N_2]$ with 1 equiv of $HBAr^F{}_4$. The resonance at 44.4 ppm corresponds to a small amount of unreacted $[K(THF)_2][P_3{}^{Si}Os\text{-}N_2]$. The signals centered at 51.3 ppm, 34.6 ppm, and 23.6 ppm correspond to $P_3{}^{Si}Os(N_2)(H)$, and the signal at 56.7 ppm corresponds to $P_3{}^{Si}OsH_3$ (see characterization data for authentic spectra of individual compounds.)

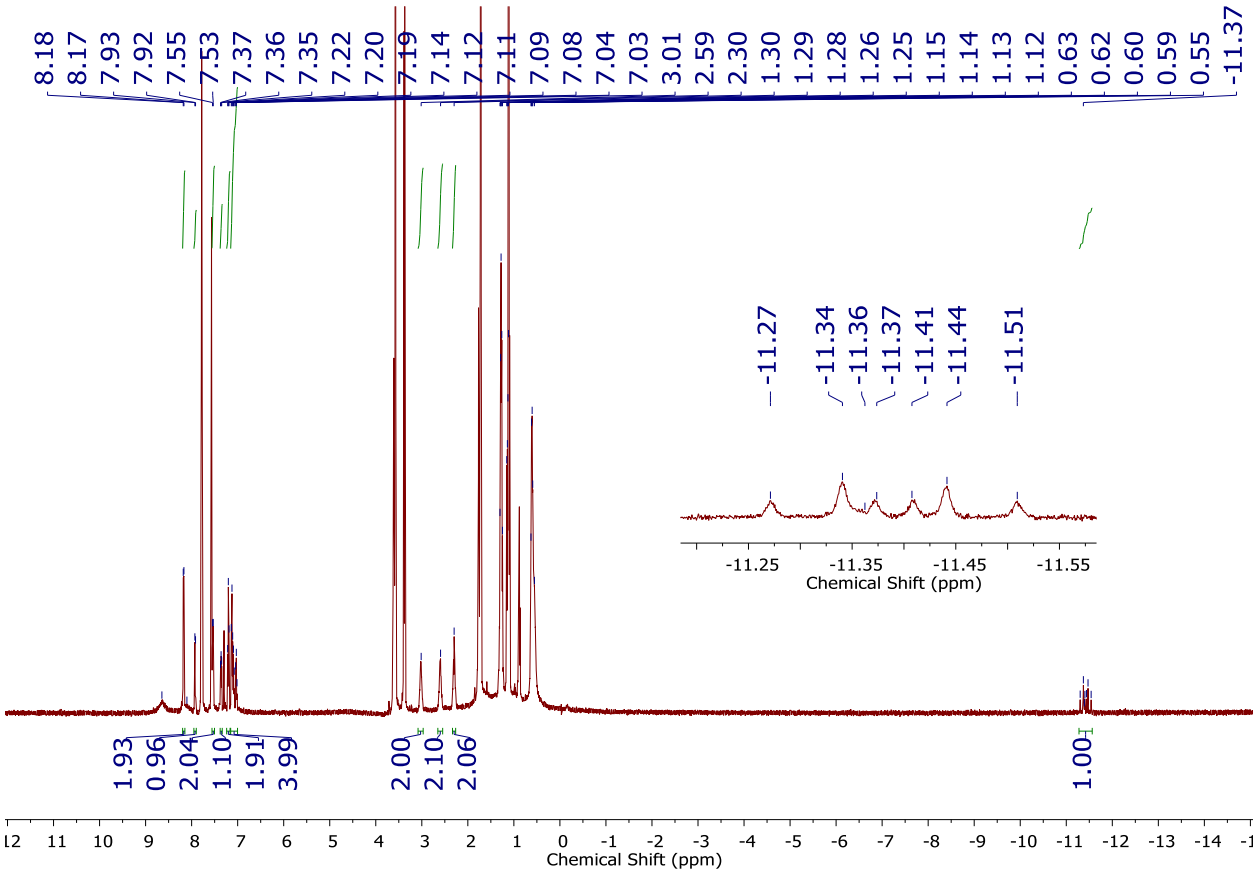

Figure S42. ^{1}H NMR spectrum (500 MHz, THF-d_8, 25 °C) for the reaction of $[K(THF)_2][P_3^{Si}Os\text{-}N_2]$ with 1 equiv of $HBAr^F{}_4$.

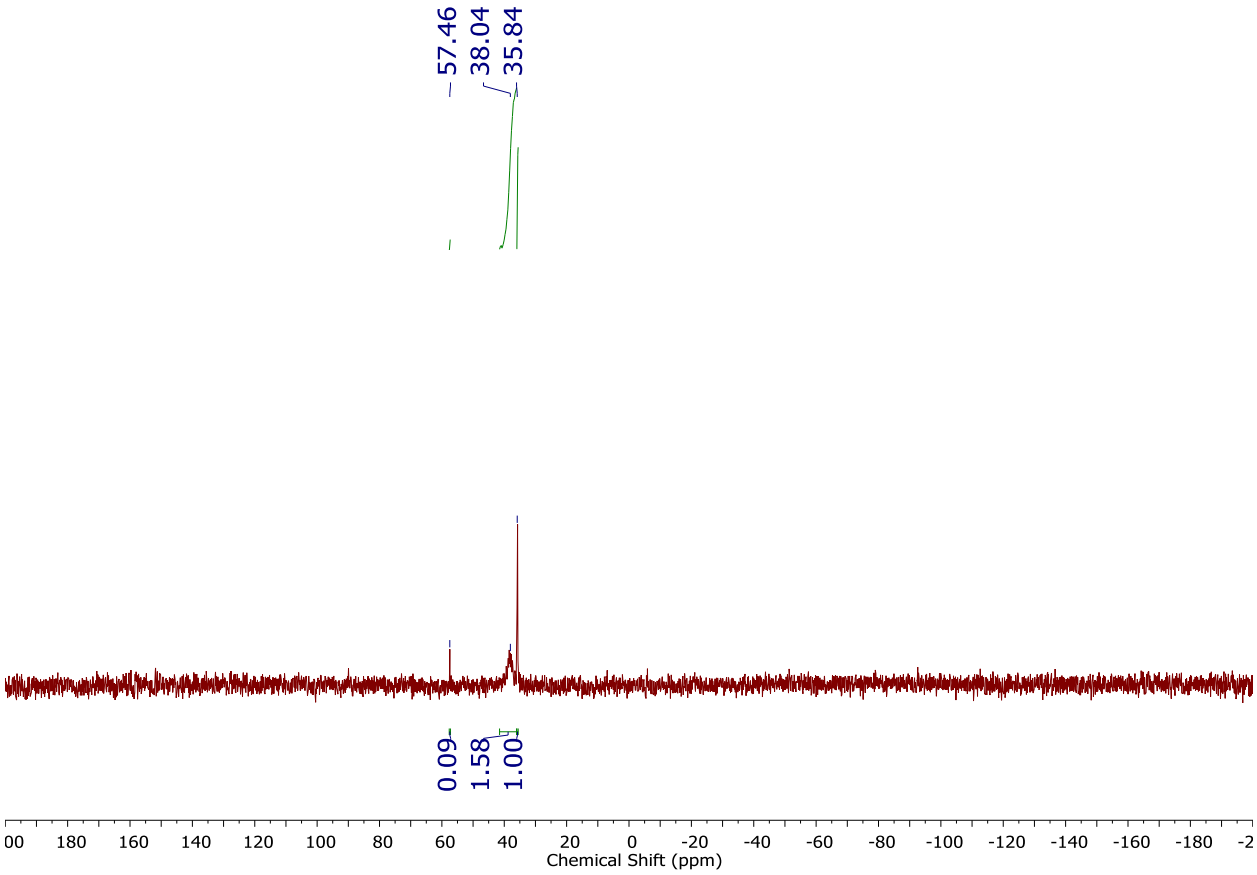

Figure S43. $^{31}P\{^{1}H\}$ NMR spectrum (202 MHz, THF-d_8, 25 °C) for the reaction of $[K(THF)_2][P_3{}^{Si}Os\text{-}N_2]$ with 1 equiv of $HBAr^F{}_4$.

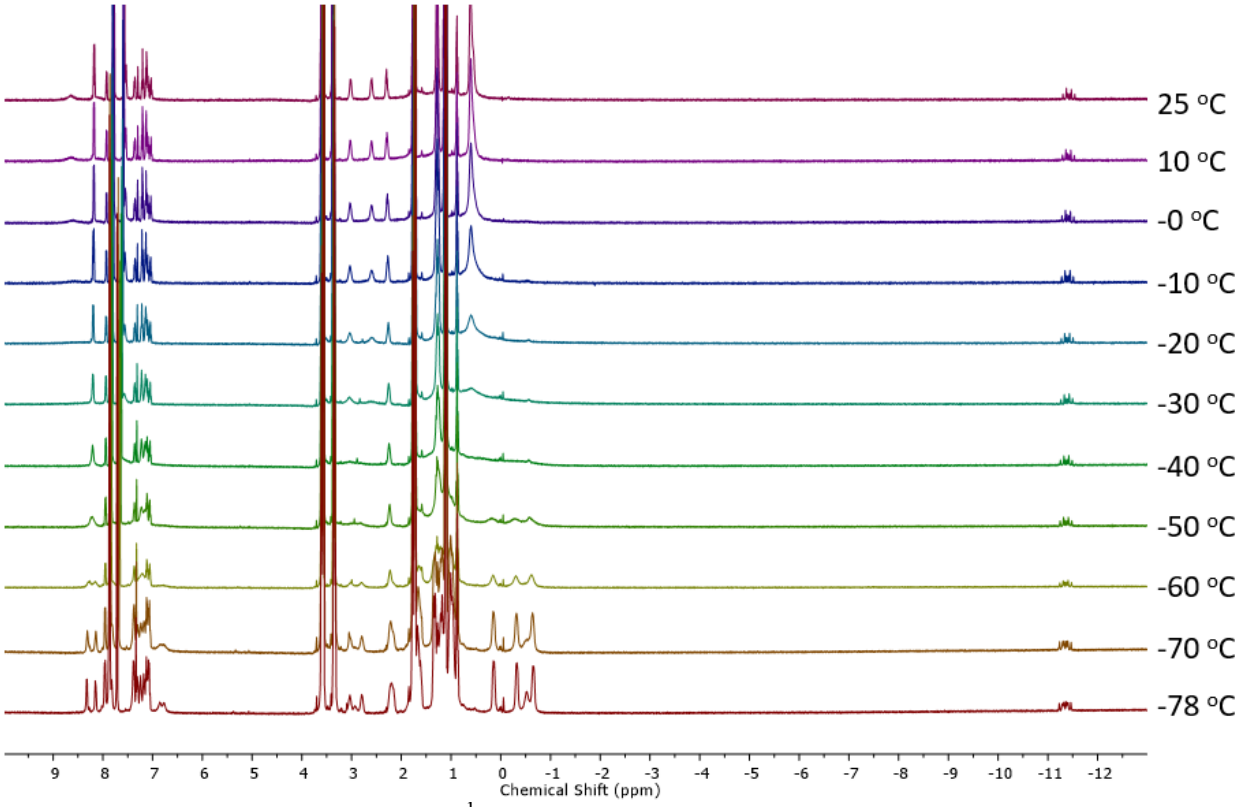

Figure S44. Variable temperature ^{1}H NMR spectra (500 MHz, THF-d_8) for the reaction of $[K(THF)_2][P_3{}^{Si}Os\text{-}N_2]$ with 1 equiv of $HBAr^F{}_4$.

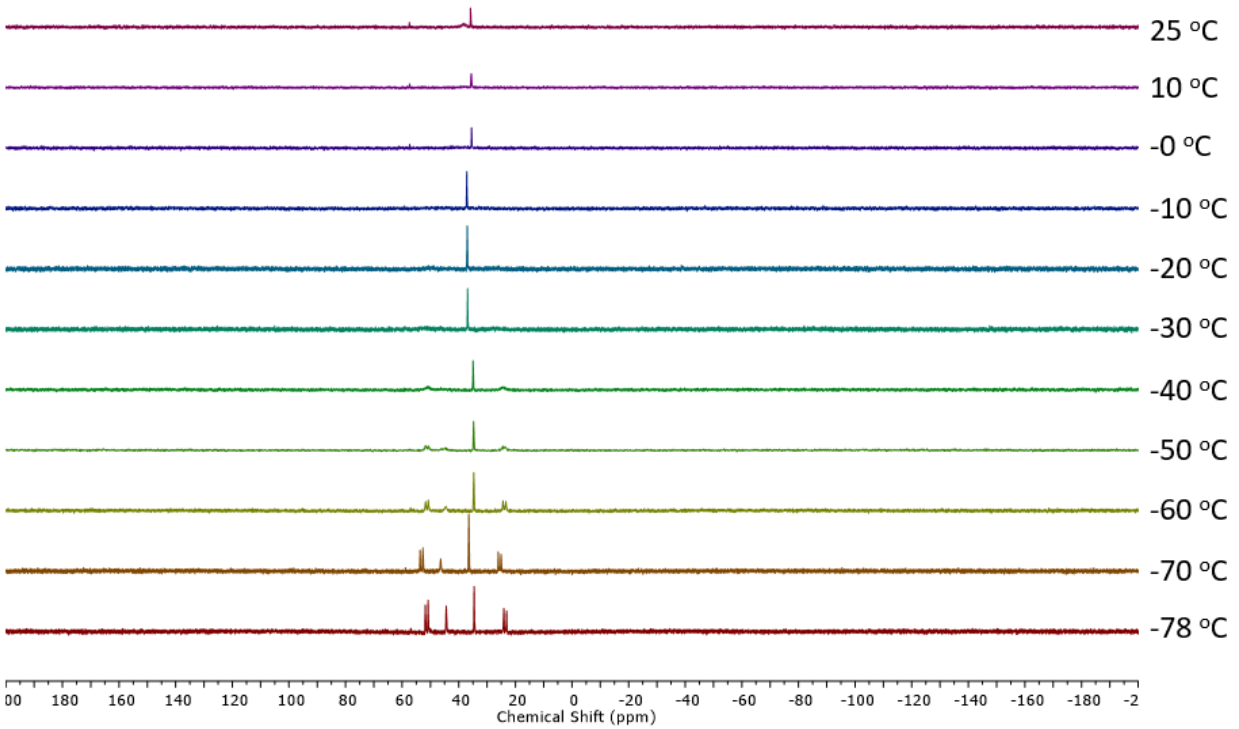

Figure S45. Variable temperature $^{31}P\{^{1}H\}$ NMR spectra (202 MHz, THF-d_8) for the reaction of $[K(THF)_2][P_3^{Si}Os\text{-}N_2]$ with 1 equiv of $HBAr^F{}_4$.

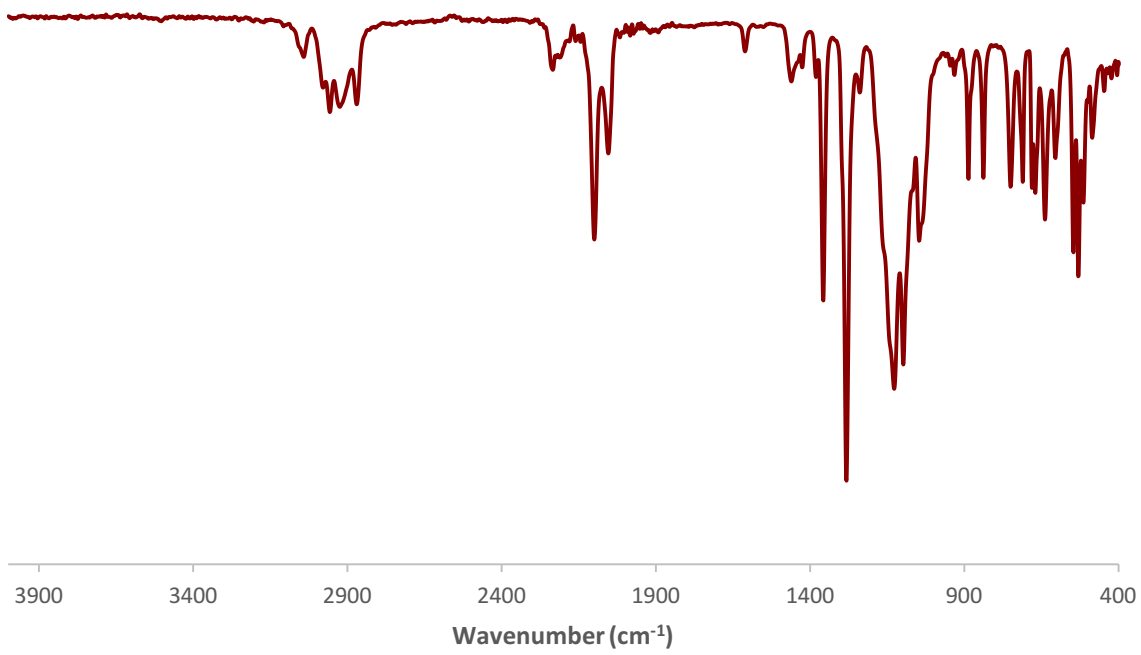

Figure S46. IR spectrum for the reaction of $[K(THF)_2][P_3^{Si}Os\text{-}N_2]$ with 1 equiv of $HBAr^F{}_4$; deposited as a thin film from THF-d_8.

General Procedure for the Variable Temperature NMR Spectral Analysis of the Reaction of $P_3^{Si}M\text{-}N_2$ (M = Os, Ru, Fe) with 5 equiv of Cp^*_2Co:

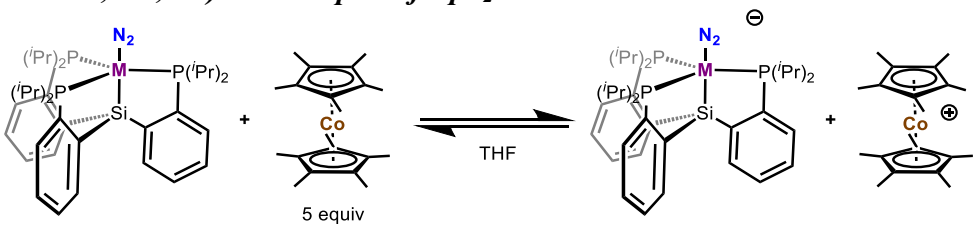

In the glovebox, $P_3^{Si}M\text{-}N_2$ and Cp^*_2Co (5 equiv with respect to $P_3^{Si}M\text{-}N_2$) were weighed out in separate vials. Both compounds were dissolved in THF-d_8, and then the solution of Cp^*_2Co was transferred to the vial containing $P_3^{Si}M\text{-}N_2$. The reaction was stirred at room temperature for 15 minutes before being filtered through glass filter paper into a J-Young NMR tube. Samples prepared in this fashion were analyzed by variable temperature NMR spectroscopy on a Varian 500 MHz instrument, allowing the probe temperature to equilibrate for 5 minutes before acquiring the spectra.

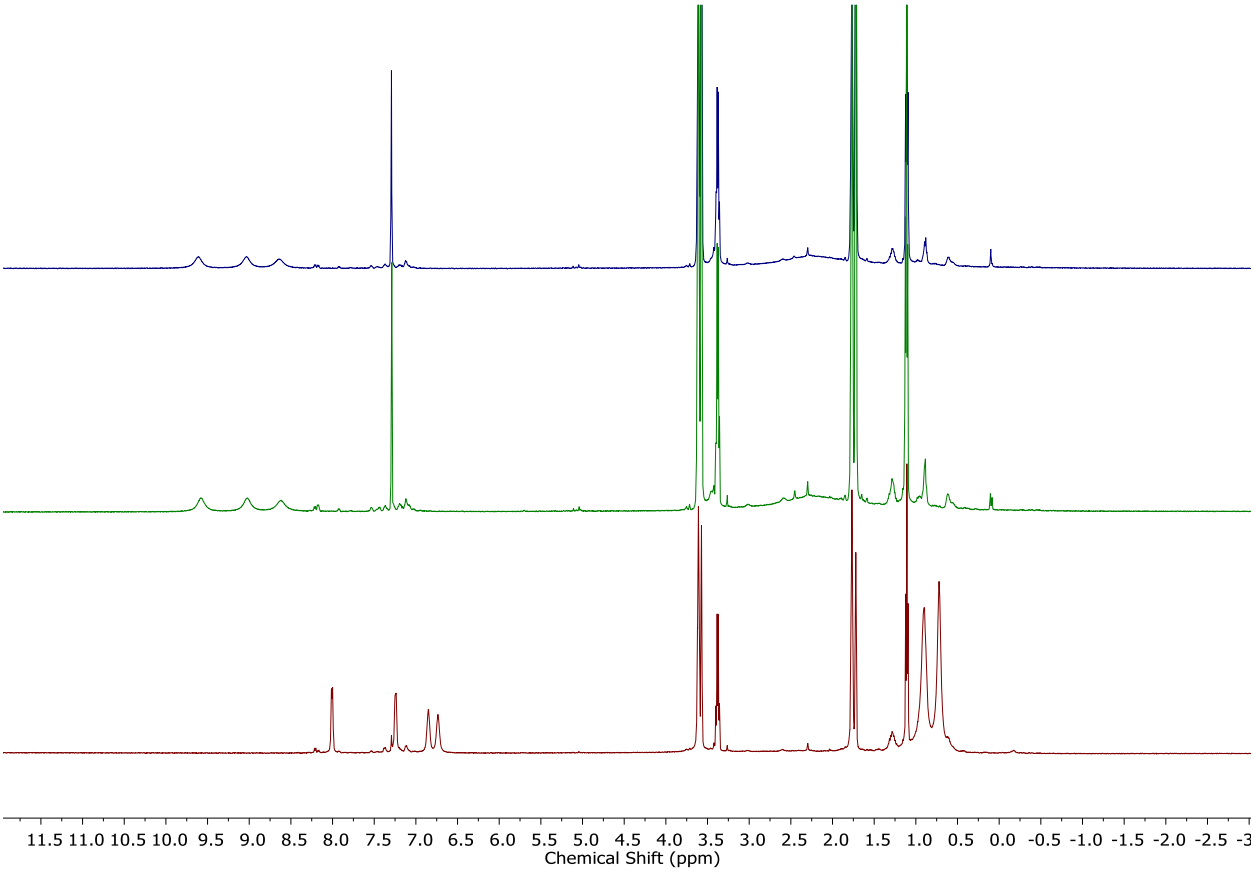

Figure S47. Stacked ^{1}H NMR spectra (500 MHz, THF-d_8, 25 °C) of an authentic sample of $P_3^{Si}Os\text{-}N_2$ (top, blue), the reaction of $P_3^{Si}Os\text{-}N_2$ with 5 equiv of Cp^*_2Co (middle, green), and an authentic sample of $[K(THF)_2][P_3^{Si}Os\text{-}N_2]$ (bottom, red). *Note:* $P_3^{Si}Os\text{-}N_2$ and $[K(THF)_2][P_3^{Si}Os\text{-}N_2]$ contain small amounts of $P_3^{Si}Os(N_2)(H)$ and $P_3^{Si}OsH_3$ present as impurities.

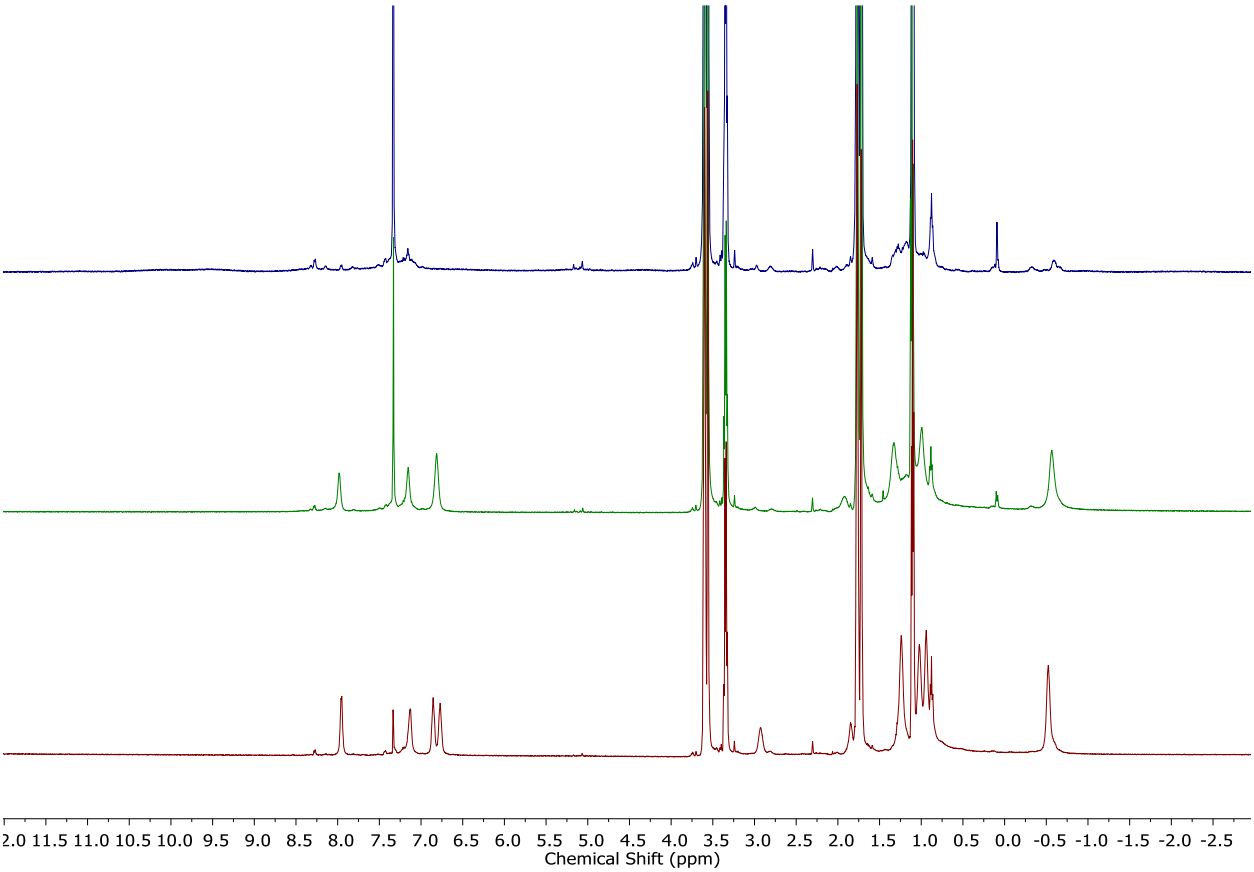

Figure S48. Stacked ^{1}H NMR spectra (500 MHz, THF-d_8, -78 °C) of an authentic sample of $P_3^{Si}Os\text{-}N_2$ (top, blue), the reaction of $P_3^{Si}Os\text{-}N_2$ with 5 equiv of Cp^*_2Co (middle, green), and an authentic sample of $[K(THF)_2][P_3^{Si}Os\text{-}N_2]$ (bottom, red). *Note:* $P_3^{Si}Os\text{-}N_2$ and $[K(THF)_2][P_3^{Si}Os\text{-}N_2]$ contain small amounts of $P_3^{Si}Os(N_2)(H)$ and $P_3^{Si}OsH_3$ present as impurities.

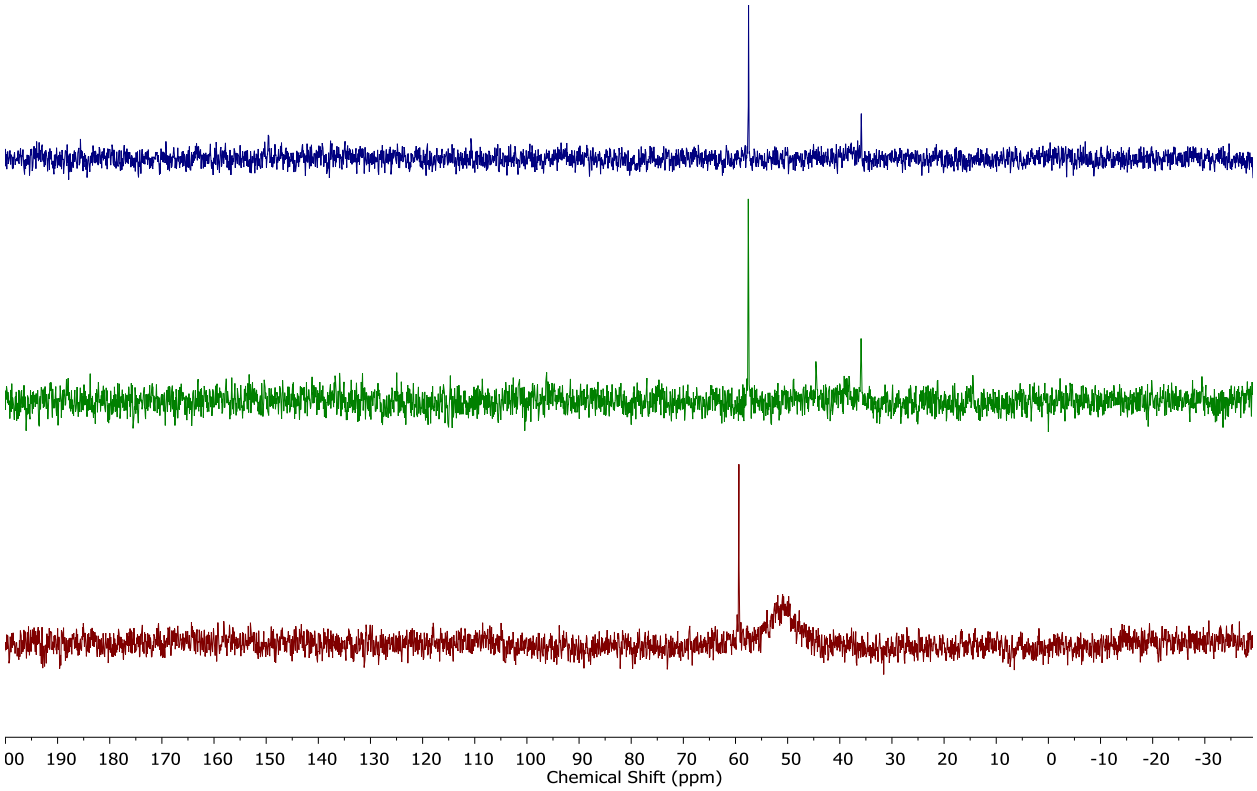

Figure S49. Stacked $^{31}P\{^{1}H\}$ NMR spectra (202 MHz, THF-d_8, 25 °C) of an authentic sample of $P_3^{Si}Os\text{-}N_2$ (top, blue), the reaction of $P_3^{Si}Os\text{-}N_2$ with 5 equiv of Cp^*_2Co (middle, green), and an authentic sample of $[K(THF)_2][P_3^{Si}Os\text{-}N_2]$ (bottom, red). *Note:* $P_3^{Si}Os\text{-}N_2$ and $[K(THF)_2][P_3^{Si}Os\text{-}N_2]$ contain small amounts of $P_3^{Si}Os(N_2)(H)$ and $P_3^{Si}OsH_3$ present as impurities that give rise to the peaks at ~35-40 ppm and ~59 ppm, respectively.

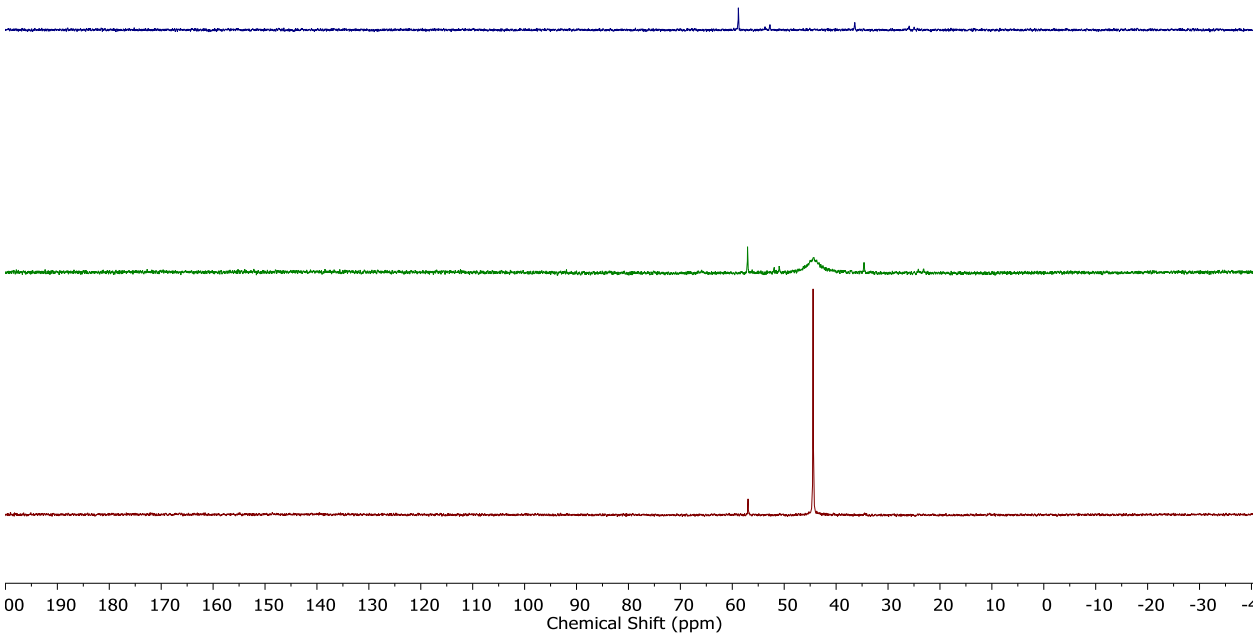

Figure S50. Stacked $^{31}P\{^{1}H\}$ NMR spectra (202 MHz, THF-d_8, -78 °C) of an authentic sample of $P_3^{Si}Os\text{-}N_2$ (top, blue), the reaction of $P_3^{Si}Os\text{-}N_2$ with 5 equiv of Cp^*_2Co (middle, green), and an authentic sample of $[K(THF)_2][P_3^{Si}Os\text{-}N_2]$ (bottom, red). *Note:* $P_3^{Si}Os\text{-}N_2$ and $[K(THF)_2][P_3^{Si}Os\text{-}N_2]$ contain small amounts of $P_3^{Si}Os(N_2)(H)$ and $P_3^{Si}OsH_3$ present as impurities. $P_3^{Si}Os(N_2)(H)$ gives rise to the doublets at ~54 ppm and ~24 ppm, and the singlet at ~35 ppm. $P_3^{Si}OsH_3$ gives rise to the singlet at ~59 ppm.

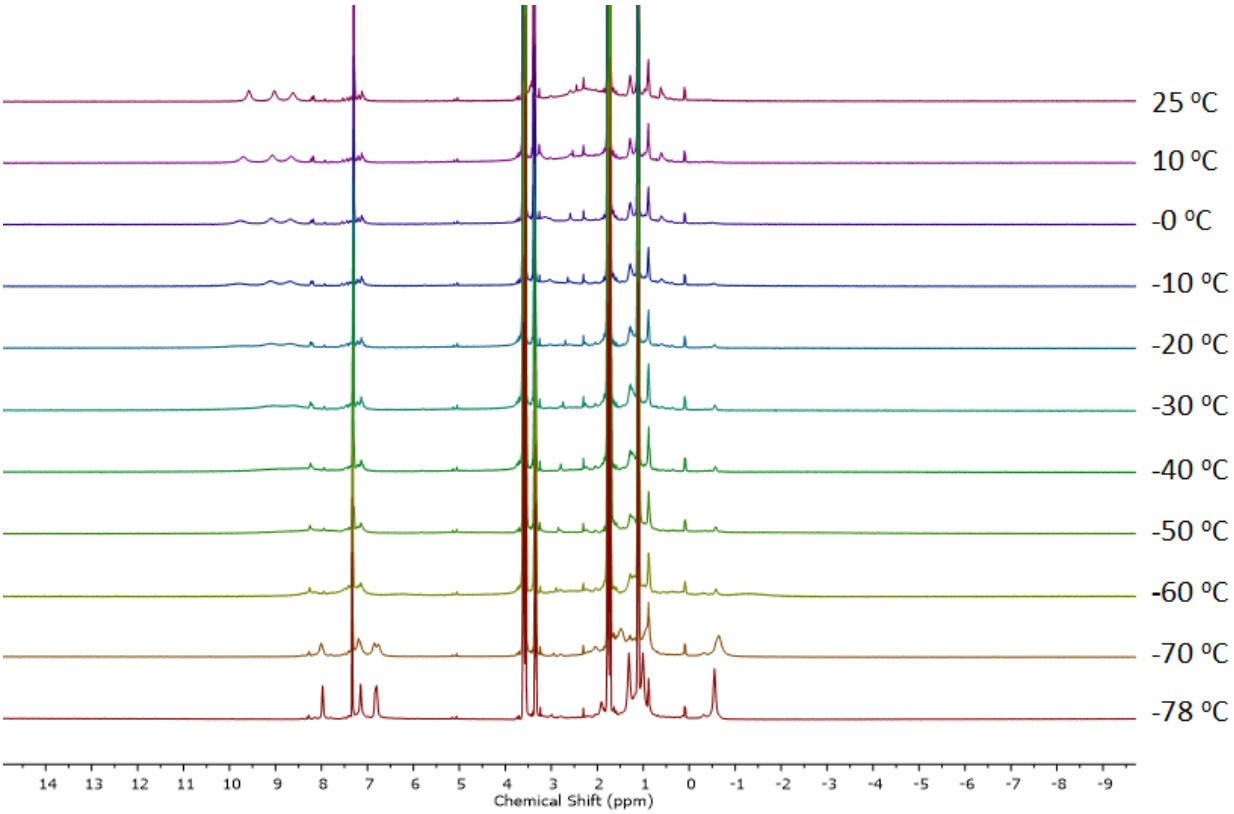

Figure S51. Variable temperature ^{1}H NMR spectra (500 MHz, THF-d_8) for the reaction of $P_3^{Si}Os$-N_2 with 5 equiv of Cp^*_2Co.

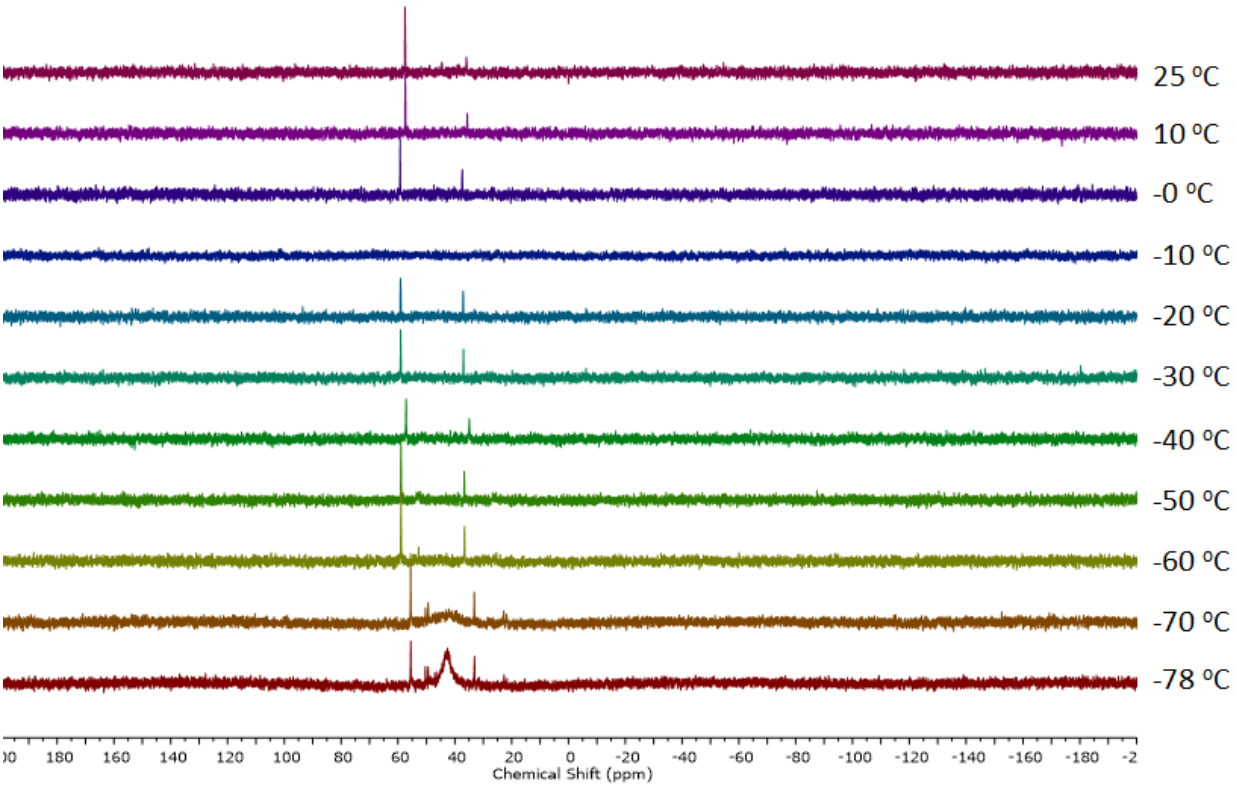

Figure S52. Variable temperature $^{31}P\{^{1}H\}$ NMR spectra (202 MHz, THF-d_8) for the reaction of $P_3^{Si}Os\text{-}N_2$ with 5 equiv of Cp^*_2Co.

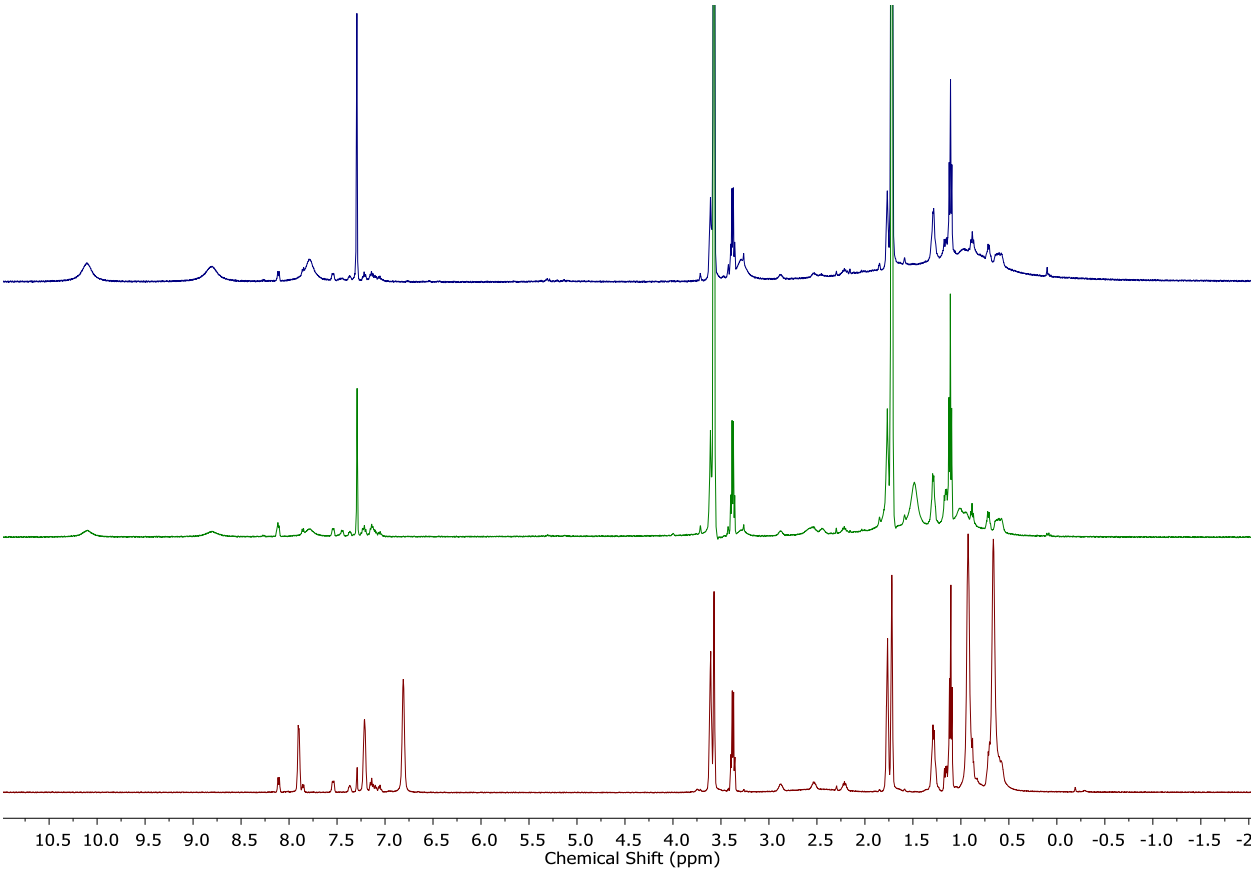

Figure S53. Stacked ^{1}H NMR spectra (500 MHz, THF-d_8, 25 °C) of an authentic sample of $P_3^{Si}Ru\text{-}N_2$ (top, blue), the reaction of $P_3^{Si}Ru\text{-}N_2$ with 5 equiv of Cp^*_2Co (middle, green), and an authentic sample of $[K(THF)_2][P_3^{Si}Ru\text{-}N_2]$ (bottom, red). *Note:* $P_3^{Si}Ru\text{-}N_2$ and $[K(THF)_2][P_3^{Si}Ru\text{-}N_2]$ contain a small amount of $P_3^{Si}Ru(N_2)(H)$ present as an impurity.

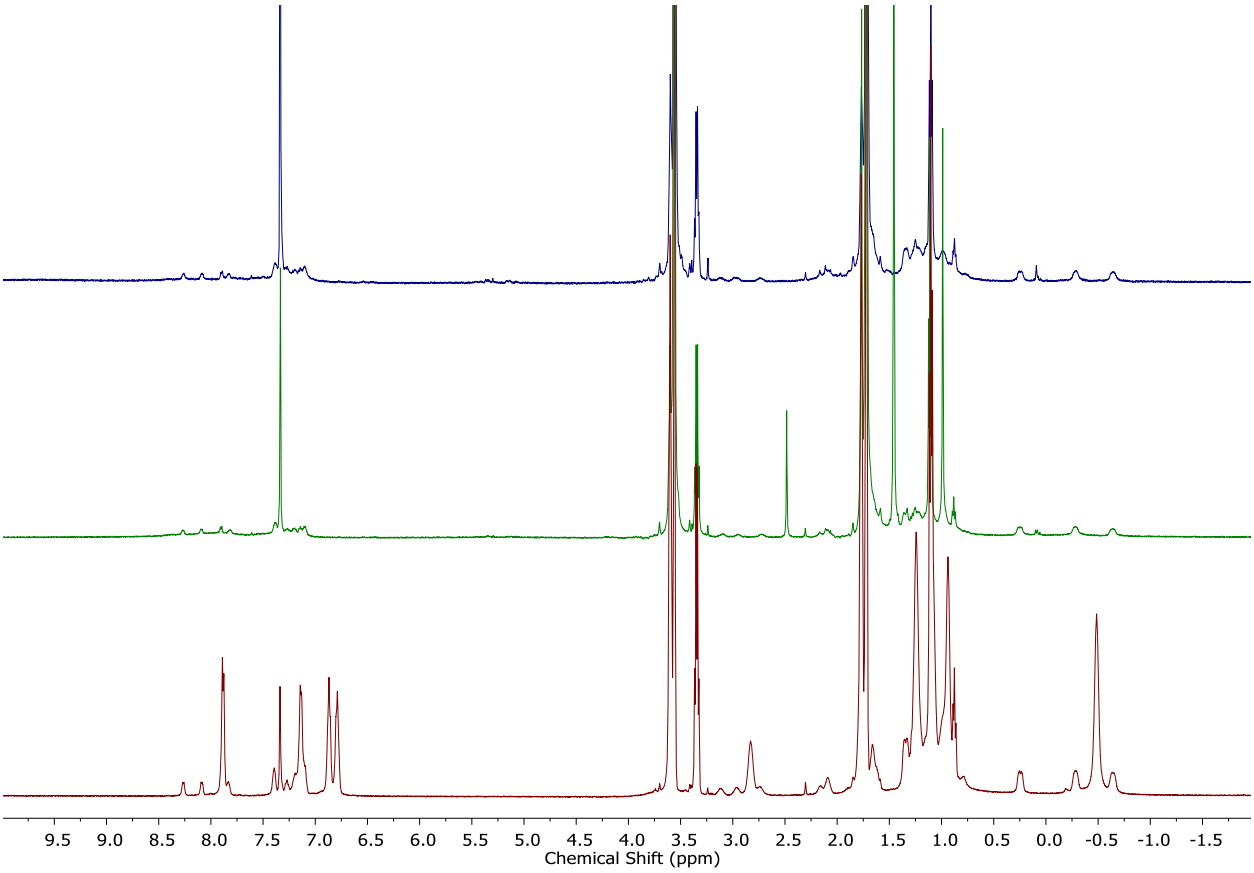

Figure S54. Stacked ^{1}H NMR spectra (500 MHz, THF-d_8, -78 °C) of an authentic sample of $P_3^{Si}Ru\text{-}N_2$ (top, blue), the reaction of $P_3^{Si}Ru\text{-}N_2$ with 5 equiv of Cp^*_2Co (middle, green), and an authentic sample of $[K(THF)_2][P_3^{Si}Ru\text{-}N_2]$ (bottom, red). *Note:* $P_3^{Si}Ru\text{-}N_2$ and $[K(THF)_2][P_3^{Si}Ru\text{-}N_2]$ contain a small amount of $P_3^{Si}Ru(N_2)(H)$ present as an impurity.

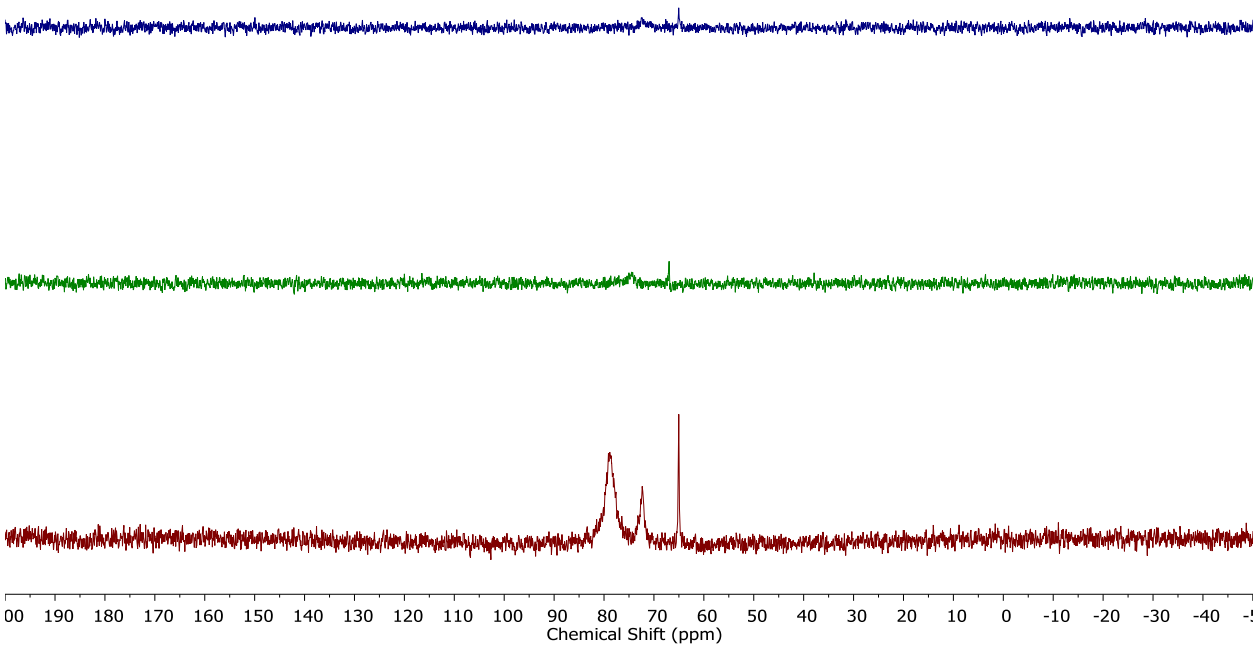

Figure S55. Stacked $^{31}P\{^{1}H\}$ NMR spectra (202 MHz, THF-d_8, 25 °C) of an authentic sample of $P_3^{Si}Ru\text{-}N_2$ (top, blue), the reaction of $P_3^{Si}Ru\text{-}N_2$ with 5 equiv of Cp^*_2Co (middle, green), and an authentic sample of $[K(THF)_2][P_3^{Si}Ru\text{-}N_2]$ (bottom, red). *Note:* $P_3^{Si}Ru\text{-}N_2$ and $[K(THF)_2][P_3^{Si}Ru\text{-}N_2]$ contain a small amount of $P_3^{Si}Ru(N_2)(H)$ present as an impurity that gives rise to the peaks at ~50 ppm and ~73 ppm.

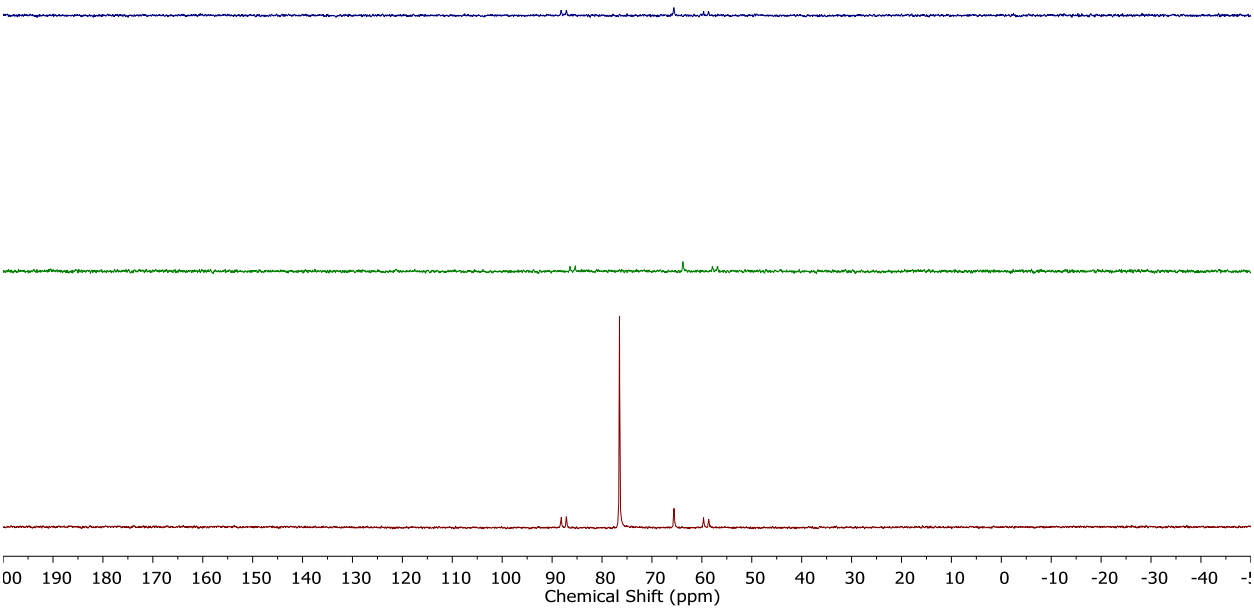

Figure S56. Stacked $^{31}P\{^{1}H\}$ NMR spectra (202 MHz, THF-d_8, -78 °C) of an authentic sample of $P_3^{Si}Ru\text{-}N_2$ (top, blue), the reaction of $P_3^{Si}Ru\text{-}N_2$ with 5 equiv of Cp^*_2Co (middle, green), and an authentic sample of $[K(THF)_2][P_3^{Si}Ru\text{-}N_2]$ (bottom, red). *Note:* $P_3^{Si}Ru\text{-}N_2$ and $[K(THF)_2][P_3^{Si}Ru\text{-}N_2]$ contain a small amount of $P_3^{Si}Ru(N_2)(H)$ present as an impurity that gives rise to the doublets at ~57 ppm and ~59 ppm, and the singlet at ~50 ppm.

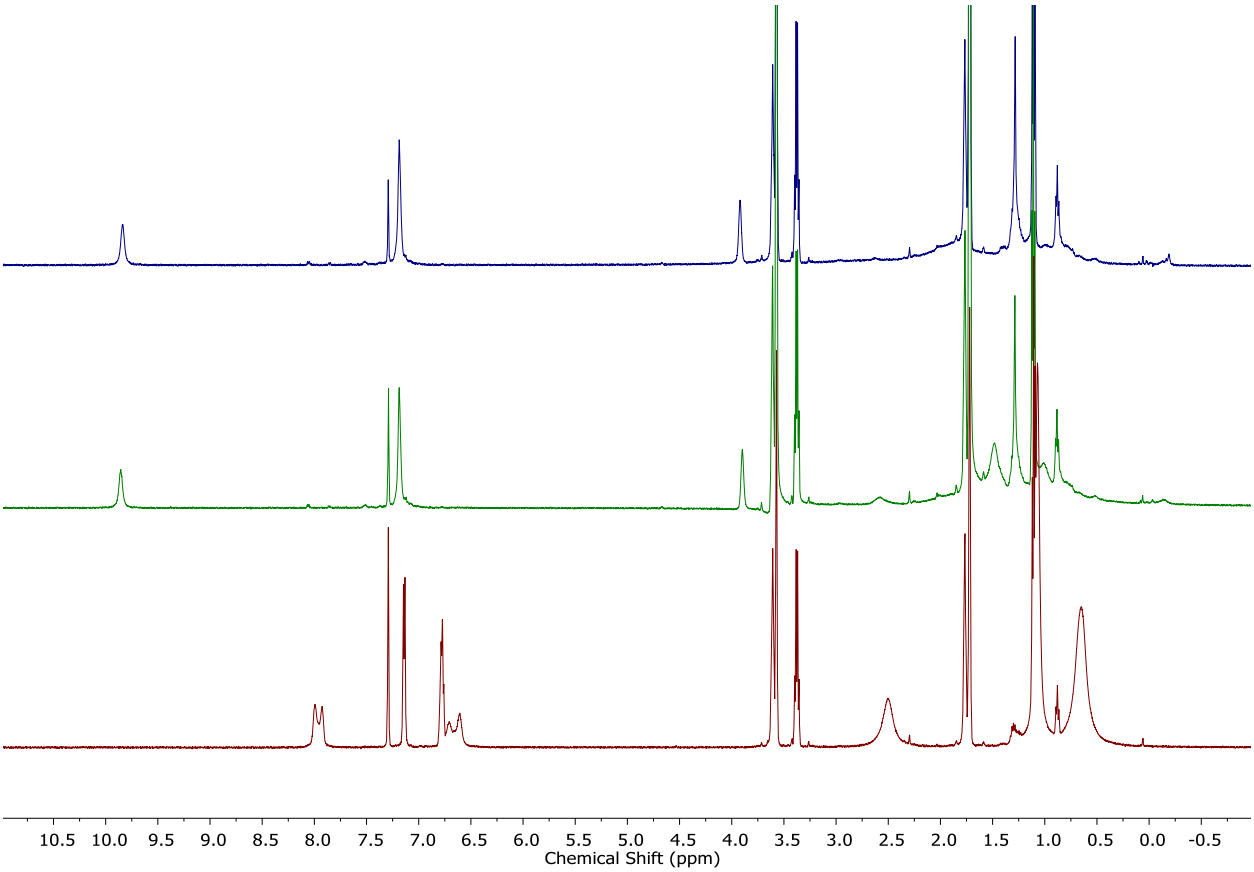

Figure S57. Stacked ^{1}H NMR spectra (500 MHz, THF-d_8, 25 °C) of an authentic sample of $P_3^{Si}Fe\text{-}N_2$ (top, blue), the reaction of $P_3^{Si}Fe\text{-}N_2$ with 5 equiv of Cp^*_2Co (middle, green), and an authentic sample of $[K(DME)_x][P_3^{Si}Fe\text{-}N_2]$ (bottom, red).

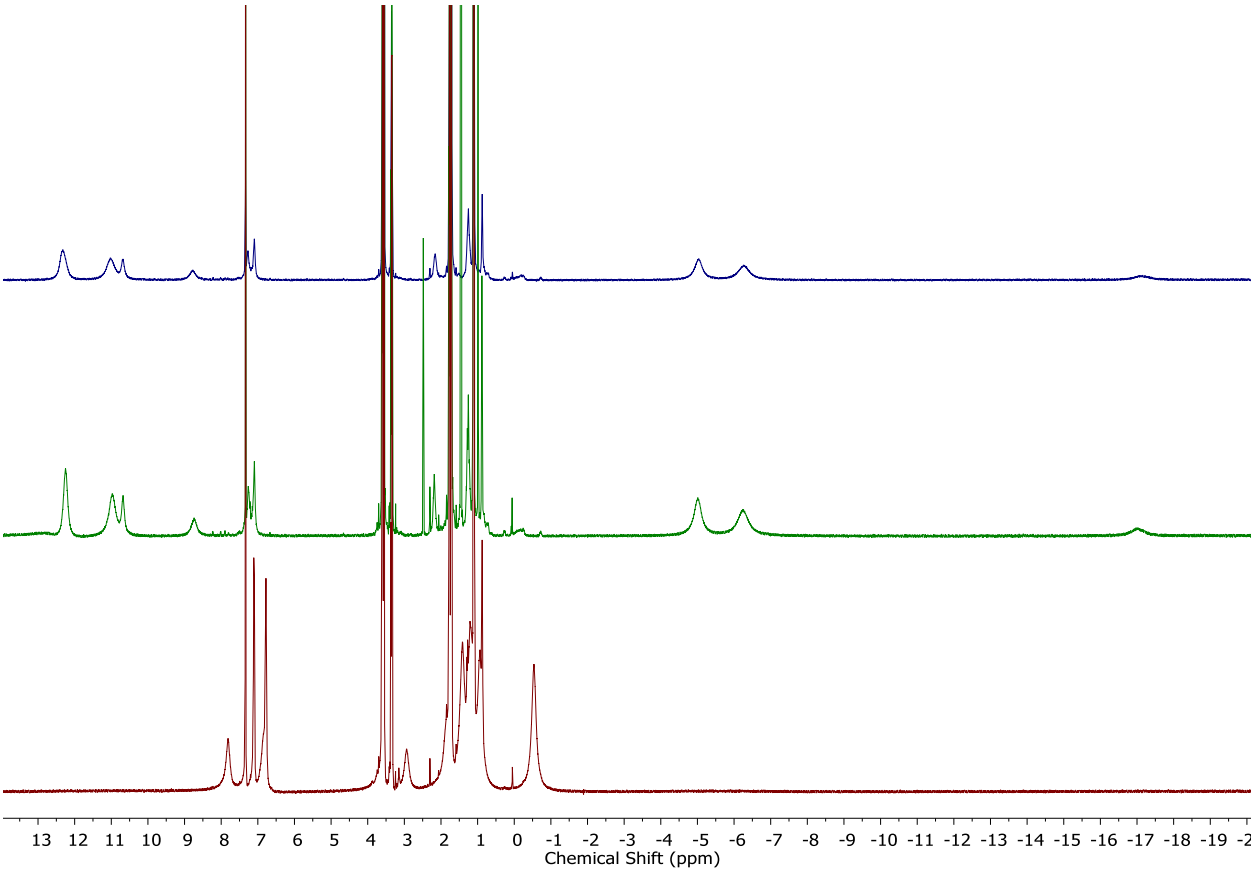

Figure S58. Stacked ^{1}H NMR spectra (500 MHz, THF-d_8, -78 °C) of an authentic sample of $P_3^{Si}Fe\text{-}N_2$ (top, blue), the reaction of $P_3^{Si}Fe\text{-}N_2$ with 5 equiv of Cp^*_2Co (middle, green), and an authentic sample of $[K(DME)_x][P_3^{Si}Fe\text{-}N_2]$ (bottom, red).

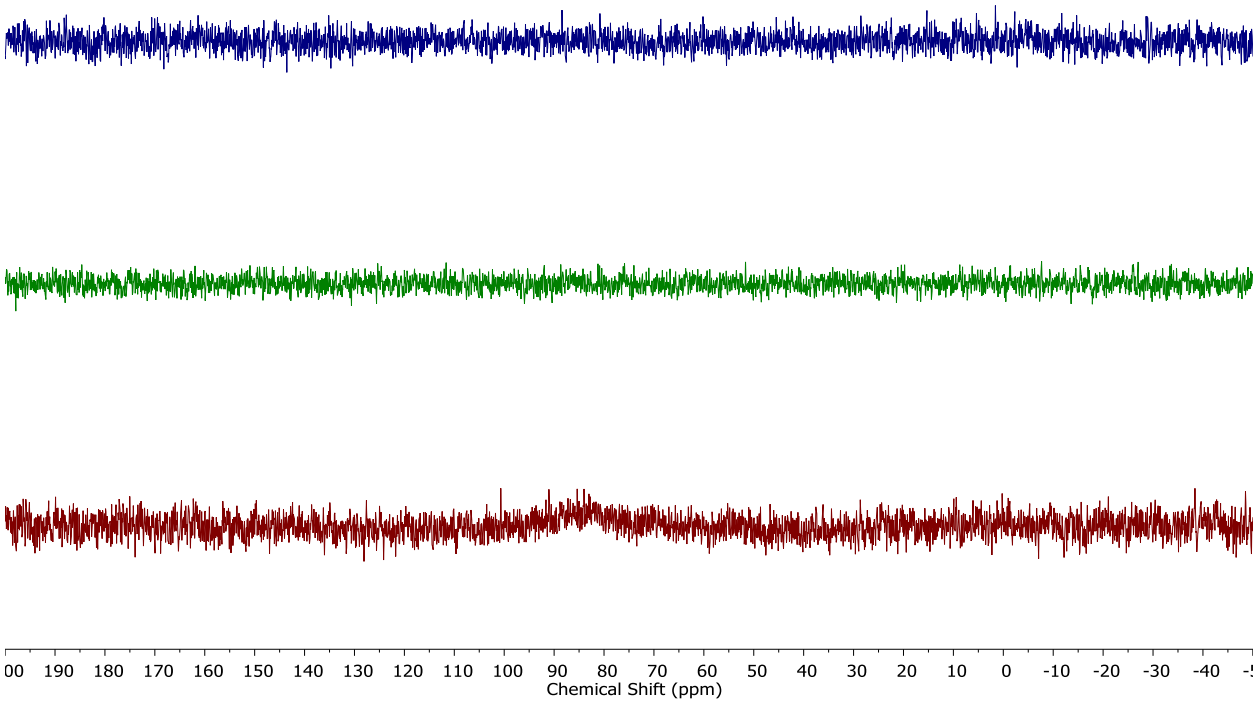

Figure S59. Stacked $^{31}P\{^{1}H\}$ NMR spectra (202 MHz, THF-d_8, 25 °C) of an authentic sample of $P_3^{Si}Fe\text{-}N_2$ (top, blue), the reaction of $P_3^{Si}Fe\text{-}N_2$ with 5 equiv of Cp^*_2Co (middle, green), and an authentic sample of $[K(DME)_x][P_3^{Si}Fe\text{-}N_2]$ (bottom, red).

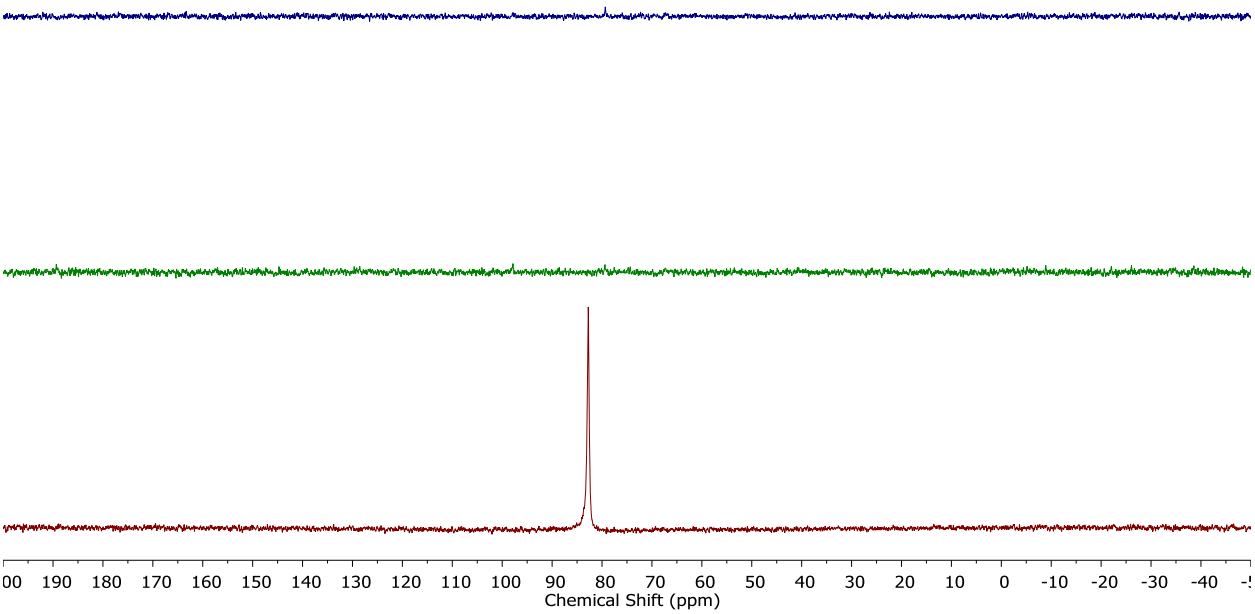

Figure S60. Stacked $^{31}P\{^{1}H\}$ NMR spectra (202 MHz, THF-d_8, -78 °C) of an authentic sample of $P_3^{Si}Fe\text{-}N_2$ (top, blue), the reaction of $P_3^{Si}Fe\text{-}N_2$ with 5 equiv of Cp^*_2Co (middle, green), and an authentic sample of $[K(DME)_x][P_3^{Si}Fe\text{-}N_2]$ (bottom, red).

UV-vis Spectral Analysis of the Reaction of $P_3^{Si}Os\text{-}N_2$ with 5 equiv of Cp^*_2Co:

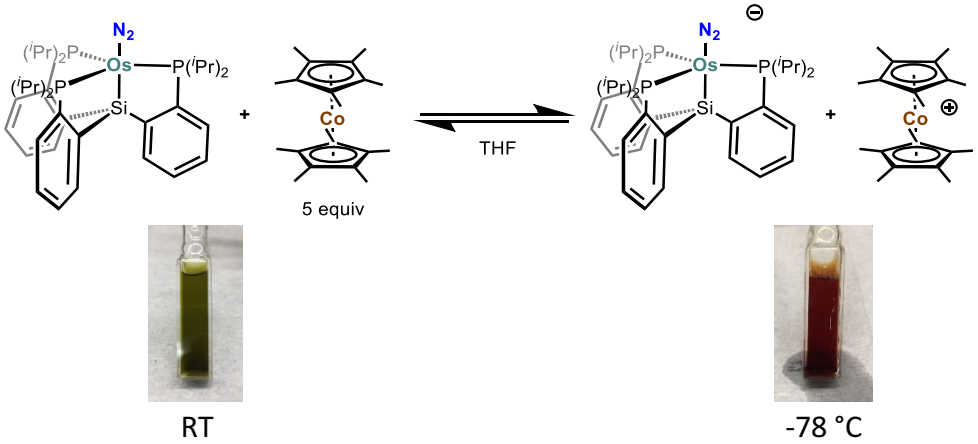

In the glovebox, $P_3^{Si}Os\text{-}N_2$ (0.0040 g, $4.8\text{x}10^{-3}$ mmol) and Cp^*_2Co (5.0 equiv, 0.024 mmol, 0.0079 g) were weighed out in separate vials. Both compounds were dissolved in 1.5 mL of THF, and then both solutions were transferred to a UV-vis cuvette. The volume of the resulting solution was then diluted to 4 mL with additional THF. The cuvette was sealed with a Teflon stopcock, removed

from the glovebox, and analyzed by variable temperature optical spectroscopy. At each temperature, the system was allowed to equilibrate for 5 minutes before collecting the spectrum.

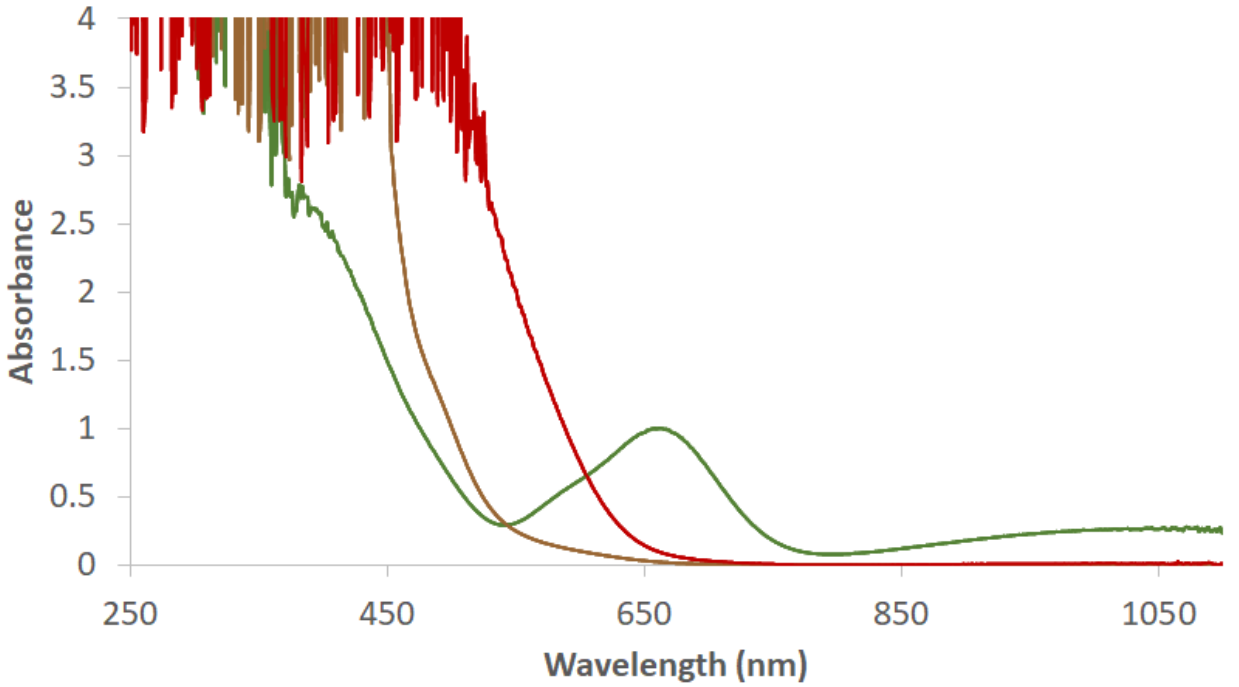

Figure S61. Overlaid UV-vis absorbance spectra (THF, -78 °C) of $P_3^{Si}Os\text{-}N_2$ (green, 1.2 mM), Cp^*_2Co (brown, 6.0 mM), and $[K(THF)_2][P_3^{Si}Os\text{-}N_2]$ (red, 1.2 mM).

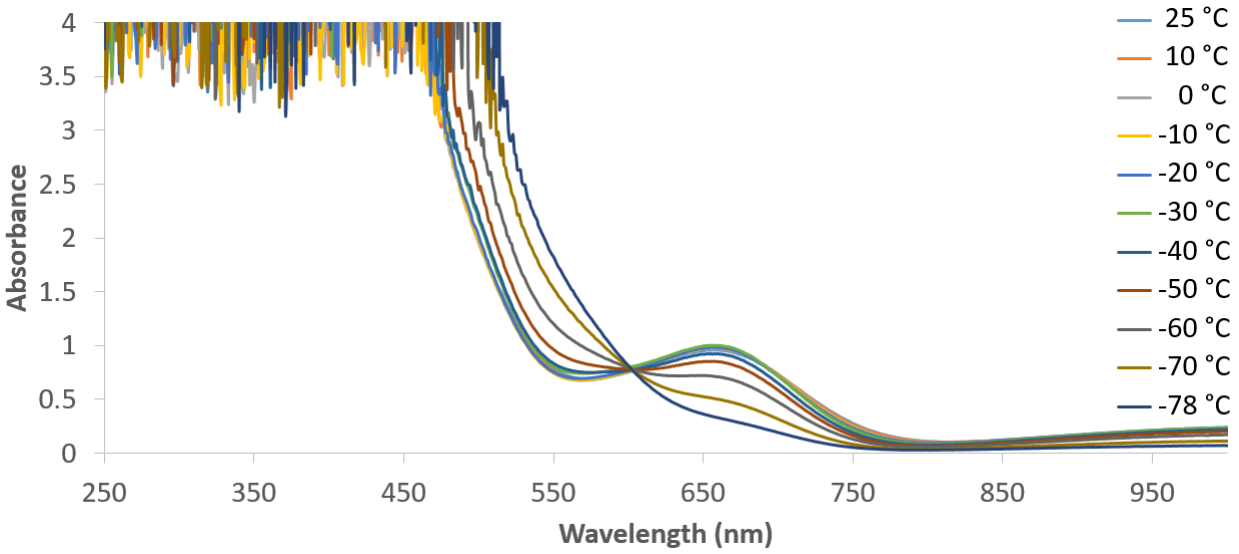

Figure S62. Variable temperature UV-vis absorbance spectra for the reaction of $P_3^{Si}Os\text{-}N_2$ (1.0 equiv, 1.2 mM) with Cp^*_2Co (5 equiv, 6.0 mM) in THF.

X-Ray Data

Table S12. Crystal data and structure refinement for $[P_3^{Si}Os{=}NNH_2][OTf]$.

Empirical formula	$C_{37}H_{56}N_2O_3F_3SiP_3SOs$
Formula weight	977.09
Temperature/K	99.98
Crystal system	orthorhombic
Space group	$P2_12_12_1$
a/Å	22.2348(15)
b/Å	12.2611(7)
c/Å	15.1377(9)
α/°	90
β/°	90
γ/°	90
Volume/Å^3	4126.9(4)
Z	4
ρ_{calc}g/cm^3	1.573
μ/mm^{-1}	3.337
F(000)	1976.0
Crystal size/mm^3	0.154 × 0.134 × 0.077
Radiation	MoKα (λ = 0.71073)
2Θ range for data collection/°	4.652 to 62.04
Index ranges	$-23 \leq h \leq 32$, $-17 \leq k \leq 17$, $-21 \leq l \leq 21$
Reflections collected	59454
Independent reflections	13119 [R_{int} = 0.0438, R_{sigma} = 0.0560]
Data/restraints/parameters	13119/0/481
Goodness-of-fit on F^2	0.998
Final R indexes [I>=2σ (I)]	R_1 = 0.0291, wR_2 = 0.0479
Final R indexes [all data]	R_1 = 0.0367, wR_2 = 0.0497
Largest diff. peak/hole / e Å^{-3}	1.34/-1.20
Flack parameter	0.009(4)

Table S13. Crystal data and structure refinement for $P_3{}^{Si}OsH_3$.

Empirical formula	$C_{36}H_{54}SiP_3Os$
Formula weight	797.99
Temperature/K	100.06
Crystal system	triclinic
Space group	P-1
a/Å	11.1667(18)
b/Å	11.2875(18)
c/Å	16.677(3)
α/°	100.081(6)
β/°	94.097(6)
γ/°	118.576(5)
Volume/Å^3	1788.0(5)
Z	2
ρ_{calc}g/cm^3	1.482
μ/mm^{-1}	3.757
F(000)	810.0
Crystal size/mm^3	0.201 × 0.16 × 0.145
Radiation	MoKα (λ = 0.71073)
2Θ range for data collection/°	4.792 to 95.518
Index ranges	$-23 \leq h \leq 23$, $-23 \leq k \leq 23$, $-34 \leq l \leq 34$
Reflections collected	426246
Independent reflections	33848 [R_{int} = 0.0727, R_{sigma} = 0.0286]
Data/restraints/parameters	33848/0/382
Goodness-of-fit on F^2	1.068
Final R indexes [I>=2σ (I)]	R_1 = 0.0205, wR_2 = 0.0483
Final R indexes [all data]	R_1 = 0.0247, wR_2 = 0.0499
Largest diff. peak/hole / e Å^{-3}	3.09/-1.50

References

(1) Hill, P. J.; Doyle, L. R.; Crawford, A. D.; Myers, W. K.; Ashley, A. E. *J. Am. Chem. Soc.* **2016**, *138*, 13521.
(2) Takaoka, A.; Gerber, L. C. H.; Peters, J. C. *Angew. Chem. Int. Ed.* **2010**, *49*, 4088.
(3) Lee, Y.; Mankad, N. P.; Peters, J. C. *Nat. Chem.* **2010**, *2*, 558.
(4) Moret, M.-E.; Peters, J. C. *Angew. Chem. Int. Ed.* **2011**, *50*, 2063.
(5) Brookhart, M.; Grant, B.; Volpe, A. F. *Organometallics* **1992**, *11*, 3920.
(6) Weitz, I. S.; Rabinovitz, M. *J. Chem. Soc., Perkin Trans. 1* **1993**, 117.
(7) Vicente, J.; Chicote, M.-T.; Guerrero, R.; Jones, P. G. *J. Chem. Soc., Dalton Trans.* **1995**, 1251.
(8) Chalkley, M. J.; Del Castillo, T. J.; Matson, B. D.; Roddy, J. P.; Peters, J. C. *ACS Cent. Sci.* **2017**, *3*, 217.
(9) Melzer, M. M.; Mossin, S.; Dai, X.; Bartell, A. M.; Kapoor, P.; Meyer, K.; Warren, T. H. *Angew. Chem. Int. Ed.* **2010**, *49*, 904.

(10) Robbins, J. L.; Edelstein, N.; Spencer, B.; Smart, J. C. *J. Am. Chem. Soc.* **1982**, *104*, 1882.
(11) (a) Carvajal, C.; Tölle, K. J.; Smid, J.; Szwarc, M. *J. Am. Chem. Soc.* **1965**, *87*, 5548. (b) Metz, D. J.; Glines, A. *J. Phys. Chem.* **1967**, *71*, 1158.
(12) Dolomanov O. V.; Bourhis, L. J.; Gildea, R. J.; Howards, J. A. K.; Puschmann, H. *J. Appl. Cryst.* **2009**, *42*, 339.
(13) Sheldrick, G. M. *Acta Cryst. A*. **2015**, *71*, 3.
(14) Sheldrick, G. M. *Acta Cryst. A*. **2008**, *64*, 112.
(15) Rittle, J.; Peters, J. C. *J. Am. Chem. Soc.* **2016**, *138*, 4243.
(16) Weatherburn, M. W., *Anal. Chem.* **1967,** *39*, 971.
(17) Watt, G.W.; Crisp, J. D. *Anal Chem.* **1952**, *24*, 2006.